

---

# SENSOR MODELLING AND ATTITUDE DETERMINATION FOR MICRO-SATELLITE

---

Bernt Ove Sunde



NTNU  
Norwegian University of  
Science and Technology

DEPARTEMENT OF ENGINEERING CYBERNETICS





## MASTEROPPGAVE

Kandidatens navn: Bernt Ove Sunde  
Fag: Teknisk Kybernetikk

Oppgavens tittel (norsk):

Oppgavens tittel (engelsk): *Sensor modelling and attitude determination for micro-satellite.*

Oppgavens tekst:

Kongsberg Defence & Aerospace er et eget forretningsområde innen Kongsberg Gruppen ASA. Resultatområdet Missile & Space, som er en del av Kongsberg Defence & Aerospace (KDA), deltar i en internasjonal studie på bruk av cluster satellitter (satellitter i gruppe). KDA har ansvaret for attitude control, determination og posisjons systemet. Satellittene skal utføre optiske målinger og radarmålinger. Mikrosatellittene skal ha 3-akse styring utført gjennom bruk av fire reaksjonshjul. Det ønskes en nøyaktighet på  $\pm 0.1^\circ$  eller bedre omkring hver akse og mikrosatellitten skal styres aktivt i azimuth, dvs omkring z-aksen. Flere satellitter observerer samme gjenstand og det er viktig at vi kjenner attitudevinklene med stor nøyaktighet, ønsket er  $0.001^\circ$  i alle akser. Oppgaven blir å utvikle en matematisk modell for satellitten og sensorene som skal brukes i satellitten, og benytte stjernesensor, solsensorer og jordsensorer til estimering av orientering. Simuleringer skal utføres i Simulink.

### **Satellittdata:**

Satellitten skal gå rett over polene og ha en sirkulær bane med en høyde på 600 km.  
Trehetsmomentene til satellitten:  $I_x=4 \text{ kgm}^2$ ,  $I_y=4 \text{ kgm}^2$ ,  $I_z=3 \text{ kgm}^2$

## Oppgaver:

1. Modeller satellitten.
2. Sett opp en matematisk modell for solsensoren. Her er det ønskelig å få et matematisk uttrykk for geometrien. (Kilder: Rapport fra KDA, Wertz)
3. Sett opp en matematisk modell for jordsensoren. Her er det ønskelig å få et matematisk uttrykk for geometrien. Se Wertz.
4. Sett opp en matematisk modell for å måle attitude vinklene (Roll, pitch og azimuth) vha av 2 eventuelt 3 GPS antenner.
5. Stjernesensoren har svært krevende modellering og denne kan modelleres som en målt vinkel addert støy, se Kyrkjebø.
6. Orienteringsnøyaktigheten skal være  $\leq 0.001$  grad om alle 3-akser. Det må velges sensorer som kan gi denne nøyaktigheten. En stjernesensor fra DTU (Danske tekniske universitetet) har en nøyaktighet på 1 arcsec i pitch og azimuth og 5 arcsec i rull. Undersøk om bruk av to stjernesensorer gir bedre nøyaktighet. Utvikl et Kalmanfilter som benytter:
  - Stjernesensor og solsensor
  - Stjernesensor, solsensor og jordsensor
7. Utfør det samme arbeid som under punkt 6, men benytt en valgfri ulineær observer.
8. Benytt realistiske støy og finn hvor nøyaktig attitudevinklene kan estimeres både med Kalmanfilter og med ulineær observer. Sammenlign.

Satellitten skal styres fra fire reaksjonshjul i tetraederkonfigurasjon. Benytt valgfri regulator til å styre satellitten.

Oppgaven gitt: 12/1-05

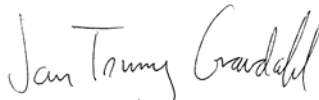
Besvarelsen leveres: 8/6-05

Besvarelsen levert:

Utført ved Institutt for teknisk kybernetikk

Veileder: Åge Skullestad, Kongsberg Defence & Aerospace

Trondheim, den 12/1-05

  
Jan Tommy Gravdahl  
Faglærer

# Preface

This work is the concluding thesis of the Siv.ing. education provided by the Norwegian University of Science and Technology (NTNU). It has been carried out at the Departments of Engineering Cybernetics (ITK). I would like to thank my advisor, associate professor Jan Tommy Gravdahl, for his support and valuable advice during this work. I would also like to thank Åge Skullestad at KDA for supplying the interesting and challenging determination problem. Finally I would like to thank my fellow satellite students at room G238 for a fun and positive work environment.

Trondheim June 8, 2005

Bernt Ove Sunde



# Contents

<b>Contents</b>	<b>iii</b>
<b>List of Figures</b>	<b>vi</b>
<b>List of Tables</b>	<b>vii</b>
<b>1 Introduction</b>	<b>1</b>
1.1 Previous work and motivation . . . . .	1
1.2 This thesis . . . . .	2
1.3 Outline of this thesis . . . . .	2
<b>2 Attitude representation</b>	<b>3</b>
2.1 Definition and notation . . . . .	3
2.1.1 Vectors . . . . .	3
2.1.2 The rotation matrix . . . . .	4
2.2 Attitude . . . . .	5
2.2.1 Reference frames . . . . .	5
2.2.2 Euler angles . . . . .	6
2.2.3 Quaternion . . . . .	7
2.3 Transformation between frames . . . . .	8
<b>3 Attitude Sensors</b>	<b>11</b>
3.1 Sensor configuration . . . . .	11
3.2 Star sensor . . . . .	12
3.2.1 Sensor model . . . . .	12
3.2.2 Star reference model . . . . .	12
3.2.3 Hardware . . . . .	12
3.2.4 Measurement noise . . . . .	12
3.3 Sun Sensor . . . . .	14
3.3.1 Sensor model . . . . .	14
3.3.2 Sun reference model . . . . .	14
3.3.3 Hardware . . . . .	15
3.3.4 Measurement noise . . . . .	15
3.4 Earth Sensor . . . . .	16
3.4.1 Sensor model . . . . .	17
3.4.2 Earth reference model . . . . .	17

3.4.3	Hardware . . . . .	17
3.4.4	Measurement noise . . . . .	18
<b>4</b>	<b>Satellite attitude</b>	<b>19</b>
4.1	Dynamic equation of motion . . . . .	19
4.1.1	kinetic equations . . . . .	19
4.1.2	Kinematic equations . . . . .	20
4.2	State space models . . . . .	20
4.2.1	Nonlinear . . . . .	20
4.2.2	Linearized . . . . .	21
4.3	Process noise . . . . .	23
4.3.1	Input noise . . . . .	23
4.3.2	Parameter noise . . . . .	24
4.3.3	Stabilizing noise . . . . .	24
4.4	Position . . . . .	24
4.5	Attitude control . . . . .	25
<b>5</b>	<b>Attitude determination</b>	<b>27</b>
5.1	Optimal nonlinear estimation . . . . .	27
5.2	Extended Kalman Filter . . . . .	27
5.2.1	Filter theory . . . . .	28
5.2.2	EKF using a single Star sensor . . . . .	30
5.2.3	EKF using two Star sensors . . . . .	31
5.2.4	EKF using Star- and Sun-sensors . . . . .	31
5.2.5	EKF using Star-, Sun- and Earth sensors . . . . .	32
5.2.6	Observability . . . . .	33
5.2.7	Modified EKF . . . . .	34
5.3	Nonlinear Observer . . . . .	35
5.3.1	Nonlinear observer theory . . . . .	35
5.3.2	Attitude observer . . . . .	36
5.3.3	Nonlinear observer using star sensors . . . . .	36
5.3.4	Nonlinear observer using Star- and Sun-sensors . . . . .	37
5.3.5	Nonlinear observer using Star-, Sun- and Earth sensors . . . . .	38
<b>6</b>	<b>Performance Analysis</b>	<b>39</b>
6.1	Simulation environment . . . . .	39
6.2	Extended kalman filter . . . . .	41
6.2.1	EKF using Star sensors . . . . .	41
6.2.2	EKF using Star-, Sun-, and Earth-sensors . . . . .	42
6.2.3	Modified EKF . . . . .	43
6.3	Nonlinear observer . . . . .	45
6.3.1	Nonlinear observer using Star sensors . . . . .	45
6.3.2	Nonlinear observer using Star-, Sun- and Earth-sensors . . . . .	46
6.4	Effect of attitude determination . . . . .	47

<b>7</b>	<b>Concluding Remarks and Recommendations</b>	<b>49</b>
7.1	Conclusion . . . . .	49
7.2	Recommendations . . . . .	50
	<b>References</b>	<b>51</b>
<b>A</b>	<b>Reference frames</b>	<b>55</b>
<b>B</b>	<b>Attitude determination summary</b>	<b>57</b>
B.1	Extended Kalman Filter . . . . .	57
B.1.1	EKF using a single Star sensor . . . . .	57
B.1.2	EKF using two Star sensors . . . . .	57
B.1.3	EKF using Star- and Sun-sensors . . . . .	58
B.1.4	EKF using Star-, Sun-, and Earth-sensors . . . . .	59
B.1.5	Modified EKF . . . . .	60
B.2	Nonlinear Observer . . . . .	61
B.2.1	Nonlinear observer using a single star sensor . . . . .	61
B.2.2	Nonlinear observer using two star sensors . . . . .	61
B.2.3	Nonlinear observer using stars and sun sensors . . . . .	62
B.2.4	Nonlinear observer using stars, sun, and earth sensors . . . . .	63
<b>C</b>	<b>Linearization</b>	<b>65</b>
C.1	Added inertia model . . . . .	65
C.2	Angular velocity model . . . . .	68
C.3	Earth sensor measurement matrix . . . . .	73
<b>D</b>	<b>CD Contents</b>	<b>75</b>

# List of Figures

2.1	Attitude expressed by Euler angles . . . . .	7
3.1	Sun position relative to the Earth . . . . .	14
3.2	Satellite's orbit and body frame relative to the Earth . . . . .	17
6.1	Simulink model overview . . . . .	39
6.2	Star filters transient errors . . . . .	41
6.3	Combined filters' transient errors . . . . .	43
6.4	Double star vs. Star and sun filter . . . . .	44
6.5	Simulated loss of star measurement . . . . .	45
6.6	Star observers transient errors . . . . .	46
6.7	Combined observers transient errors . . . . .	46
6.8	Satellite propagation simulink overview . . . . .	48
A.1	ECI, ECEF, and Orbit frame . . . . .	55
A.2	Body, Orbit, and ECI frame . . . . .	56

# List of Tables

3.1	DTU Star sensor main technical data . . . . .	13
3.2	DSS main technical data . . . . .	16
3.3	13-470-RH main data . . . . .	18
6.1	Satellite parameters . . . . .	40
6.2	Initial values . . . . .	41
6.3	Star filters steady-state errors . . . . .	42
6.4	Combined filters steady-state errors . . . . .	43
6.5	Star observers steady-state errors . . . . .	46
6.6	Combined observers steady-state errors . . . . .	47



# Abstract

This thesis describes the development of attitude determination schemes for a small active stabilized and gravity-gradient stable satellite using the relative positions of the Sun, the Earth, and the surrounding stars. The systems determines the attitude well within the desired accuracy demands, and the resulting attitude control meets the accuracy requirement of  $0.1^\circ$  about all axes. The satellite's attitude and angular velocity are estimated using either a extended kalman filter (EKF), or a nonlinear observer, with the attitude represented by Euler parameters to ensure global solutions.

The attitude is determined based on observations made by the star, sun, and earth sensors in four different configurations. The sensor are modeled as ideal, with performances reflecting available hardware. The satellite's attitude and dynamics model are represented relative to the orbit frame, and extended to include dynamics of reaction wheels placed in a tetrahedron structure. The linearized model is updated to include the added dynamics. The EKF and nonlinear observer are designed based on the satellite's model and modified, enabling them to determine the attitude from the sensors.

The satellite equations are implemented in continuous-time, while the determinations are implemented discrete with update rates according to chosen sensor configuration. Attitude control is using a simple PD-scheme with the estimated states as state feedback. Greatest accuracy is attained using the sun and earth measurements, at an output rate of 40 Hz, as main sensors, and performing corrections with two star sensors at every fifth iteration. The determination produces the attitude within a  $0.00002^\circ$  root-mean square error of the actual values. The nonlinear observer displays best performances when the determination system is exactly determined or overdetermined, while the EKF displays best performances when the determination system is underdetermined.



# Chapter 1

## Introduction

Small satellites may perform complex tasks as surveillance and communication, and are to some degree in demand of directional attitude control. In order to achieve required attitude control, the satellite's attitude, i.e. its relative orientation in space, must be known to some degree of accuracy. The control performance is dependent on the accuracy of the attitude determination. Because the satellite's low weight budget and small size, inertial navigation systems (INS) becomes too large and heavy, and the attitude must be derived from the relative positions of the Sun, Earth, and stars and the Earth's magnetic field.

### 1.1 Previous work and motivation

This thesis is a part of the ongoing study at Kongsberg Defence and Aerospace (KDA) on cluster satellites. KDA's Missile and Space division is participating in an international study of cluster satellites, and are responsible for attitude control and determination, and the positioning system. The satellites are to perform optical and radar measurements in unison, and requires accurately 3-axis directional attitude control executed by reaction wheels. To ensure a control performance of  $0.1^\circ$ , an attitude determination accuracy of  $0.001^\circ$  is desired. The attitude will be derived from sensor measuring the relative position of the stars, the Sun, and the Earth. The satellite has a planned circular polar orbit at 600km altitude.

There exist numerous papers and articles on the problem of attitude determination of spacecrafts, and extended kalman filters and nonlinear observers are two among many methods presented. Leferts, Markley and Shuster (1982) introduces spacecraft attitude determination using quaternion based Kalman filter, while the use of a nonlinear observer is addressed by Salcudean (1991), and extended by Krogstad (2005) to include reaction wheel dynamics. Employing vector observation in attitude determination is presented by Shuster (1981).

The satellite is based on the previously studied Norwegian mini-satellites, NSAT-1 and NISSE (Norwegian Ionospheric Small Satellite Experiment). The study is presently extended to the field of cluster satellites, but attitude determination may be treated as a separate and independent part. A relevant study is the attitude determination for NSAT-1, addressed in Kyrkjebø (2000). The strict attitude demands of the satellite suggests a study of attainable attitude determination using the proposed sensors.

## 1.2 This thesis

This thesis investigates two attitude determination systems using Star, Sun, and Earth sensors in various configurations for a small active stabilized and gravity-gradient stable satellite. The sensor modeling assumes ideal models, with performances reflecting available hardware. The Kalman filters and nonlinear observers will be designed to treat the attitude case, and allow different sensor output rates. While the performances of the attitude determinations are investigated with a given set of satellite parameters, the work presented has an general approach and may be employed to a large set of similar satellite configurations.

## 1.3 Outline of this thesis

### Chapter 2

Basic definitions and notations used throughout the report are described. The definition of rigid body attitude represented by Euler angles and Euler parameters are presented.

### Chapter 3

The selection of attitude sensor and their configurations are presented. The sensor models together with corresponding reference- and noise-models are derived.

### Chapter 4

The dynamic model of the satellite's attitude is presented and linearized, and an active stabilizing torque is introduced.

### Chapter 5

The extended kalman filter and the nonlinear observer are presented, and according to sensor configurations modified to determine the satellite's attitude.

### Chapter 6

The performance of the attitude determination schemes are presented and discussed.

### Chapter 7

Conclusions based on the performance analysis are presented, and recommendations for further work are given.

## Chapter 2

# Attitude representation

In order to perform attitude determination, knowledge of attitude representing is needed. This chapter presents the basic notations and definitions used to develop a representation of the attitude by Euler angles and Euler parameters.

### 2.1 Definition and notation

This section introduces the basic notation and definitions used when describing rigid body motion.

#### 2.1.1 Vectors

Vectors are useful in describing forces, torques, velocities and accelerations because they represent both magnitude and direction. This characteristic makes the use of vectors eligible when dealing with rigid body dynamics and kinematics.

#### Vector description

Vectors can be described as coordinate-free, or in relation with a coordinate frame. Using a Cartesian coordinate frame in describing vectors, introduces two alternative vector representations (Egeland and Gravdahl 2002). First as a vector  $\vec{u}$  expressed as a linear combination of frame  $a$ 's orthogonal unit vectors  $\vec{a}_1, \vec{a}_2$  and  $\vec{a}_3$  by

$$\vec{u} = u_1\vec{a}_1 + u_2\vec{a}_2 + u_3\vec{a}_3 \quad (2.1)$$

where  $u_i$  are the unique components or coordinates of  $\vec{u}$  in frame  $a$ . Secondly as a coordinate vector from where the frame coordinates of the vector are written as a column vector

$$\mathbf{u}^a = \begin{bmatrix} u_1 \\ u_2 \\ u_3 \end{bmatrix} \quad (2.2)$$

where the superscripted  $a$  denotes the coordinate frame in which the vector is expressed. In this thesis the latter notation will be used.

### The vector cross product

The vector cross product  $\times$  is given by

$$\mathbf{u} \times \mathbf{v} = \mathbf{S}(\mathbf{u})\mathbf{v} \quad (2.3)$$

where  $\mathbf{S}(\mathbf{u}) \in SS(3)$  is a skew-symmetric matrix, defined as (Fossen 2002)

$$\mathbf{S}(\mathbf{u}) = -\mathbf{S}(-\mathbf{u}) = -\mathbf{S}^T(\mathbf{u}) = \begin{bmatrix} 0 & -u_3 & u_2 \\ u_3 & 0 & -u_1 \\ -u_2 & u_1 & 0 \end{bmatrix} \quad (2.4)$$

and often referred to as the skew-symmetric of vector  $\mathbf{u}$ .

### 2.1.2 The rotation matrix

In this section the rotation matrix and its properties are briefly presented (Egeland et.al. 2002).

#### Coordinate transformation for vectors

As shown in section 2.1.1, a vector may be described by its components in a Cartesian coordinate frame  $a$  with orthogonal unit vectors  $\vec{a}_1, \vec{a}_2$  and  $\vec{a}_3$ . The dynamic model of the satellite used throughout this report will incorporate several different coordinate frames, and a way to convert a vector from one frame to another is thus needed. This can be done by introducing the coordinate transformation from frame  $b$  to frame  $a$  given by

$$\mathbf{v}^a = \mathbf{R}_b^a \mathbf{v}^b \quad (2.5)$$

where

$$\mathbf{R}_b^a = \{\vec{a}_i \cdot \vec{b}_j\} \quad (2.6)$$

is called the rotation matrix from  $a$  to  $b$ . The elements  $r_{ij} = \vec{a}_i \cdot \vec{b}_j$  of the rotation matrix  $\mathbf{R}_b^a$  are called the direction cosines.

#### Simple rotations

A rotation about a fixed axis is called a simple rotation. By expressing the vectors in Cartesian coordinate frames, there are a total of three simple rotations. They are

$$\mathbf{R}_x(\phi) = \begin{bmatrix} 1 & 0 & 0 \\ 0 & \cos \phi & -\sin \phi \\ 0 & \sin \phi & \cos \phi \end{bmatrix} \quad (2.7)$$

$$\mathbf{R}_y(\theta) = \begin{bmatrix} \cos \theta & 0 & \sin \theta \\ 0 & 1 & 0 \\ -\sin \theta & 0 & \cos \theta \end{bmatrix} \quad (2.8)$$

$$\mathbf{R}_z(\psi) = \begin{bmatrix} \cos \psi & -\sin \psi & 0 \\ \sin \psi & \cos \psi & 0 \\ 0 & 0 & 1 \end{bmatrix} \quad (2.9)$$

where the notation  $\mathbf{R}_x(\phi)$  represents a rotation of angle  $\phi$  about the x axis.

### Properties of the rotation matrix

The Rotation matrix has some useful properties that will be presented in this section. It has been proven that the rotation matrix is orthogonal and satisfies

$$\mathbf{R}_a^b = (\mathbf{R}_a^b)^{-1} = (\mathbf{R}_b^a)^T \quad (2.10)$$

The rotation matrix has two interpretations. First it acts as a coordinate transformation matrix when transforming the coordinate vector  $\mathbf{v}^b$  to  $\mathbf{v}^a$  according to (2.5), and secondly as a rotation matrix when rotating the coordinate vector  $\mathbf{p}^a$  to the coordinate vector  $\mathbf{q}^b$  where  $\mathbf{q}^b = \mathbf{p}^a$  by

$$\mathbf{q}^b = \mathbf{R}_b^a \mathbf{p}^a \quad (2.11)$$

The latter interpretation is later used to define the attitude of a rigid body.

It is also proven that the rotation matrix has a determinant equal to unity, and one defines the rotation matrix by its inclusion in the  $SO(3)$ , which is

$$SO(3) = \{\mathbf{R} | \mathbf{R} \in R^{3 \times 3}, \mathbf{R}^T \mathbf{R} = \mathbf{I} \text{ and } \det \mathbf{R} = 1\} \quad (2.12)$$

The kinematic differential equation of the rotation matrix is given by the two alternative forms

$$\dot{\mathbf{R}}_b^a = \mathbf{S}(\boldsymbol{\omega}_{ab}^a) \mathbf{R}_b^a = \mathbf{R}_b^a \mathbf{S}(\boldsymbol{\omega}_{ab}^b) \quad (2.13)$$

where  $\boldsymbol{\omega}_{ab}^b$  is the angular velocity vector of frame  $b$  relative to frame  $a$ , given in the  $b$  frame.

A rotation matrix can also be described as a composite rotation, i.e. a product of two or more rotation matrices. In the case of three rotations we have

$$\mathbf{R}_d^a = \mathbf{R}_b^a \mathbf{R}_c^b \mathbf{R}_d^c \quad (2.14)$$

## 2.2 Attitude

Attitude of a rigid body is its relative orientation between itself and a reference system, and may be described by an rotation using either Euler angles or Euler parameters.

### 2.2.1 Reference frames

Before presenting the attitude representation, it is convenient to define the various reference frames that determines the attitude. This section presents the selection of frames that are commonly used in satellite navigation, (Vallado 2001) and (Fossen 2002). Illustrations are given in appendix A.

#### Earth-Centered Inertial (ECI) frame

The ECI frame is a non-accelerated reference frame in which Newton's laws are valid. The frame is fixed in space with origin at the Earth's center and the z-axis pointing towards the North Pole. The x-axis points toward vernal equinox, the point where the plane of the Earth's orbit about the Sun crosses the Equator going from south to north, and the y-axis completes the right hand Cartesian coordinate system. The frame is denoted I.

### Earth-Centered Earth Fixed (ECEF) frame

This frame has also its origin at the Earth's center. The coordinate axes are fixed to the earth and rotates relative to the ECI-frame with a frequency of

$$\omega_{ie} \approx \frac{1 + 365.25 \text{cycles}}{(365.25)(24)h} \frac{2\pi \text{rad/cycle}}{3600s/h} \approx 7.292115 \times 10^{-5} \text{rad/s} \quad (2.15)$$

because of the Earth's daily rotation and its yearly rotation around the sun (Farrell 1976). Because of Earth's rotation, the ECEF frame is not an inertia reference frame. The z-axis points towards the North Pole, x-axis points towards the intersection between the Greenwich meridian and the Equator, and the y-axis completes the right handed orthogonal system. The frame is denoted E.

### Orbit frame

The orbit frame moves with the satellite, and is also known as the satellite coordinate system. Instead of pointing from the Earth, the z axis is here set to always point towards the Earth's center. The x axis points in the direction motion along the orbit trajectory and is perpendicular to the radius vector. The x axis is usually not aligned with the velocity vector except for circular orbits or for elliptical orbits at apogee and perigee. The y axis is normal to the orbital plane. The frame is denoted O.

### Body frame

The body frame is fixed to the satellite and of practical reasons the origin is placed at the satellite's center of mass. The x- and y-axis are defined according to the right-handed coordinate system along the the symmetrical axes. As with the orbit frame the body frames z-axis points towards the Earth's center. The body frame is aligned with the body frame when the satellite has an attitude of  $0^\circ$  in roll, pitch and yaw. It is this deviation between the Orbit frame and the Body frame that describe the satellite's attitude. The frame is denoted B.

#### 2.2.2 Euler angles

The Euler angles,  $\Theta = [\phi \ \theta \ \psi]^T$ , of the roll-pitch yaw type are commonly used to describe the motion of rigid bodies that move freely, like satellites (Fossen 2002). Here the satellites attitude is determined by the rotation between the body frame and the orbit frame. In this description the rotation from body frame to orbit frame may be considered as a composite rotation consisting of a rotation  $\psi$  about the  $z_b$ , then a rotation  $\theta$  about the current (rotated) y axis, and finally a rotation  $\phi$  about the current x axis, illustrated in figure 2.1. The resulting rotation matrix becomes

$$\mathbf{R}_b^o = \mathbf{R}_z(\psi)\mathbf{R}_y(\theta)\mathbf{R}_x(\phi) \quad (2.16)$$

where  $\mathbf{R}_z(\psi)$ ,  $\mathbf{R}_y(\theta)$ , and  $\mathbf{R}_x(\phi)$  are given by (2.7), (2.8), and (2.9) which yields

$$\mathbf{R}_b^o(\Theta) = \begin{bmatrix} c\theta c\psi & s\theta s\phi s\psi - c\phi s\psi & s\theta c\phi c\psi + s\phi s\psi \\ c\theta s\psi & s\theta s\phi c\psi + c\phi c\psi & s\theta c\phi s\psi - s\phi c\psi \\ -s\theta & c\theta s\phi & c\theta c\phi \end{bmatrix} \quad (2.17)$$

where  $c = \cos$  and  $s = \sin$ . It is seen from (2.17) that the matrix will be singular at  $\pm 90^\circ$ , an an alternative representation of the attitude is needed. The singularity can be shifted to other angles

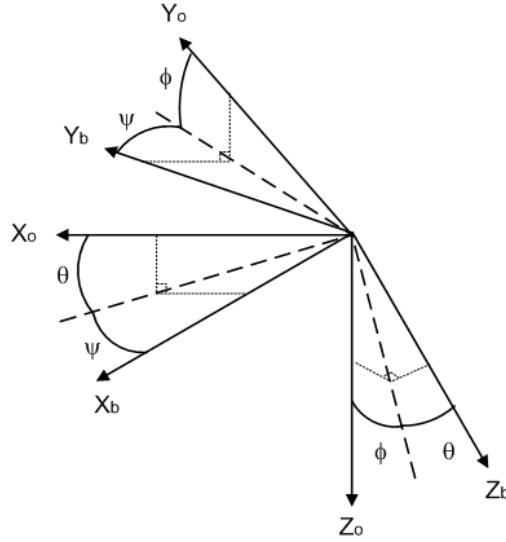


**Figure 2.1:** Attitude expressed by Euler angles

by changing the order of rotation, but it is always present in the mathematical description Euler angle attitude.

### 2.2.3 Quaternion

A quaternion is defined as a vector

$$\mathbf{q} = \begin{bmatrix} \alpha \\ \boldsymbol{\beta} \end{bmatrix} \quad (2.18)$$

of dimension 4 where  $\alpha$  is the real part and  $\boldsymbol{\beta} = [\beta_1 \beta_2 \beta_3]^T$  is the vector part.

#### Unit quaternion

A unit quaternion is a quaternion, (2.18), with unit length, i.e. it satisfies

$$\mathbf{p}^T \mathbf{p} = \eta^2 + \boldsymbol{\epsilon}^T \boldsymbol{\epsilon} = 1 \quad (2.19)$$

#### The quaternion product

The quaternion product of two unit quaternions  $\mathbf{p}_1$  and  $\mathbf{p}_2$  is a unit quaternion defined by (Chou 1992)

$$\mathbf{p} := \mathbf{p}_1 \otimes \mathbf{p}_2 = \begin{bmatrix} \eta_1 \eta_2 - \boldsymbol{\epsilon}_1^T \boldsymbol{\epsilon}_2 \\ \eta_1 \boldsymbol{\epsilon}_2 + \eta_2 \boldsymbol{\epsilon}_1 + S(\boldsymbol{\epsilon}_1) \boldsymbol{\epsilon}_2 \end{bmatrix} \quad (2.20)$$

### Euler parameters

Because of the existence of singularities in (2.17), Euler parameters are introduced to represent the satellite's attitude. The Euler parameters are defined by

$$\eta = \cos \frac{\theta}{2}, \quad \boldsymbol{\epsilon} = \mathbf{k} \sin \frac{\theta}{2} \quad (2.21)$$

where  $\boldsymbol{\epsilon} = [\epsilon_1 \ \epsilon_2 \ \epsilon_3]^T$  and  $\theta$  is the rotation about the unit vector  $\mathbf{k}$ . The vector,  $\mathbf{p} = (\eta \ \boldsymbol{\epsilon})^T$ , of Euler parameters can be treated as a unit quaternion vector, and therein useful mathematical tools becomes available.

### Rotation by Euler parameters

By using the Euler parameters the rotation matrix,  $\mathbf{R}_b^o$ , can now be expressed as

$$\mathbf{R}_b^o = \mathbf{R}_e(\eta, \boldsymbol{\epsilon}) = \mathbf{I} + 2\eta\mathbf{S}(\boldsymbol{\epsilon}) + 2\mathbf{S}(\boldsymbol{\epsilon})\mathbf{S}(\boldsymbol{\epsilon}) \quad (2.22)$$

Any given rotation will correspond to two sets of Euler parameters as

$$\mathbf{R}_e(-\eta, -\boldsymbol{\epsilon}) = \mathbf{R}_e(\eta, \boldsymbol{\epsilon}) \quad (2.23)$$

and the inverse rotation is given by

$$\mathbf{R}_e(\eta, \boldsymbol{\epsilon})^{-1} = \mathbf{R}_e(\eta, \boldsymbol{\epsilon})^T = \mathbf{R}_e(\eta, -\boldsymbol{\epsilon}) \quad (2.24)$$

## 2.3 Transformation between frames

This section presents the rotation matrices between the different frames used in this report.

### ECEF to ECI

The rotation of the ECEF frame relative that of the ECI frame is a rotation about the coincident  $z_i$  and  $z_e$  axes. This rotation can be described by a simple rotation of type (2.9), with  $\alpha = \omega_{ie}t$  where  $\omega_{ie}$  is the Earth's rotation, given by (2.15), and  $t$  is the time passed since the ECEF and ECI frames were aligned. Since the rotation,  $\alpha$ , is defined as negative right handed, the rotation matrix from frame  $e$  to to frame  $i$  becomes

$$\mathbf{R}_e^i = \mathbf{R}_{z_i}(-\alpha) = \begin{bmatrix} \cos \alpha & \sin \alpha & 0 \\ -\sin \alpha & \cos \alpha & 0 \\ 0 & 0 & 1 \end{bmatrix} \quad (2.25)$$

given the fact that  $\cos(-\alpha) = \cos \alpha$  and  $\sin(-\alpha) = -\sin \alpha$ .

### ECI to Orbit

The rotation between the ECI frame and the Orbit frame is dependent on the satellite orbit. In this thesis the orbit is assumed polar and circular at 600km altitude, and the rotation may be

represented as an rotation consisting of two simple rotations. First a time-varying rotation about the  $y_i$  axis, where the rotation velocity is defined as

$$\omega_o = \sqrt{\frac{\mu_g}{R}} = 0.001083 \text{ rad/sec} \quad (2.26)$$

where  $\mu_g$  is the Earth gravitational constant and  $R$  is the satellite Earth center distance. The second rotation is due to the orbit frame's z-axis pointing towards the Earth, and may be represented as an constant rotation of  $180^\circ$  about the  $x_i$ -axis. The rotation from ECI to orbit frame may now be represented as the two simple rotations in succession as

$$\mathbf{R}_i^o = \mathbf{R}_{x,\pi} \mathbf{R}_{y,\mu} = \begin{bmatrix} \cos \mu & 0 & \sin \mu \\ 0 & -1 & 0 \\ \sin \mu & 0 & -\cos \mu \end{bmatrix} \quad (2.27)$$

where  $\mu$  is the latitude position of the satellite, given by  $\mu = \beta_0 + \omega_o t$ , where  $\beta_0$  is the satellite's drop angle, and  $t$  is the time since last passing  $0^\circ$  latitude.

### Orbit to Body

This is the contrary rotation of the rotation defined by the satellites attitude,  $\mathbf{R}_e(\eta, \epsilon)$ , and is used to produce measurements and reference values. By computing (2.22) and using the properties (2.24) and (2.10),  $\mathbf{R}_o^b$  becomes

$$\mathbf{R}_o^b = [ \mathbf{c}_1^b \quad \mathbf{c}_2^b \quad \mathbf{c}_3^b ] = \begin{bmatrix} \eta^2 + \epsilon_1^2 - \epsilon_2^2 - \epsilon_3^2 & 2(\epsilon_1\epsilon_2 + \eta\epsilon_3) & 2(\epsilon_1\epsilon_3 - \eta\epsilon_2) \\ 2(\epsilon_1\epsilon_2 - \eta\epsilon_3) & \eta^2 - \epsilon_1^2 + \epsilon_2^2 - \epsilon_3^2 & 2(\epsilon_2\epsilon_3 + \eta\epsilon_1) \\ 2(\epsilon_1\epsilon_3 + \eta\epsilon_2) & 2(\epsilon_2\epsilon_3 - \eta\epsilon_1) & \eta^2 - \epsilon_1^2 - \epsilon_2^2 + \epsilon_3^2 \end{bmatrix} \quad (2.28)$$

where  $\mathbf{c}_i^b = [ c_{ix}^b \quad c_{iy}^b \quad c_{iz}^b ]^T$  is the directional cosines . This rotation has the property that when the  $z_o$  and  $z_b$  are aligned  $\mathbf{c}_3^b$  becomes  $[ 0 \quad 0 \quad \pm 1 ]$  which gives us a quantity of the deviation between the two frames (Ose 2004).



## Chapter 3

# Attitude Sensors

This chapter presents the chosen attitude sensors and configurations. Each sensor is studied and mathematical models, with conjunction reference models, will be derived. Concluding each sensor presentation will be investigation of available sensor hardware and their measurement noise.

### 3.1 Sensor configuration

This thesis deals with attitude determination based on four different sensor configuration. The sensor configurations will be

- Single star sensor
- Double star sensor
- Star and sun sensor
- Star, sun, and earth sensor

With exception of the first, the configurations define the satellite as a multiple sensor system, i.e. it has redundant attitude measurements. The combination of information from multiple sensors to achieve performance exceeding those of individual sensors is referred to as multi sensor fusion or simply sensor fusion (Rao 2002). By this definition, attitude determination may be; in the case of overdetermined attitude information, considered as an solution to the sensor fusion problem.

An general sensor model may be represented as

$$\mathbf{y}_s = (\mathbf{I} + \Delta)\mathbf{y} + \mathbf{b} + \mathbf{w} \quad (3.1)$$

where  $\Delta$  is the sensor misalignment,  $\mathbf{b}$  the sensor bias, and  $\mathbf{w}$  its random noise. By assuming bias-free and perfect aligned sensors, the above model is reduced to

$$\mathbf{y}_s = \mathbf{y} + \mathbf{w} \quad (3.2)$$

Because of its simple form and ability to render the noise representation as additive, the reduced model desirable when modeling sensors.

## 3.2 Star sensor

Stars provide an highly accurate reference to the satellite, and since they are orbit independent, available anywhere in the sky. They are superior to any other attitude references, and determines attitude within a few arcseconds of the true attitude.

### 3.2.1 Sensor model

The star sensor compares pictures of star coordinates in the satellite's body frame to a on-board star catalog. The comparament provides a well defined 3-axis attitude representation, such as the Euler parameters. The sensor may be modeled as the true attitude with added noise (Kyrkjebø 2000). Because of the required unity of  $\mathbf{q}_{star}$ , the model (3.2) is not applicable, and the star sensor may be modeled as

$$\mathbf{q}_{star} = \mathbf{q} \otimes \mathbf{q}_n \quad (3.3)$$

where  $\mathbf{q}$  is the actual attitude, and  $\mathbf{q}_n$  is the star sensor measurement noise, represented as Euler parameters.

### 3.2.2 Star reference model

Since the star sensor produces Euler parameters describing the satellite's attitude, it is directly comparable and no further model is needed.

### 3.2.3 Hardware

The star sensor is the most accurate attitude sensor, but is also heavier, more expensive, and require more power than most other attitude sensors. This comes from the fact that star sensors have extensive computer processing in order to produce their measurements from only a picture. Several types of star sensor exists, and depending on their method of attitude acquisition they are star scanners, fixed head star trackers, and gimbaled star tracker.

In the past a main disadvantage of the star sensors has been their operating range and weight. They had low update rates, and could not operate if the operating rates became to large, usually  $10^\circ/\text{min}$ . The Danish technical university, DTU, have developed a star sensor,  $\mu\text{ASC}$  that has greatly increased performances (Jørgensen, Denver, Betto and Jørgensen 2001), and this is used to develop the sensor model. The sensors main technical data is given in table 3.1. Here it is seen that the presented star sensor is small and light, and has an greatly increased operating range.

### 3.2.4 Measurement noise

As stated above the chosen star sensor has an accuracy of 1 arcsecond around all axis. Arcseconds is a alternative measure of angles and one arcsecond is equivalent to 0.000278 degrees. Since the sensor model produces the attitude as a quaternion, it is convenient to represent the accuracy in the magnitude of the quaternion. By regarding the individual axis angles accuracies as an composite rotation, the accuracies may be represented as the unit quaternion,  $\mathbf{q}_n$ , by applying algorithm 2.2

**Table 3.1:** DTU Star sensor main technical data

Property	Value
Dimension:	10x10x4,5 cm
Mass:	400 gr
Accuracy:	1 arcsec
Attitude rate	up to 10 deg/sec
Reliability	99.999%
Update rate:	8 Hz

(Fossen 2002) as

$$\Theta_a = \begin{bmatrix} \phi_a \\ \theta_a \\ \psi_a \end{bmatrix} = \begin{bmatrix} 0.000278 \\ 0.000278 \\ 0.000278 \end{bmatrix} \xrightarrow{\text{Alg.2.2}} \mathbf{q}_a \approx \begin{bmatrix} 1 \\ 2.4 \cdot 10^{-6} \\ 2.4 \cdot 10^{-6} \\ 2.4 \cdot 10^{-6} \end{bmatrix} \quad (3.4)$$

By using the result of (3.4), the star sensor measurement noise may now be modeled as

$$\mathbf{q}_n = \begin{bmatrix} \sqrt{1 - \|\boldsymbol{\epsilon}_n\|^2} \\ \boldsymbol{\epsilon}_n \end{bmatrix} \quad (3.5)$$

where  $\boldsymbol{\epsilon}_n$  is represented by Gaussian white noise with the properties

$$\mathbf{E}[\boldsymbol{\epsilon}_{n,i}^2] = \sigma_{\boldsymbol{\epsilon}_{n,i}}^2, \quad \text{for } i = 1, 2, 3 \quad (3.6)$$

where

$$\sigma_{\boldsymbol{\epsilon}_{n,i}} = 2.4 \cdot 10^{-6} \quad (3.7)$$

When using the measurement in attitude determination it is sometimes required that the measurement noise is modeled as additive. By representing (3.3) in the form of (3.2), the additive measurement noise,  $\mathbf{v}_{star}$ , may be represented as

$$\mathbf{v}_{star} = \mathbf{q} \otimes \mathbf{q}_n - \mathbf{q} \quad (3.8)$$

It is seen from the above equation that by representing the sensor model as (3.2), the measurement noise becomes scaled. By expanding (3.8), the noise model may be represented on component for as

$$\mathbf{v}_{star} = \begin{bmatrix} \eta\eta_n - \boldsymbol{\epsilon}^T \boldsymbol{\epsilon}_n - \eta \\ \eta\boldsymbol{\epsilon} + \eta_n\boldsymbol{\epsilon} + \mathbf{S}(\boldsymbol{\epsilon})\boldsymbol{\epsilon}_n - \boldsymbol{\epsilon} \end{bmatrix} \quad (3.9)$$

and the noise covariance may then be derived by

$$E[\mathbf{v}_{star}^2] = \sigma_{\mathbf{v}_{star}}^2 = \begin{bmatrix} \eta E[\eta_n^2] - \boldsymbol{\epsilon}^T E[\boldsymbol{\epsilon}_n^2] - \eta \\ \eta E[\boldsymbol{\epsilon}_n^2] + E[\eta_n^2]\boldsymbol{\epsilon} + \mathbf{S}(\boldsymbol{\epsilon})E[\boldsymbol{\epsilon}_n^2] - \boldsymbol{\epsilon} \end{bmatrix} \quad (3.10)$$

One may assuming that  $\eta_n = \sqrt{1 - \|\boldsymbol{\epsilon}_n\|^2} \simeq 1$ , which implies that  $E[\eta_n^2] \simeq 1$ , and (3.10) may now be reduced to

$$\sigma_{\mathbf{v}_{star}}^2 \simeq \begin{bmatrix} \boldsymbol{\epsilon}^T E[\boldsymbol{\epsilon}_n^2] \\ \eta E[\boldsymbol{\epsilon}_n^2] + \mathbf{S}(\boldsymbol{\epsilon})E[\boldsymbol{\epsilon}_n^2] \end{bmatrix} \quad (3.11)$$

### 3.3 Sun Sensor

The Sun provides an reference when the satellite is in line of view of it. The Sun's visibility from the satellite is dependent on orbit, and in occurrence of eclipse, the reference availability ceases.

#### 3.3.1 Sensor model

In principle the Sun sensor is a measurement of the Sun's relative position with respect to the satellite's body frame. This position, expressed as a direction by a vector, is called the Sun vector measurement, and may be modeled as

$$\mathbf{s}^b = \mathbf{R}_o^b \mathbf{s}_{ref}^o + \mathbf{v}_{sun} \quad (3.12)$$

where  $\mathbf{R}_o^b$  is the actual rotation matrix,  $\mathbf{v}_{sun} = [v_{sun,1} \ v_{sun,2} \ v_{sun,3}]^T$  is the measurement noise, and  $\mathbf{s}_{ref}^o$  is the sun vector reference produced by (3.17).

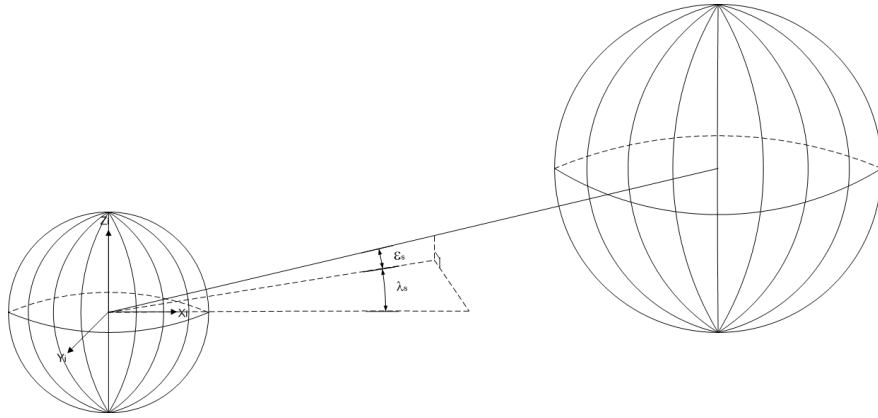


**Figure 3.1:** Sun position relative to the Earth

#### 3.3.2 Sun reference model

In order to utilize the Sun vector measurement, knowledge of the Sun's position relative to the satellite's orbital position is needed for comparison. The reference model presented in this section is based on the work done by Svartveit (2003). Here a model simplification is presented by describing the Sun-Earth related motion as seen from the Earth, i.e. the Sun revolves around the Earth as the Earth revolves around the Sun, illustrated in 3.1. The elevation of the Sun,  $\varepsilon_s$ , varies periodically through a year and is given by

$$\varepsilon_s = \frac{23\pi}{180} \sin\left(\frac{T_s}{365} 2\pi\right) \quad (3.13)$$

where  $T_s$  is the time given in days, since the first day of spring. By a period of 365 days the Sun's orbit around the Earth is given by

$$\lambda_s = \frac{T_s}{365} 2\pi \quad (3.14)$$

where  $\lambda_s$  is called the Sun's orbit parameter. The Sun's position at a given time relative to the ECI frame can now be expressed as

$$\mathbf{s}_{ref}^i = \mathbf{R}_y(\varepsilon_s)\mathbf{R}_z(\lambda_s)\mathbf{s}_0^i \quad (3.15)$$

where

$$\mathbf{s}_0^i = [1 \ 0 \ 0]^T \quad (3.16)$$

is the Sun's position when the Earth passes vernal equinox,  $\mathbf{R}_y$  and  $\mathbf{R}_z$  are the simple rotations given by (2.8) and (2.9). By using the result of (3.15) and (2.27) the Sun's position relative to the satellite is given by

$$\mathbf{s}_{ref}^o = \mathbf{R}_i^o \mathbf{s}_{ref}^i \quad (3.17)$$

Because much of the light detected by the Sun sensor is the Earth albedo, i.e. Sun light reflected from the Earth's surface, a correction of the sun sensor measurement is needed before further use. The albedo light changes due to the varying reflectivity of the Earth's surface, the satellite's position and the Sun's position. Because of the usual limited on-board computation power and memory space on small satellites, it is convenient to model the albedo as a polynomial function. This model has proven to yield good results in attitude determination (Appel 2004). The albedo effect on the sun vector measurement may also be compensated for by using certain sensor hardware, as explained in the next section.

### 3.3.3 Hardware

There exist numerous ways of measuring the sun vector. A common property is that they have medium/high accuracy, wide field of view, high reliability, radiation tolerance, small size, and low mass, all of which are important for use in ADCS of small satellites. Depending on the mission requirements a number of different types of sun sensors may be used. They range from coarse sun sensors such as the Sun acquisition sensor(SAS) and attitude anomaly detector(AAD), further to the analog fine sun sensor such as the quadrant sun sensor(QSS), and finally to the digital fine sun sensor(DSS).

A DSS has limited field of view, FOV, but is not affected by the Earth albedo unless the Earth is adjacent to the sun spot (Boldrini and Monnini 2001). Due to these properties and the strict attitude determination requirement, the DSS is chosen as the Sun sensor in which the model (3.12) is based on. There are numerous manufacturers of a DSS, but the sensor presented by Boldrini et.al. (2001) is chosen as reference, and its main technical data is given in table 3.2.

### 3.3.4 Measurement noise

As seen from table 3.2 the accuracy of the sun sensor is  $0.02^\circ$  for all axes. The measurement noise may be represented by incorporating the sensor error into the rotation matrix in (3.12). As with the star sensor, the sensor's individual angle errors can be combined to represent a composite rotation  $\mathbf{R}_e(\eta_{sn}, \boldsymbol{\epsilon}_{sn})$  by using

$$\mathbf{q}_{sn} = \begin{bmatrix} \sqrt{1 - \|\boldsymbol{\epsilon}_{sn}\|^2} \\ \boldsymbol{\epsilon}_{sn} \end{bmatrix} \quad (3.18)$$

---

<sup>1</sup>10 Hz in sun acquisition mode and up to 100 Hz in sun tracking mode

**Table 3.2:** DSS main technical data

Property	Value
Dimension:	110x110x50 mm
Mass:	0.425 kg
FOV:	128x128°
Accuracy:	<0.02°
Resolution:	<0.005°
Update rate:	10/100 Hz <sup>1</sup>

The sensor model now becomes

$$\mathbf{s}^b = \mathbf{R}_e(\eta, -\epsilon)\mathbf{R}_e(\eta_{sn}, -\epsilon_{sn})\mathbf{s}_{ref}^o \quad (3.19)$$

, and by comparing (3.19) and (3.12), the noise may be represented as additive by

$$\mathbf{v}_{sun} = (\mathbf{R}_e(\eta, -\epsilon)\mathbf{R}_e(\eta_{sn}, -\epsilon_{sn}) - \mathbf{R}_e(\eta, -\epsilon))\mathbf{s}_{ref}^o = \mathbf{R}_e(\eta, -\epsilon)(\mathbf{R}_e(\eta_{sn}, -\epsilon_{sn}) - \mathbf{I})\mathbf{s}_{ref}^o \quad (3.20)$$

By substituting (2.22) into (3.20), it is reduced to

$$\begin{aligned} \mathbf{v}_{sun} &= \mathbf{R}_e(\eta, -\epsilon)(2\eta_{sn}\mathbf{S}(-\epsilon_{sn}) + 2\mathbf{S}(-\epsilon_{sn})\mathbf{S}(-\epsilon_{sn}))\mathbf{s}_{ref}^o \\ &= \mathbf{R}_e(\eta, -\epsilon)(2\mathbf{S}(\epsilon_{sn})\mathbf{S}(\epsilon_{sn}) - 2\eta_{sn}\mathbf{S}(\epsilon_{sn}))\mathbf{s}_{ref}^o \end{aligned} \quad (3.21)$$

The covariance of the measurement matrix may now be determined by

$$\mathbf{E}[v_{sun}^2] = \mathbf{R}_e(\eta, -\epsilon)(2\mathbf{S}(\mathbf{E}[\epsilon_{sn}^2])\mathbf{S}(\mathbf{E}[\epsilon_{sn}^2]) - 2\mathbf{E}[\eta_{sn}^2]\mathbf{S}(\mathbf{E}[\epsilon_{sn}^2]))\mathbf{s}_{ref}^o \quad (3.22)$$

Because the sensor error is represented as an unit quaternion one may assume that the  $\eta_{sn} \simeq 1$ , which further implies that  $\mathbf{E}[\eta_{sn}^2] \simeq 1$ . Equation (3.22) can now be reduced to

$$\mathbf{E}[v_{sun}^2] \simeq \mathbf{R}_e(\eta, -\epsilon)(2\mathbf{S}(\mathbf{E}[\epsilon_{sn}^2])\mathbf{S}(\mathbf{E}[\epsilon_{sn}^2]) - 2\mathbf{S}(\mathbf{E}[\epsilon_{sn}^2]))\mathbf{s}_{ref}^o \quad (3.23)$$

where

$$\mathbf{E}[\epsilon_{sn}^2] = 1.7450 \cdot 10^{-4} \cdot \mathbf{I}_{3 \times 3} \quad (3.24)$$

is the covariance of the noise quaternion  $\mathbf{q}_{sn}$ , generated by Gaussian white noise.

### 3.4 Earth Sensor

The Earth is always visible for satellites orbiting it, and with the knowledge of the orbit, a reference may be acquired anywhere.

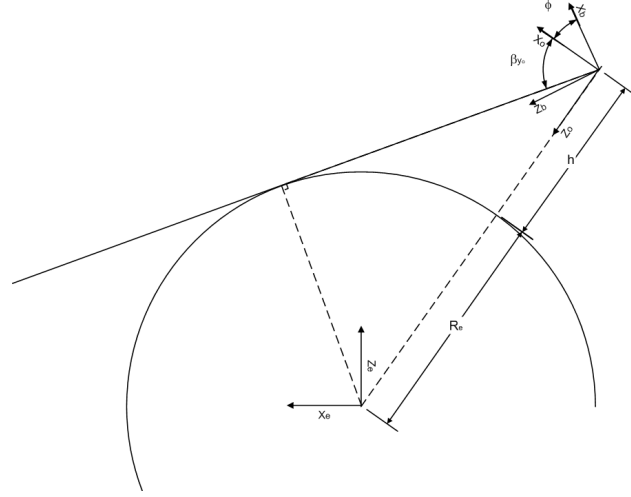


**Figure 3.2:** Satellite's orbit and body frame relative to the Earth

### 3.4.1 Sensor model

An Earth sensor, or horizon scanners as they are also known as, determines the Earth's position relative to the satellite. Because of the approximated circular shape of the Earth, only the roll and pitch part of the Euler angles can be determined from the measurements. A model of the sensor can take the form

$$\mathbf{y}_e = \begin{bmatrix} \phi_e \\ \theta_e \end{bmatrix} = \begin{bmatrix} \phi \\ \theta \end{bmatrix} + \begin{bmatrix} \beta_{x_o} \\ \beta_{y_o} \end{bmatrix} + \mathbf{v}_e \quad (3.25)$$

where  $\phi$  and  $\theta$  are the true roll and pitch attitude of the satellite,  $\beta_{x_o}$  and  $\beta_{y_o}$  are the roll and pitch attitude between the Earth's horizon and the orbit frame, and  $\mathbf{v}_e$  is the measurement noise.

### 3.4.2 Earth reference model

Figure 3.2 shows the  $xz$ -cross-section of the relative positions of the Earth, orbit frame, and body frame. The figure applies also to the  $yz$ -plane, and under the assumption of a circular Earth, the relative roll and pitch angle between the orbit frame and the Earth's horizon is constant, and be determined by

$$\beta_{x_o} = \beta_{y_o} = 90^\circ - \sin^{-1}\left(\frac{R_e}{R_e + h}\right) \quad (3.26)$$

where  $R_e$  is the Earth's radius and  $h$  is the satellite's orbit altitude. When (3.26) is subtracted from (3.25), the resulting sensor measurement becomes comparable with the roll and pitch attitude of the satellite.

### 3.4.3 Hardware

Most Earth sensors determine the horizon angles,  $\phi_e$  and  $\theta_e$ , by using the infrared domain to detect the Earth/space transition. EADS Sodern delivers digital optronic sensors with accuracies in the  $0.03^\circ$  region, and output data rates of about 1Hz. Goodrich provides two sensors, where one is similar

to EADS's and the other is an analog version. The analog sensor has poorer accuracies but the measurements may be sampled at any chosen rate. Due to this property the analog sensor, model 13-470-RH, is chosen to represent the horizon sensor, and its main features are given in table 3.3.

**Table 3.3:** 13-470-RH main data

Property	Value
Dimension:	19 cm in diameter, 12.2 cm deep
Mass:	0.190 kg
Operating range:	$\pm 10^\circ$ around nadir
Accuracy:	$< 0.2^\circ$

#### 3.4.4 Measurement noise

The chosen horizon sensor has an accuracy of  $0.2^\circ$ , which corresponds to 0.0035 rad. Since the sensor measurement is also represented in Euler angles the measurement noise may be represented by Gaussian white noise with the property

$$\mathbf{E}[v_{e,i}^2] = \sigma_{v_{e,i}}^2, \quad \text{for } i = 1, 2 \quad (3.27)$$

where

$$\sigma_{v_{e,i}} = 0.0035 \quad (3.28)$$

# Chapter 4

## Satellite attitude

This section presents the deduction of the satellite's mathematical model. It is derived by using the model presented by Kyrkjebø (2000) and extending it to include reaction wheel dynamics (Goeree and Chatel 1999) and (Wiger 2003). The model is the basis for both the Kalman Filter and the nonlinear observer, and is essential in accurately determining the attitude.

### 4.1 Dynamic equation of motion

#### 4.1.1 kinetic equations

Derived from elementary mechanics, the satellite's inital kinetic equations of motion is given in body frame by

$$\dot{\boldsymbol{\omega}}_{ib}^b = (\mathbf{I}^b)^{-1}[-\mathbf{S}(\boldsymbol{\omega}_{ib}^b)\mathbf{I}^b\boldsymbol{\omega}_{ib}^b + \boldsymbol{\tau}^b + \mathbf{g}^b] \quad (4.1)$$

where  $\mathbf{I}^b$  is the satellite's inertia given in the body frame,  $\boldsymbol{\omega}_{ib}^b = [\omega_{ib,x}^b \ \omega_{ib,y}^b \ \omega_{ib,z}^b]^T$  is the angular velocity of the body frame relativ to the ECI frame given in body frame,  $\boldsymbol{\tau}^b$  is the control torque, and  $\mathbf{g}^b$  is the gravitation force acting on the satellite.

The control torques,  $\boldsymbol{\tau}^b$ , are generate by the reaction wheels placed in a tetrahedron structure, (Wiger 2003). The resulting torques are given by

$$\boldsymbol{\tau}^b = -\mathbf{S}(\boldsymbol{\omega}_{ib}^b)\mathbf{A}\mathbf{I}_w(\boldsymbol{\omega}_w + \mathbf{A}^T\boldsymbol{\omega}_{ib}^b) \quad (4.2)$$

$$\dot{\boldsymbol{\omega}}_w = (\mathbf{I}_w)^{-1}\boldsymbol{\tau}_w - \mathbf{A}^T\dot{\boldsymbol{\omega}}_{ib}^b \quad (4.3)$$

where  $\boldsymbol{\omega}_w = [\omega_{w,1} \ \omega_{w,2} \ \omega_{w,3} \ \omega_{w,4}]^T$  are the angular rates of the individual wheels,  $\boldsymbol{\tau}_w$  is the control input,  $\mathbf{A}$  is the reaction wheels configuration matrix defined as

$$\mathbf{A} = [\mathbf{t}_1 \ \mathbf{t}_2 \ \mathbf{t}_3 \ \mathbf{t}_4] = \{a_{ji}\}, \ j = 1, \dots, 3, \ i = 1, \dots, 4 \quad (4.4)$$

, and  $\mathbf{I}_w$  is the diagonal matrix containing the inertias of the reaction wheels about their spin axes on its diagonal given by

$$\mathbf{I}_w = \begin{bmatrix} i_1 & 0 & 0 & 0 \\ 0 & i_2 & 0 & 0 \\ 0 & 0 & i_3 & 0 \\ 0 & 0 & 0 & i_4 \end{bmatrix} \quad (4.5)$$

It is desirable to express the model in reference to the orbit frame in stead of the ECI frame. This is done using the known relation between the body-orbit and the body-ECI angular velocities as

$$\boldsymbol{\omega}_{ib}^b = \boldsymbol{\omega}_{io}^b + \boldsymbol{\omega}_{ob}^b = \mathbf{R}_o^b \boldsymbol{\omega}_{io}^o + \boldsymbol{\omega}_{ob}^b \quad (4.6)$$

where  $\mathbf{R}_o^b$  is the rotation matrix from orbit to body frame as defined in (2.28),  $\boldsymbol{\omega}_{ob}^b = [\omega_{ob,x}^b \ \omega_{ob,y}^b \ \omega_{ob,z}^b]^T$  is the angular velocity of the body frame relative to the orbit frame given in body frame, and  $\boldsymbol{\omega}_{io}^o$  is the constant rotation of the orbit frame relative to the ECI-frame given by

$$\boldsymbol{\omega}_{io}^o = [0 \ -\omega_o \ 0]^T \quad (4.7)$$

where  $\omega_o$  is defined by (2.26).

By using (4.6) and the rotation matrix property (2.13), the derivative of the angular velocity vector relative to the orbit frame may be derived by

$$\dot{\boldsymbol{\omega}}_{ib}^b = \frac{\delta}{\delta t} (\mathbf{R}_o^b \boldsymbol{\omega}_{io}^o + \boldsymbol{\omega}_{ob}^b) = \dot{\mathbf{R}}_o^b \boldsymbol{\omega}_{io}^o + \dot{\boldsymbol{\omega}}_{ob}^b = \dot{\boldsymbol{\omega}}_{ob}^b - \mathbf{R}_o^b \mathbf{S}(\boldsymbol{\omega}_{ob}^b) \boldsymbol{\omega}_{io}^o \quad (4.8)$$

The gravitation torque,  $\mathbf{g}^b$ , acting on the satellite due to the gravitational field of the planets, the Moon and the Sun is modeled as

$$\mathbf{g}^b = 3\omega_o^2 \mathbf{c}_3 \times \mathbf{I}^b \mathbf{c}_3 \quad (4.9)$$

where  $\mathbf{c}_3$  is the direct cosine defined in (2.28).

### 4.1.2 Kinematic equations

The attitude motion of the satellite is described as

$$\dot{\boldsymbol{\epsilon}} = \frac{1}{2} [\eta \mathbf{I} + \mathbf{S}(\boldsymbol{\epsilon})] \boldsymbol{\omega}_{ob}^b \quad (4.10)$$

$$\dot{\eta} = -\frac{1}{2} \boldsymbol{\epsilon}^T \boldsymbol{\omega}_{ob}^b \quad (4.11)$$

## 4.2 State space models

### 4.2.1 Nonlinear

By choosing the state vector as

$$\mathbf{x}_a = [\mathbf{q} \ \boldsymbol{\omega}_{ob}^b \ \boldsymbol{\omega}_w]^T \quad (4.12)$$

where  $a$  denotes the use of all the states. By substituting (4.6) and (4.8) into (4.1)-(4.3), the nonlinear state space model becomes

$$\dot{\mathbf{x}}_a = \begin{bmatrix} \dot{\eta} \\ \dot{\boldsymbol{\epsilon}} \\ \dot{\boldsymbol{\omega}}_{ob}^b \\ \dot{\boldsymbol{\omega}}_w \end{bmatrix} = \mathbf{f}(\mathbf{x}_a, \boldsymbol{\tau}_w, t) + \mathbf{E}w \quad (4.13)$$

where  $\mathbf{w}$  is the process noise,  $\mathbf{E}$  is the process noise matrix, and  $\mathbf{f}(\mathbf{x}_a, \boldsymbol{\tau}_w, t)$  is defined as

$$\mathbf{f}(\mathbf{x}_a, \boldsymbol{\tau}_w, t) = \begin{bmatrix} \frac{1}{2}\boldsymbol{\epsilon}^T\boldsymbol{\omega}_{ob}^b \\ \frac{1}{2}[\eta\mathbf{I} + \mathbf{S}(\boldsymbol{\epsilon})]\boldsymbol{\omega}_{ob}^b \\ \mathbf{f}_{inert} + \mathbf{f}_{addinert} + \mathbf{f}_{rot} + \mathbf{f}_w + \mathbf{f}_{ext} \\ \tilde{\mathbf{f}}_{inert} + \tilde{\mathbf{f}}_{addinert} + \tilde{\mathbf{f}}_{rot} + \tilde{\mathbf{f}}_w \end{bmatrix} \quad (4.14)$$

where

$$\mathbf{f}_{inert} = -(\mathbf{I}^b)^{-1}[-\mathbf{S}(\boldsymbol{\omega}_{ob}^b + \mathbf{R}_o^b\boldsymbol{\omega}_{io}^o)(\mathbf{I}^b)^{-1}(\boldsymbol{\omega}_{ob}^b + \mathbf{R}_o^b\boldsymbol{\omega}_{io}^o)] \quad (4.15a)$$

$$\mathbf{f}_{addinert} = -(\mathbf{I}^b)^{-1}[-\mathbf{S}(\boldsymbol{\omega}_{ob}^b + \mathbf{R}_o^b\boldsymbol{\omega}_{io}^o)(\mathbf{A}\mathbf{I}_w)^{-1}(\boldsymbol{\omega}_w + \mathbf{A}^T(\boldsymbol{\omega}_{ob}^b + \mathbf{R}_o^b\boldsymbol{\omega}_{io}^o))] \quad (4.15b)$$

$$\mathbf{f}_{rot} = \mathbf{S}(\boldsymbol{\omega}_{ob}^b)\mathbf{R}_o^b\boldsymbol{\omega}_{io}^o \quad (4.15c)$$

$$\mathbf{f}_w = -(\mathbf{I}^b)^{-1}\mathbf{A}\boldsymbol{\tau}_w \quad (4.15d)$$

$$\mathbf{f}_{ext} = (\mathbf{I}^b)^{-1}\mathbf{g}^b \quad (4.15e)$$

$$\tilde{\mathbf{f}}_{inert} = -\mathbf{A}^T\mathbf{f}_{inert} \quad (4.15f)$$

$$\tilde{\mathbf{f}}_{addinert} = -\mathbf{A}^T\mathbf{f}_{addinert} \quad (4.15g)$$

$$\tilde{\mathbf{f}}_{rot} = -\mathbf{A}^T\mathbf{f}_{rot} \quad (4.15h)$$

$$\tilde{\mathbf{f}}_w = -(\mathbf{I}_w)^{-1}\boldsymbol{\tau}_w \quad (4.15i)$$

$$(4.15j)$$

### 4.2.2 Linearized

A linearization of the satellite's model is needed in calculating the Kalman gains, section 5.2.1. The states that are to be determined are the  $\mathbf{q}$  and  $\boldsymbol{\omega}_{ob}^b$ , and corresponding dynamics is reduced by removing the  $\dot{\boldsymbol{\omega}}_w$  from (4.13). The new state vector is now

$$\mathbf{x} = [\mathbf{q} \quad \boldsymbol{\omega}_{ob}^b]^T \quad (4.16)$$

and the new state space model becomes where  $\mathbf{f}(\mathbf{x}_a, \boldsymbol{\tau}_w, t)$  is defined as

$$\dot{\mathbf{x}} = \mathbf{f}(\mathbf{x}, \boldsymbol{\tau}_w, \boldsymbol{\omega}_w, t) = \begin{bmatrix} \frac{1}{2}\boldsymbol{\epsilon}^T\boldsymbol{\omega}_{ob}^b \\ \frac{1}{2}[\eta\mathbf{I} + \mathbf{S}(\boldsymbol{\epsilon})]\boldsymbol{\omega}_{ob}^b \\ \mathbf{f}_{inert} + \mathbf{f}_{addinert} + \mathbf{f}_{rot} + \mathbf{f}_w + \mathbf{f}_{ext} \end{bmatrix} \quad (4.17)$$

where the angular rates of the reaction wheels,  $\boldsymbol{\omega}_w$ , are assumed known and now treated as a constant.

The linearization converts the system (4.17) to the form

$$\Delta\dot{\mathbf{x}} = \mathbf{F}\Delta\mathbf{x} + \mathbf{B}\Delta\boldsymbol{\tau}_w \quad (4.18)$$

where  $\mathbf{F}$  is the differentiation of (4.17) with respect to  $\mathbf{x}$ , and  $\mathbf{B}$  is with respect to the input  $\boldsymbol{\tau}_w$  as

$$\mathbf{F} = \frac{\delta\mathbf{f}(\mathbf{x}, \boldsymbol{\tau}_w, \boldsymbol{\omega}_w, t)}{\delta\mathbf{x}}, \quad \mathbf{B} = \frac{\delta\mathbf{f}(\mathbf{x}, \boldsymbol{\tau}_w, \boldsymbol{\omega}_w, t)}{\delta\boldsymbol{\tau}_w} \quad (4.19)$$

As a simplification of the linearization process, the nonlinear function  $\mathbf{f}(\mathbf{x}, \boldsymbol{\tau}, \boldsymbol{\omega}_w, t)$  can be divided into two parts; an attitude part consisting of the Euler parameters and a angular velocity part. By performing this partition the derived linear system matrix,  $\mathbf{F}$ , can now be separated in the same manner by

$$\mathbf{F} = \begin{bmatrix} \mathbf{F}_{att} \\ \mathbf{F}_{vel} \end{bmatrix} = \begin{bmatrix} \frac{\delta \dot{\mathbf{q}}}{\delta x_1} & \cdots & \frac{\delta \dot{\mathbf{q}}}{\delta x_7} \\ \frac{\dot{\boldsymbol{\omega}}_{ob}^b}{\delta x_1} & \cdots & \frac{\dot{\boldsymbol{\omega}}_{ob}^b}{\delta x_7} \end{bmatrix} \quad (4.20)$$

The linearized attitude part becomes (Kyrkjebø 2000)

$$\mathbf{F}_{att} = \begin{bmatrix} 0 & -\frac{1}{2}(\boldsymbol{\omega}_{ob}^b) & -\frac{1}{2}\boldsymbol{\epsilon}^T \\ \frac{1}{2}\boldsymbol{\omega}_{ob}^b & -\frac{1}{2}\mathbf{S}(\boldsymbol{\omega}_{ob}^b) & \frac{1}{2}[\eta\mathbf{I} + \mathbf{S}(\boldsymbol{\epsilon})] \end{bmatrix} \quad (4.21)$$

Before linearizing the angular velocity part, it is convenient to express the dynamics in component form. As presented above the angular velocity of the satellites is expressed by

$$\boldsymbol{\omega}_{ob}^b = \mathbf{f}_{inert} + \mathbf{f}_{addinert} + \mathbf{f}_{rot} + \mathbf{f}_w + \mathbf{f}_{ext} \quad (4.22)$$

where each part of (4.22) can be expressed in components as presented following. The effect of the satellites own inertia can now be expressed as

$$\mathbf{f}_{inert} = \begin{bmatrix} k_x(\omega_{ob,2}^b - c_{22}\omega_o)(\omega_{ob,3}^b - c_{32}\omega_o) \\ k_y(\omega_{ob,1}^b - c_{12}\omega_o)(\omega_{ob,3}^b - c_{32}\omega_o) \\ k_z(\omega_{ob,1}^b - c_{12}\omega_o)(\omega_{ob,2}^b - c_{22}\omega_o) \end{bmatrix} \quad (4.23)$$

where  $k_x = \frac{I_y - I_z}{I_x}$ ,  $k_y = \frac{I_x - I_z}{I_y}$ , and  $k_z = \frac{I_y - I_x}{I_z}$ , and the direction cosines,  $c_{ij}$ , for  $i = 1, \dots, 3$ ,  $j = 1, \dots, 3$ , are defined by (2.28). and

$$\mathbf{f}_{inertadd} = \begin{bmatrix} \frac{1}{I_x}(-e_2(\omega_{ob,3}^b - c_{32}\omega_o) + e_3(\omega_{ob,2}^b - c_{22}\omega_o)) \\ \frac{1}{I_y}(e_1(\omega_{ob,3}^b - c_{32}\omega_o) - e_3(\omega_{ob,1}^b - c_{12}\omega_o)) \\ \frac{1}{I_z}(-e_1(\omega_{ob,2}^b - c_{22}\omega_o) + e_2(\omega_{ob,1}^b - c_{12}\omega_o)) \end{bmatrix} \quad (4.24)$$

where

$$\mathbf{e}_j = i_w \sum_{i=1}^4 a_{ji}(\omega_{w,i} + \sum_{k=1}^3 (a_{ki}(\omega_{ob,k}^b - c_{k2}\omega_o))), \quad \text{for } j = 1, \dots, 3 \quad (4.25)$$

is the added inertia to the satellite due to the spinning reaction wheels. The added effect of expressing the attitude with regards to the orbit frame is

$$\mathbf{f}_{rot} = \begin{bmatrix} -\omega_{ob,3}^b(\omega_{ob,2}^b - c_{22}\omega_o) + \omega_{ob,2}^b(\omega_{ob,3}^b - c_{32}\omega_o) \\ \omega_{ob,3}^b(\omega_{ob,1}^b - c_{12}\omega_o) - \omega_{ob,1}^b(\omega_{ob,3}^b - c_{32}\omega_o) \\ -\omega_{ob,2}^b(\omega_{ob,1}^b - c_{12}\omega_o) + \omega_{ob,1}^b(\omega_{ob,2}^b - c_{22}\omega_o) \end{bmatrix} \quad (4.26)$$

and the gravitation effect is

$$\mathbf{f}_{ext} = 3\omega_o^2 \begin{bmatrix} k_x c_{23} c_{33} \\ k_y c_{13} c_{33} \\ k_z c_{13} c_{23} \end{bmatrix} \quad (4.27)$$

The satellites angular velocity model, (4.22), may now be differentiated with respect to the state vector, (4.16), as

$$\mathbf{F}_{vel} = \frac{\partial \mathbf{f}_{inert}}{\partial \mathbf{x}} + \frac{\partial \mathbf{f}_{inertadd}}{\partial \mathbf{x}} + \frac{\partial \mathbf{f}_{rot}}{\partial \mathbf{x}} + \frac{\partial \mathbf{f}_{ext}}{\partial \mathbf{x}} \quad (4.28)$$

where  $\frac{\partial \mathbf{f}_{inert}}{\partial \mathbf{x}}$ ,  $\frac{\partial \mathbf{f}_{rot}}{\partial \mathbf{x}}$ , and  $\frac{\partial \mathbf{f}_{ext}}{\partial \mathbf{x}}$  have been calculated by Kyrkjebø (2000). This leaves  $\frac{\partial \mathbf{f}_{inertadd}}{\partial \mathbf{x}}$  to be calculated as

$$\frac{\partial \mathbf{f}_{inertadd}}{\partial \mathbf{x}} = \begin{bmatrix} \frac{\partial \mathbf{f}_{inertadd,1}}{\partial \eta} & \dots & \frac{\partial \mathbf{f}_{inertadd,1}}{\partial \omega_{ob,3}^b} \\ \vdots & \ddots & \vdots \\ \frac{\partial \mathbf{f}_{inertadd,1}}{\partial \eta} & \dots & \frac{\partial \mathbf{f}_{inertadd,1}}{\partial \omega_{ob,3}^b} \end{bmatrix} \quad (4.29)$$

The computation of  $\frac{\partial \mathbf{f}_{inertadd}}{\partial \mathbf{x}}$  is performed in appendix C.1, and the linearized velocity matrix,  $\mathbf{F}_{vel}$ , now becomes

$$\mathbf{F}_{vel} = \begin{bmatrix} b_{51} & b_{52} & b_{53} & b_{54} & b_{55} & b_{56} & b_{57} \\ b_{61} & b_{62} & b_{63} & b_{64} & b_{65} & b_{66} & b_{67} \\ b_{71} & b_{72} & b_{73} & b_{74} & b_{75} & b_{76} & b_{77} \end{bmatrix} \quad (4.30)$$

where the components,  $a_{ij}$ , are defined in appendix C.2.

The Linearization of the system with respect to the input  $\boldsymbol{\tau}_w$  may also be separated as

$$\mathbf{B} = \begin{bmatrix} \mathbf{B}_{att} \\ \mathbf{B}_{vel} \end{bmatrix} \quad (4.31)$$

From (4.17), it is noted that the satellite's attitude part is independent on  $\boldsymbol{\tau}_w$ , and the corresponding linearization,  $\mathbf{B}_{att}$ , becomes zero. The attitude part is linearized as

$$\mathbf{B}_{vel} = \frac{\partial}{\partial \boldsymbol{\tau}_w} (\mathbf{f}_{inert} + \mathbf{f}_{addinert} + \mathbf{f}_{rot} + \mathbf{f}_w + \mathbf{f}_{ext}) = -(\mathbf{I}^b)^{-1} \mathbf{A} \quad (4.32)$$

### 4.3 Process noise

The process noise accounts for the differences between the above modeled satellite and the actual behavior of the satellite. It is assumed that the disturbances only acts on the  $\mathbf{q}$  and  $\boldsymbol{\omega}_{ob}^b$  part of the model and that they are uncorrelated and additive making

$$\mathbf{E} = \begin{bmatrix} \mathbf{I}_{7 \times 7} \\ \mathbf{0}_{4 \times 7} \end{bmatrix} \quad (4.33)$$

and

$$\mathbf{w} = [w_1 \ w_2 \ w_3 \ w_4 \ w_5 \ w_6 \ w_7]^T \quad (4.34)$$

where  $w_1$  thorough  $w_7$  are modeled as white Gaussian noise with the property

$$E[\mathbf{w}^2] = \mathbf{Q} \ , \ \mathbf{Q} = \mathbf{Q}^T > 0 \quad (4.35)$$

The process noise can be divided into input noise and parameter noise.

#### 4.3.1 Input noise

Input noise is defines as the disturbances that produces acting torques on the satellite, and the main factor is due to aerodynamic drag. Aerodynamic drag is caused by the residual atmosphere,

and is dependent on angular velocity. The individual elements of the disturbance may be assumed uncorrelated and modeled as white noise with covariance

$$\mathbf{Q}_{ad} = \text{diag}(\sigma_{\omega_{ib,x}^b}, \sigma_{\omega_{ib,y}^b}, \sigma_{\omega_{ib,z}^b}) \quad (4.36)$$

Bak (2000) suggested that the aerodynamic drag for a micro-satellite is in the magnitude range of  $10^{-8}$  to  $10^{-13}$  Nm.

### 4.3.2 Parameter noise

Despite the best efforts, the satellite parameters are usually only known to a certain degree. The main error component is the modeling error related to the moments of inertia, and these can be represent by introducing noise in (4.1). The noise cannot be directly modeled as Gaussian white noise, but as a rate noise by (Bak 2000)

$$\mathbf{Q}_i = \mathbf{G}_d \mathbf{Q}_s \mathbf{G}_d^T + \mathbf{G}_g \mathbf{Q}_s \mathbf{G}_g^T \quad (4.37)$$

where  $\mathbf{G}_d$  and  $\mathbf{G}_g$  are the noise input matrices defined as

$$\mathbf{G}_d = \text{diag}(\omega_{ob,y}^b \omega_{ob,z}^b, \omega_{ob,x}^b \omega_{ob,z}^b, \omega_{ob,x}^b \omega_{ob,y}^b) \quad (4.38)$$

$$\mathbf{G}_g = \text{diag}(-c_{23}c_{33}, -c_{13}c_{33}, -c_{13}c_{23}) \quad (4.39)$$

and  $\mathbf{Q}_s$  is covariance of the Gaussian white noise defined as

$$\mathbf{Q}_s = k_s \text{diag}(\Delta k_x^2, \Delta k_y^2, \Delta k_z^2) \quad (4.40)$$

with  $k_s$  as a tuning parameter.

### 4.3.3 Stabilizing noise

Truncation of the system by Taylor expansion may introduce errors if the system is highly nonlinear. There are no physical arguments for introducing stabilizing noise, but when using the truncated system in a Kalman filter it ensures proper filter behavior. Different scenarios may require different level of noise, and must therefor be determined empirical.

The accumulate noise model description is now given as

$$\mathbf{Q} = \begin{bmatrix} \mathbf{Q}_q & \mathbf{0}_{3 \times 3} \\ \mathbf{0}_{3 \times 3} & \mathbf{Q}_i + \mathbf{Q}_{ad} + \mathbf{Q}_\omega \end{bmatrix} \quad (4.41)$$

where  $\mathbf{Q}_q$  and  $\mathbf{Q}_\omega$  are the covariance of the stabilizing noise in the Euler parameters and angular velocity, respectively.

## 4.4 Position

The satellite's attitude is independent on its position, but the position is important in determining it. The reference sun vector is computed from knowledge of the ECI latitude and longitude position.

As presented in section 2.3, the ECI position of the satellite is represented as an rotation about the  $y_i$  axis, making the longitude position constant at zero. The position model is thus based on propagating the latitude position,  $\mu$ , which defines the rotation  $\mathbf{R}_i^o$ , rather than Keplerian equations. The presented model is sufficient for simulation purposes, and given by

$$\mathbf{r}^i = \mathbf{R}_{y,\mu} \mathbf{r}^p \quad (4.42)$$

where  $\mathbf{r}^p$  is defined as the distance from the center of the Earth to the satellite as

$$\mathbf{r}^p = [0 \ 0 \ R]^T \quad (4.43)$$

and the propagation of the latitude, as presented in section 2.3, is defined as

$$\mu = \beta_0 + \omega_o t \quad (4.44)$$

## 4.5 Attitude control

Attitude control is not essential for accurate attitude determination, but when performed it is necessary to include its effect on the satellite model as done above. Control design is not performed in detail and thus not optimum, but its performance is used to illustrate the attitude determinations effect on the control.

The satellite will be controlled active in azimuth, i.e. around the z-axis, and the control torque acting on the satellite is generated from the change in spin of the reaction wheels. The change in spin is driven by the control inputs  $\boldsymbol{\tau}_w$ . A simple PD controller is introduced as

$$\boldsymbol{\tau}_w = \mathbf{K}_p \mathbf{A}^\dagger \tilde{\Delta} \boldsymbol{\epsilon} + \mathbf{K}_d \mathbf{A}^\dagger \tilde{\Delta} \boldsymbol{\omega}_{ob}^b \quad (4.45)$$

where  $\tilde{\Delta} \boldsymbol{\epsilon}$  and  $\tilde{\Delta} \boldsymbol{\omega}_{ob}^b$  are the control errors, and  $^\dagger$  denotes the use of the pseudo inverse of  $\mathbf{A}$  defined as

$$\mathbf{A}^\dagger = \mathbf{A}^T (\mathbf{A} \mathbf{A}^T)^{-1} \quad (4.46)$$

For simplicity the reference trajectories are chosen to be zero attitude and zero angular velocity, s.t.  $\tilde{\Delta} \boldsymbol{\epsilon}$  and  $\tilde{\Delta} \boldsymbol{\omega}_{ob}^b$  are exchanged with  $\boldsymbol{\epsilon}$  and  $\boldsymbol{\omega}_{ob}^b$ .



## Chapter 5

# Attitude determination

The determination of the satellite's attitude may be considered as an optimal nonlinear estimation problem, and the extended kalman filter and the nonlinear observer may be considered as approximated solutions to this problem. The topic of this chapter are the approximations assumed and the following modifications to the two determinations schemes enabling them to produce the attitude from the sensor measurements.

### 5.1 Optimal nonlinear estimation

Although the optimal nonlinear estimation problem is well defined, its solution, which relies on infinite-dimensional description of probability density functions, can generally not be solved exactly (Huster 2003). Combined with the fact that the attitude determination algorithms using vector measurements are either underdetermined or overdetermined, most solutions to nonlinear estimation must be considered as approximations, achieved by choosing appropriate approximations for the particular problem. By considering the noise sources as being driven by white Gaussian noise and using the presented sensors, suboptimal solutions may be derived.

The solving of the optimal nonlinear estimation problem has been widely discussed in the literature. Stengel (1994) and Gelb (1974) provides an outline of the problem, while Jazwinski (1970) and Maybeck (1982) analyze the problem in greater detail.

### 5.2 Extended Kalman Filter

Since it was introduced by Kalman (1960), the Kalman filter has become a standard design tool for estimation. Its popularity comes from its flexible approach that can generate good solutions to a wide range of estimation problems. For linear problems with white Gaussian noise sources, it generates an optimal solution. For nonlinear problems, many modifications to the Kalman filter have been developed to generate good, sub-optimal solutions. One such modification is the extended kalman filter (EKF) (Schmidt 1970), which constructs a linear system that approximates the nonlinear system near the current best estimate. It must be noted that with the EKF, no guarantees for optimality or even convergence can be stated as with the Kalman filter. However, countless nonlinear problems have been solved successfully with the EKF approach.

### 5.2.1 Filter theory

The Kalman filter and its extension, the EKF, have been described in countless textbooks, including (Gelb 1974), (Kailath, Sayed, and Hassibi 2000), (Stengel 1994), and (Farrell and Barth 1998). Before presenting the EKF equations, the discrete implementation of the satellite model must be derived. The conversion can be done by introducing fictitious samplers and holding devices into the continuous-time model, and the error introduced by discretization may be made discarded by using sufficiently small sampling period. Based on continuous system discretization theory, (Chen 1999), the model may be expressed as

$$\mathbf{x}_{k+1} = \Phi_k \mathbf{x}_k + \Gamma_k \boldsymbol{\tau}_{w,k} + \mathbf{E}_k \mathbf{w}_k \quad (5.1a)$$

$$\mathbf{y}_k = \mathbf{H}_k \mathbf{x}_k + \mathbf{v}_k \quad (5.1b)$$

where  $k$  denotes the sample step,  $\mathbf{w}_k = [w_{1,k} \ w_{2,k} \ w_{3,k} \ w_{4,k} \ w_{5,k} \ w_{6,k} \ w_{7,k}]^T$  is the discrete process noise,  $\mathbf{v}_k$  is the discrete measurement noise, and  $\mathbf{E}_k$  is the discrete process noise matrix defined as

$$\mathbf{E}_k = \mathbf{E} \Delta t \quad (5.2)$$

$\Phi_k$  is the state matrix exponential defined as

$$\Phi_k = e^{\mathbf{F}_k \Delta t} = \sum_{k=0}^{\infty} \frac{\mathbf{F}_k^k \Delta t^k}{k!} \quad (5.3)$$

where  $\Delta t$  is the step size and  $\mathbf{F}_k$  is the linearized system matrix, (4.20), at step  $k$ , and  $\Gamma_k$  is the input matrix defined as

$$\Gamma_k = (e^{\mathbf{F}_k \Delta t} - \mathbf{I}) \mathbf{F}_k^{-1} \mathbf{B}_k \quad (5.4)$$

under the assumption of nonsingular  $\mathbf{F}_k$ . The two expressions, (5.3) and (5.4), are approximated by using the first three elements in the series, as

$$\Phi_k \simeq \mathbf{I} + \mathbf{F}_k \Delta t + \frac{1}{2} \mathbf{F}_k^2 \Delta t^2 \quad (5.5)$$

$$\Gamma_k \simeq (\mathbf{I} \Delta t + \frac{1}{2} \mathbf{F}_k \Delta t^2) \mathbf{B}_k \quad (5.6)$$

The design of the extended Kalman filter is based on the above presented satellite model. The model is used in the filter to obtain an overview of the measurement to state interactions, and to predict future outputs. The EKF algorithm for system (4.17) is defined as

$$\mathbf{K}_k = \bar{\mathbf{P}}_k \mathbf{H}_k^T [\mathbf{H}_k \bar{\mathbf{P}}_k \mathbf{H}_k^T + \mathbf{R}_k]^{-1} \quad (5.7a)$$

$$\hat{\mathbf{x}}_k = \bar{\mathbf{x}}_k + \mathbf{K}_k [\mathbf{y}_k - \mathbf{H}_k \bar{\mathbf{x}}_k] \quad (5.7b)$$

$$\hat{\mathbf{P}}_k = [\mathbf{I} - \mathbf{K}_k \mathbf{H}_k] \bar{\mathbf{P}}_k [\mathbf{I} - \mathbf{K}_k \mathbf{H}_k]^T + \mathbf{K}_k \mathbf{R}_k \mathbf{K}_k^T \quad (5.7c)$$

$$\bar{\mathbf{x}}_{k+1} = \hat{\Phi}_k \hat{\mathbf{x}}_k + \Gamma_k \boldsymbol{\tau}_{w,k} \quad (5.7d)$$

$$\bar{\mathbf{P}}_{k+1} = \hat{\Phi}_k \hat{\mathbf{P}}_k \hat{\Phi}_k^T + \mathbf{E}_k \mathbf{Q}_k \mathbf{E}_k^T \quad (5.7e)$$

where (5.7a) is the calculation of the kalman gain matrix, (5.7b) is the state estimate update, (5.7c) is the error covariance update, (5.7d) the state estimation propagation, and (5.7e) is the error covariance propagation.  $\mathbf{R}_k$  and  $\mathbf{Q}_k$  are design matrices describing the expected covariance

of the measurement noise,  $\mathbf{v}_k$ , and the process noise,  $\mathbf{w}_k$ .  $\hat{\Phi}_k$  is determined by deriving  $\mathbf{F}_k$  with the estimated states.

It is convenient to rewrite (5.7b) into an innovation process and a pure state estimate update as

$$\boldsymbol{\nu}_k = \mathbf{y}_{m,k}^b - \mathbf{H}_k \bar{\mathbf{x}}_k \quad (5.8)$$

$$\hat{\mathbf{x}}_k = \bar{\mathbf{x}}_k + \mathbf{K}_k \boldsymbol{\nu}_k \quad (5.9)$$

where (5.8) is the innovation process and (5.9) is the state estimate update.

### Euler parameters in filter

When employing unit quaternion in representing the attitude it is crucial to maintain the constraint on the quaternion norm. This suggests the use of a quaternion normalization algorithm (Bar-Itzhack, Markley and Deutchmann 1991). The quaternion part of the state estimation update and the state estimation propagation must be normalized in order to maintain the physical content of the unit quaternion. The normalization in the state estimation propagation can be done as

$$\bar{\mathbf{q}}_{k+1} = \frac{\bar{\mathbf{q}}_{k+1}}{\|\bar{\mathbf{q}}_{k+1}\|} \quad (5.10)$$

Due to numerical round offs, the introduction of (5.10) leads to difficulties in maintaining a singular covariance matrix,  $\mathbf{P}_k$ , (Lefferts et.al. 1982). The solution is to reduce the dimension of  $\mathbf{P}_k$  by one, and is done by removing  $\eta$  from the state vector, (4.16). The corresponding design model now becomes

$$\mathbf{x}_{r,k+1} = \begin{bmatrix} \boldsymbol{\epsilon}_{k+1} \\ \boldsymbol{\omega}_{ob,k+1}^b \end{bmatrix} = \Phi_{r,k} \mathbf{x}_{r,k} + \Gamma_{r,k} \boldsymbol{\tau}_{w,k} + \mathbf{E}_{r,k} \mathbf{w}_{r,k} \quad (5.11a)$$

$$\mathbf{y}_{r,k} = \mathbf{H}_{r,k} \mathbf{x}_{r,k} + \mathbf{v}_{r,k} \quad (5.11b)$$

where  $r$  denotes the use of the reduced state vector.  $\Phi_{r,k}$  and  $\Gamma_{r,k}$  are now defined as

$$\Phi_{r,k} \simeq \mathbf{I} + \mathbf{F}_{r,k} \Delta t + \frac{1}{2} \mathbf{F}_{r,k}^2 \Delta t^2 \quad (5.12)$$

$$\Gamma_{r,k} \simeq (\mathbf{I} \Delta t + \frac{1}{2} \mathbf{F}_{r,k} \Delta t^2) \mathbf{B}_{r,k} \quad (5.13)$$

and  $\mathbf{F}_{r,k}$  and  $\mathbf{B}_{r,k}$  are the reduced linearized state and input matrices at step  $k$ , determined by

$$\mathbf{F}_{r,k} = \left. \frac{\delta \mathbf{f}_r(\mathbf{x}_r, \boldsymbol{\tau}_{w,k}, \boldsymbol{\omega}_{w,k}, t)}{\delta \mathbf{x}_k} \right|_{\mathbf{x}_r = \mathbf{x}_{r,k}} \quad (5.14)$$

$$\mathbf{B}_{r,k} = \left. \frac{\delta \mathbf{f}_r(\mathbf{x}_r, \boldsymbol{\tau}_{w,k}, \boldsymbol{\omega}_{w,k}, t)}{\delta \boldsymbol{\tau}_w} \right|_{\mathbf{x}_r = \mathbf{x}_{r,k}} \quad (5.15)$$

It is important to note that (5.11a) is used in the calculation of the kalman gain matrix, (5.7a), the error covariance update, (5.7c), and in the error covariance propagation, (5.7e), but not in calculating the state propagation, (5.7d), where (5.1a) is still used.

By using the reduced system (5.7a), (5.7b), (5.7c), and (5.7e) can now be expressed as

$$\mathbf{K}_{r,k} = \bar{\mathbf{P}}_{r,k} \mathbf{H}_{r,k}^T [\mathbf{H}_{r,k} \bar{\mathbf{P}}_{r,k} \mathbf{H}_{r,k}^T + \mathbf{R}_r]^{-1} \quad (5.16a)$$

$$\hat{\mathbf{x}}_{r,k} = \bar{\mathbf{x}}_{r,k} + \mathbf{K}_{r,k} [\mathbf{y}_{r,k} - \mathbf{H}_{r,k} \bar{\mathbf{x}}_{r,k}] \quad (5.16b)$$

$$\hat{\mathbf{P}}_{r,k} = [\mathbf{I} - \mathbf{K}_{r,k} \mathbf{H}_{r,k}] \bar{\mathbf{P}}_{r,k} [\mathbf{I} - \mathbf{K}_{r,k} \mathbf{H}_{r,k}]^T + \mathbf{K}_{r,k} \mathbf{R}_r \mathbf{K}_{r,k}^T \quad (5.16c)$$

$$\bar{\mathbf{P}}_{r,k+1} = \hat{\boldsymbol{\Phi}}_{r,k} \hat{\mathbf{P}}_{r,k} \hat{\boldsymbol{\Phi}}_{r,k}^T + \mathbf{E}_{r,k} \mathbf{Q}_r \mathbf{E}_{r,k}^T \quad (5.16d)$$

Because of the unit constraint on the quaternion, the above presented filter still contains full state information, and it may be derived by

$$\hat{\mathbf{x}}_k = \begin{bmatrix} \sqrt{1 - \|\hat{\boldsymbol{\epsilon}}_k\|^2} \\ \hat{\mathbf{x}}_{r,k} \end{bmatrix} \quad (5.17)$$

The effect of the various sensor configuration on the extended kalman filter will manifest itself in the innovation process and in the state estimation update. By increasing or decreasing the dimension of the measurements,  $\mathbf{y}_{m,k}$ , or altering its physical nature, the measurement matrix,  $\mathbf{H}_k$ , must be altered to accommodate these changes and thus maintaining the physical effect of the measurement on the filter. Altering the measurement matrix will in turn change the kalman gain calculation, error covariance update and propagation in dimension or/and value. Consequently all the presented kalman filters in this section will utilize (5.7d), (5.16a), (5.16c) and (5.16d), while depending on the sensor configuration each filter will have different (5.8), (5.9), and measurement covariance,  $\mathbf{R}_{r,k}$ .

Consequently, the following presented EKF designs will only treat the design of the innovation processes and the estimate state updates.

### 5.2.2 EKF using a single Star sensor

As presented in section 3.2.1, the star sensor measures the attitude of the satellite, represented by Euler parameters. The estimation error can be interpreted as an rotation, and be used in the estimation update as

$$\hat{\mathbf{q}}_k = \bar{\mathbf{q}}_k \otimes \begin{bmatrix} \sqrt{1 - \|\mathbf{K}_{star,\epsilon,k} \Delta \boldsymbol{\epsilon}_k\|^2} \\ \mathbf{K}_{star,\epsilon,k} \Delta \boldsymbol{\epsilon}_k \end{bmatrix} \quad (5.18)$$

where  $\Delta \boldsymbol{\epsilon}_k$  is derived from

$$\Delta \mathbf{q}_k = \begin{bmatrix} \Delta \eta_k \\ \Delta \boldsymbol{\epsilon}_k \end{bmatrix} = \mathbf{q}_{star,k} \otimes \bar{\mathbf{q}}_k^{-1} \quad (5.19)$$

where  $\mathbf{q}_{star,k}$  is the discrete star sensor measurement defined in (3.3).

While the innovation and state update process for the quaternion part differ from usual practice, the angular velocity part is done the usual way by the innovation

$$\bar{\Delta} \boldsymbol{\epsilon}_k = \boldsymbol{\epsilon}_{star,k} - \bar{\boldsymbol{\epsilon}}_k \quad (5.20)$$

and the state update as

$$\hat{\boldsymbol{\omega}}_{ob,k}^b = \bar{\boldsymbol{\omega}}_{ob,k}^b + \mathbf{K}_{star,\omega,k} \bar{\Delta} \boldsymbol{\epsilon}_k \quad (5.21)$$

$\mathbf{K}_{star,\epsilon,k}$  and  $\mathbf{K}_{star,\omega,k}$  are the two parts of the kalman gains produced by (5.16a) and defined as

$$\mathbf{K}_{star,k} = \begin{bmatrix} \mathbf{K}_{star,\epsilon,k} \\ \mathbf{K}_{star,\omega,k} \end{bmatrix} \quad (5.22)$$

The measurements matrix becomes constant and given by

$$\mathbf{H}_{star} = \begin{bmatrix} \mathbf{I}_{3 \times 3} & \mathbf{0}_{3 \times 3} \end{bmatrix} \quad (5.23)$$

and the measurement noise covariance matrix is determined by

$$\mathbf{R}_{star,k} = \text{diag}(\sigma_{\bar{v}_{star,2,k}}^2, \dots, \sigma_{\bar{v}_{star,4,k}}^2) \quad (5.24)$$

where

$$\sigma_{\bar{v}_{star,i,k}}^2 = \mathbf{E}[\bar{v}_{star,i,k}^2] \quad (5.25)$$

is derived by using the predicted attitude in equation (3.11).

### 5.2.3 EKF using two Star sensors

This filter is similar to the previous one, distinguished by having twice the number of star measurements,  $\mathbf{q}_{star1,k}$  and  $\mathbf{q}_{star2,k}$ . The innovation processes (5.19) and (5.20) are used on each of the two measurements, and they are incorporated in the state update as

$$\hat{\mathbf{q}}_k = \bar{\mathbf{q}}_k \otimes \left[ \sqrt{1 - \frac{\|\mathbf{K}_{star1,\epsilon,k}\Delta\epsilon_{k,1} + \mathbf{K}_{star2,\epsilon,k}\Delta\epsilon_{k,2}\|^2}{\mathbf{K}_{star1,\epsilon,k}\Delta\epsilon_{k,1} + \mathbf{K}_{star2,\epsilon,k}\Delta\epsilon_{k,2}}} \right] \quad (5.26)$$

and

$$\hat{\omega}_{ob,k}^b = \bar{\omega}_{ob,k}^b + \mathbf{K}_{star1,\omega,k}\bar{\Delta}\epsilon_{k,1} + \mathbf{K}_{star2,\omega,k}\bar{\Delta}\epsilon_{k,2} \quad (5.27)$$

The kalman gain and measurement matrices are now extended to incorporate two star measurements as

$$\mathbf{K}_{stars,k} = \begin{bmatrix} \mathbf{K}_{star1,\epsilon,k} & \mathbf{K}_{star2,\epsilon,k} \\ \mathbf{K}_{star1,\omega,k} & \mathbf{K}_{star2,\omega,k} \end{bmatrix} \quad (5.28)$$

and

$$\mathbf{H}_{stars} = \begin{bmatrix} \mathbf{I}_{3 \times 3} & \mathbf{0}_{3 \times 3} \\ \mathbf{I}_{3 \times 3} & \mathbf{0}_{3 \times 3} \end{bmatrix} \quad (5.29)$$

The predicted measurement noise covariance is also extended to

$$\mathbf{R}_{stars,k} = \text{diag}(\sigma_{\bar{v}_{star1,2,k}}^2, \dots, \sigma_{\bar{v}_{star1,4,k}}^2, \sigma_{\bar{v}_{star2,2,k}}^2, \dots, \sigma_{\bar{v}_{star2,4,k}}^2) \quad (5.30)$$

### 5.2.4 EKF using Star- and Sun-sensors

The main factor in designing an extended kalman filter with sun and star sensor, is the different update rates of the two sensors. Seen from table 3.1 and 3.2, the sun sensor produces measurements up to 100 times per second, while the star sensor at 8 times per second. One alternative is to fashion separate EKF's for each sensor, while a more elegant method is to design a combined filter. The combined filter is strictly speaking an filter using the sun sensor as main measurements

, and when available, corrected by star measurements.

The sun filter innovation process is defined as

$$\boldsymbol{\nu}_{s,k} = \mathbf{s}_k^b - \bar{\mathbf{s}}_k^b \quad (5.31)$$

where  $\mathbf{s}_k^b$  is the sun vector measurement defined by (3.12), and  $\bar{\mathbf{s}}_k^b$  is the predicted sun vector derived from

$$\bar{\mathbf{s}}_k^b = \bar{\mathbf{R}}_e(\bar{\boldsymbol{\eta}}, \bar{\boldsymbol{\epsilon}}) \mathbf{s}_k^o \quad (5.32)$$

The innovation process may now be used in updating the states as

$$\hat{\mathbf{q}}_k = \bar{\mathbf{q}}_k \otimes \left[ \begin{array}{c} \sqrt{1 - \|\mathbf{K}_{sun,\epsilon,k} \boldsymbol{\nu}_{s,k}\|^2} \\ \mathbf{K}_{sun,\epsilon,k} \boldsymbol{\nu}_{s,k} \end{array} \right] \quad (5.33)$$

and

$$\hat{\boldsymbol{\omega}}_{ob,k}^b = \bar{\boldsymbol{\omega}}_{ob,k}^b + \mathbf{K}_{sun,\omega,k} \boldsymbol{\nu}_{s,k} \quad (5.34)$$

where the kalman gains are

$$\mathbf{K}_{r,k} = \begin{bmatrix} \mathbf{K}_{sun,\epsilon,k} \\ \mathbf{K}_{sun,\omega,k} \end{bmatrix} \quad (5.35)$$

The predicted sun vector,  $\bar{\mathbf{s}}_k^b$ , is the result of a nonlinear measurement function and Bak (2000) proposed the following measurement matrix when using vector measurement in kalman filters as

$$\mathbf{H}_{sun,k} = \left. \frac{\partial}{\partial \mathbf{x}_r} (\bar{\mathbf{s}}_k^b) \right|_{\mathbf{x}_r = \bar{\mathbf{x}}_r} \simeq [2\mathbf{S}(\bar{\mathbf{s}}_k^b) \quad 0_{3 \times 3}] \quad (5.36)$$

and the measurement noise covariance matrix

$$\mathbf{R}_{sun,k} = \text{diag}(\sigma_{\bar{v}_{sun,1,k}}^2, \sigma_{\bar{v}_{sun,2,k}}^2, \sigma_{\bar{v}_{sun,3,k}}^2) \quad (5.37)$$

where

$$\sigma_{\bar{v}_{sun,i,k}}^2 = \mathbf{E}[\bar{v}_{sun,i,k}^2] \quad (5.38)$$

The above filter derives the attitude in the time span when only sun measurements are available, but when star measurements are accessible the filter takes on a little different shape. Firsts the sun measurement correction of the predicted estimates is performed, followed by the star measurement correction of the sun corrected estimates, finished by the state propagation. The presented filter design gives two state update sequences at every iteration the star sensor measurements is available. The additional equations to the above sun filter is (5.16a), (5.26), (5.27), and (5.16c).

### 5.2.5 EKF using Star-, Sun- and Earth sensors

The design of this filter is similar to the previous filter, with the distinction that this uses measurements from both the sun sensor and earth sensor as main sensors, and gets corrections from the star measurements. The main innovation process is now

$$\boldsymbol{\nu}_{se,k} = \begin{bmatrix} \boldsymbol{\nu}_{sun,k} \\ \boldsymbol{\nu}_{earth,k} \end{bmatrix} = \begin{bmatrix} \mathbf{s}_k^b - \bar{\mathbf{s}}_k^b \\ \mathbf{y}_e^b - \bar{\mathbf{y}}_e^b \end{bmatrix} \quad (5.39)$$

where  $\bar{\mathbf{y}}_e^b$  and  $\mathbf{y}_e^b$  are the predicted and measured earth's horizon angles. The prediction is the Euler parameter to Euler angle conversion given by the nonlinear equations

$$\bar{\mathbf{y}}_e^b = \begin{bmatrix} \bar{\phi} \\ \bar{\theta} \end{bmatrix} = \begin{bmatrix} \tan^{-1}\left(\frac{2(\bar{\epsilon}_2\bar{\epsilon}_3 + \bar{\eta}\bar{\epsilon}_1)}{\bar{\eta}^2 - \bar{\epsilon}_1^2 - \bar{\epsilon}_2^2 + \bar{\epsilon}_3^2}\right) \\ -\tan^{-1}\left(\frac{2(\bar{\epsilon}_1\bar{\epsilon}_3 + \bar{\eta}\bar{\epsilon}_2)}{\sqrt{1 - 2(\bar{\epsilon}_1\bar{\epsilon}_3 + \bar{\eta}\bar{\epsilon}_2)}}\right) \end{bmatrix} \quad (5.40)$$

The state update is now done according to

$$\hat{\mathbf{q}}_k = \bar{\mathbf{q}}_k \otimes \begin{bmatrix} \sqrt{1 - \|\mathbf{K}_{se,\epsilon,k}\boldsymbol{\nu}_{se,k}\|^2} \\ \mathbf{K}_{se,\epsilon,k}\boldsymbol{\nu}_{se,k} \end{bmatrix} \quad (5.41)$$

for the quaternion part, and

$$\hat{\boldsymbol{\omega}}_{ob,k}^b = \bar{\boldsymbol{\omega}}_{ob,k}^b + \mathbf{K}_{se,\omega,k}\boldsymbol{\nu}_{se,k} \quad (5.42)$$

for the angular velocity part. The measurement matrix,  $\mathbf{H}_{se,k}$ , is defined as

$$\mathbf{H}_{se,k} = \begin{bmatrix} \mathbf{H}_{sun,k} \\ \mathbf{H}_{earth,k} \end{bmatrix} \quad (5.43)$$

where  $\mathbf{H}_{sun,k}$  is given in the previous section, and  $\mathbf{H}_{earth,k}$  is the earth sensor measurement matrix defined as

$$\mathbf{H}_{earth,k} = \left. \frac{\partial}{\partial \mathbf{x}_r} (\mathbf{y}_e^b) \right|_{\mathbf{x}_r = \bar{\mathbf{x}}_r} \quad (5.44)$$

and the linearization is performed in appendix C.3.

### 5.2.6 Observability

Observability of a system may be achieved in two different ways. The system may exploits static observability if it is observable at any time, or dynamic observability if it is observable, but does not satisfy static observability. In this sense, static observability is achieved if the matrix

$$\mathbf{O} = \begin{bmatrix} \mathbf{H}_k \\ \mathbf{H}_k \boldsymbol{\Phi}_k \\ \vdots \\ \mathbf{H}_k \boldsymbol{\Phi}_k^{n-1} \end{bmatrix} \quad (5.45)$$

has rank  $n$ . Dynamic observability occurs when the system relies on variations in the system states or time-varying measurement matrices to achieve observability. The criteria for dynamic observability is obtained if the observability Gramian, defines as

$$\mathcal{O} = \sum_{k=1}^N \boldsymbol{\Phi}_k^T \mathbf{H}_k^T \mathbf{H}_k \boldsymbol{\Phi}_k \quad (5.46)$$

is nonsingular (Psiaki, Martel, and Pal 1990)

### Satellite observability

Preliminary investigations show that by using one of the presented measurement matrices,  $\mathbf{H}_{star}$ ,  $\mathbf{H}_{sun}$  or  $\mathbf{H}_{earth}$ , results in a static observable system. If only the quaternion part of the model is examined, only the star measurement matrix exploits static observability. The two other measurement matrices utilize the relations between the observable quaternion-values, the angular velocities and the missing quaternion-value to produce static observability, in that order. These relations are small and may lead to unobservability. The sun measurements and earth measurement must then rely on their dynamic observability properties to produce an observable system.

#### 5.2.7 Modified EKF

Several researchers have reported poor EKF performance for a system that exploits dynamic observability. It is a significant factor in estimator design when the necessary variations of the system are slow compared to the rate at which new measurements are acquired, and it implies that long intervals of subsequent measurements do not generate observability of the complete states. If the star sensor is not accessible, the resulting filter becomes either a sun filter or a sun and earth filter. By the above discussion, the resulting filter exploits dynamic observability. Since the sun filter only has a single vector measurement, it is in addition underdetermined and attitude determination becomes difficult. The star and earth filter has five measurement parameters available and is thus overdetermined. This suggests a modification of the filter, performed by combining the sun and earth measurement to produce a filter exploiting static observability.

By defining a reference vector as

$$\mathbf{e}_{r,k}^o = [0 \ 0 \ 1]^T \quad (5.47)$$

the earth measurements may be represented as a vector measurement by

$$\mathbf{e}_{m,k}^b = (\mathbf{R}_y(\theta_{e,k})\mathbf{R}_x(\phi_{e,k}))^T \mathbf{e}_{r,k}^o \quad (5.48)$$

and be fused with the sun measurement by using the Gauss-Newton algorithm (Marins, Yun, Bachmann, McGhee, and Zyda 2001). The Gauss-Newton method is a numerical optimization algorithm that uses line search in minimizing the squared error function, (Nocedal and Wright 1999), given by

$$\mathbf{Q}_k^o = \boldsymbol{\varepsilon}^T \boldsymbol{\varepsilon} = (\mathbf{y}_{r,k}^o - \mathbf{M}\mathbf{y}_{m,k}^b)^T (\mathbf{y}_{r,k}^o - \mathbf{M}\mathbf{y}_{m,k}^b) \quad (5.49)$$

where

$$\mathbf{y}_{r,k}^o = [\mathbf{s}_{r,k}^o \ \mathbf{e}_{r,k}^o]^T \quad (5.50)$$

are the reference vectors in orbit frame, and

$$\mathbf{y}_{m,k}^b = [\mathbf{s}_{m,k}^b \ \mathbf{e}_{m,k}^b]^T \quad (5.51)$$

are the measured vectors in body frame, and  $\mathbf{M}_k$  is the total rotation matrix defined as

$$\mathbf{M}_k = \begin{bmatrix} \mathbf{R}_e(\hat{\boldsymbol{\eta}}_{g,k}, \hat{\boldsymbol{\epsilon}}_{g,k}) & \mathbf{0}_{3 \times 3} \\ \mathbf{0}_{3 \times 3} & \mathbf{R}_e(\hat{\boldsymbol{\eta}}_{g,k}, \hat{\boldsymbol{\epsilon}}_{g,k}) \end{bmatrix} \quad (5.52)$$

where  $\mathbf{q}_{g,k}$  is the quaternion defining the attitude. The actual algorithm that minimizing the error function, and determines  $\mathbf{q}_{g,k}$  is given by

$$\hat{\mathbf{q}}_{g,k+1} = \hat{\mathbf{q}}_{g,k} - [J^T(\hat{\mathbf{q}}_{g,k})J(\hat{\mathbf{q}}_{g,k})]^{-1} J^T(\hat{\mathbf{q}}_{g,k})\boldsymbol{\varepsilon}_k^g(\hat{\mathbf{q}}_{g,k}) \quad (5.53)$$

where  $\hat{\mathbf{q}}_{g,k}$  is a unit quaternion at sample  $k$ , and  $J$  is the Jacobian matrix defined as

$$J = - \left[ \left( \frac{\partial \mathbf{M}_k}{\partial \eta_{g,k}} \mathbf{y}_m^b \right) \left( \frac{\partial \mathbf{M}_k}{\partial \epsilon_{g,1,k}} \mathbf{y}_m^b \right) \left( \frac{\partial \mathbf{M}_k}{\partial \epsilon_{g,2,k}} \mathbf{y}_m^b \right) \left( \frac{\partial \mathbf{M}_k}{\partial \epsilon_{g,3,k}} \mathbf{y}_m^b \right) \right] \quad (5.54)$$

The convergence of the Gauss-Newton algorithm has undergone comprehensive testing and results show that the best quaternion is achieved in 3-4 iterations (Marins 2000).

The resulting quaternion from the Gauss-Newton algorithm can now be used in the EKF as the star sensor measurement is used in the star EKF. The measurement matrix becomes linear as

$$\mathbf{H}_{g,k} = [\mathbf{I}_{3 \times 3} \quad 0_{3 \times 3}] \quad (5.55)$$

and the measurement covariance matrix

$$\mathbf{R}_{g,k} = \text{diag}(\sigma_{v_{g,1}}^2, \sigma_{v_{g,2}}^2, \sigma_{v_{g,3}}^2) \quad (5.56)$$

where

$$\sigma_{v_{g,i}}^2 = \mathbf{E}[v_{g,i}^2] \quad (5.57)$$

is the covariance of the noise on the quaternion produced by the Gauss-Newton algorithm to be determined later.

## 5.3 Nonlinear Observer

Nonlinear observers solve the nonlinear estimation problem in an ad hoc manner. Their design is performed by proposing an arbitrary filter, with parameters, then tuned according to some criteria. The most important criteria is convergence, and through Lyapunov analyze it may be proven. The motivations for choosing nonlinear observers are their ability to find an Lyapunov function that proves convergens.

### 5.3.1 Nonlinear observer theory

Consider the nonlinear time-varying system

$$\dot{\mathbf{x}} = \mathbf{f}(\mathbf{x}, \mathbf{u}, t) \quad (5.58)$$

$$\mathbf{y} = h(\mathbf{x}) \quad (5.59)$$

where  $\mathbf{x}$  are the states,  $\mathbf{u}$  are the inputs, and  $\mathbf{y}$  are the measurements. A full state observer, under the assumption that  $\mathbf{u}$  and  $\mathbf{y}$  are available, is defined as

$$\dot{\hat{\mathbf{x}}} = \mathbf{f}(\hat{\mathbf{x}}, \mathbf{u}, t) + \mathbf{L}(\mathbf{y} - h(\hat{\mathbf{x}})) \quad (5.60)$$

where  $\hat{\mathbf{x}}$  are the estimated states and  $\mathbf{L}$  are the observer gains. Stability of the observer is done by defining the estimation error dynamics as

$$\dot{\mathbf{e}}(t) = \dot{\mathbf{x}}(t) - \dot{\hat{\mathbf{x}}}(t) \quad (5.61)$$

and analyzing for stability.

### 5.3.2 Attitude observer

This section introduces the attitude observer presented by Krogstad (2005). The observer is based on the work done by Salcudean (1991), but extended to incorporate reaction wheel dynamics. In presenting this observer it is convenient to represent the satellite's equation of motion in a simpler fashion. The Satellite's angular motion in relation to its angular momentum may be described as

$$\mathbf{h}^b = \mathbf{I}\boldsymbol{\omega}_{ob}^b + \mathbf{h}_w^b \quad (5.62)$$

where  $\mathbf{h}$  is the total angular momentum of the satellite and  $\mathbf{h}_w$  is the angular momentum created by the reaction wheels defined as

$$\mathbf{h}_w^b = \mathbf{A}\mathbf{I}_w(\boldsymbol{\omega}_w + \mathbf{A}^T\boldsymbol{\omega}_{ob}^b) \quad (5.63)$$

By differentiating (5.62) the angular velocity part of (4.14) is obtained. Using the property (5.62) and a quaternion measurement  $\mathbf{q}_m = [\eta_m \quad \boldsymbol{\epsilon}_m]^T$ , a discrete nonlinear attitude observer may now be described by the following dynamics

$$\hat{\mathbf{g}}^b = 3\omega_o^2\hat{\mathbf{c}}_3 \times \mathbf{I}^b\hat{\mathbf{c}}_3 \quad (5.64a)$$

$$\dot{\hat{\mathbf{h}}}^b = \mathbf{R}_e(\hat{\eta}_m, \hat{\boldsymbol{\epsilon}}_m)[\hat{\mathbf{g}}^b + \frac{1}{2}k_p(\mathbf{I}^b)^{-1}\mathbf{e}\text{sgn}(\mathbf{e}_o)] \quad (5.64b)$$

$$\dot{\hat{\mathbf{h}}}_w^b = \mathbf{A}\mathbf{I}_w(\boldsymbol{\omega}_w + \mathbf{A}^T\hat{\boldsymbol{\omega}}_{ob}^b) \quad (5.64c)$$

$$\hat{\boldsymbol{\omega}}_{ob}^b = (\mathbf{I}^b)^{-1}\mathbf{R}_e(\eta_m, \boldsymbol{\epsilon}_m)^T(\hat{\mathbf{h}}^b - \hat{\mathbf{h}}_w^b) \quad (5.64d)$$

$$\dot{\hat{\mathbf{q}}} = \frac{1}{2} \begin{bmatrix} -\hat{\boldsymbol{\epsilon}}^T \\ \hat{\eta}\mathbf{I} + \mathbf{S}(\hat{\boldsymbol{\epsilon}}) \end{bmatrix} (\hat{\boldsymbol{\omega}}_{ob}^b + \frac{1}{2}k_v\mathbf{R}_e(\eta_m, \boldsymbol{\epsilon}_m)(\mathbf{I}^b)^{-1}\mathbf{R}_e(\eta_m, \boldsymbol{\epsilon}_m)^T\mathbf{e}\text{sgn}(\mathbf{e}_o)) \quad (5.64e)$$

where  $\mathbf{R}_e(\eta_m, \boldsymbol{\epsilon}_m)$  is the rotation matrix defined by (2.22), and

$$\mathbf{e}_o = \eta_m\hat{\boldsymbol{\eta}} + \boldsymbol{\epsilon}_m^T\hat{\boldsymbol{\epsilon}} \quad (5.64f)$$

$$\mathbf{e} = \hat{\eta}\boldsymbol{\epsilon}_m - \eta_m\hat{\boldsymbol{\epsilon}} + \mathbf{S}(\boldsymbol{\epsilon}_m)\hat{\boldsymbol{\epsilon}} \quad (5.64g)$$

is the quaternion,  $[\mathbf{e}_o \quad \mathbf{e}^T]^T$ , describing the rotation error  $\mathbf{R}_e(\eta_m, \boldsymbol{\epsilon}_m)\mathbf{R}_e(\hat{\eta}, \hat{\boldsymbol{\epsilon}})^T$ .

### 5.3.3 Nonlinear observer using star sensors

When using single star measurement the nonlinear attitude observer takes the discrete form of the above observer with  $\mathbf{q}_m$  exchanged by  $\mathbf{q}_{s,k}$  as

$$\hat{\mathbf{g}}_k^b = 3\omega_o^2\hat{\mathbf{c}}_{3,k} \times \mathbf{I}^b\hat{\mathbf{c}}_{3,k} \quad (5.65a)$$

$$\hat{\mathbf{h}}_{k+1}^b = \hat{\mathbf{h}}_k^b + \mathbf{R}_e(\eta_{s,k}, \boldsymbol{\epsilon}_{s,k})[\hat{\mathbf{g}}_k^b + \frac{1}{2}k_p(\mathbf{I}^b)^{-1}\mathbf{e}_k\text{sgn}(\mathbf{e}_{0,k})]\Delta t \quad (5.65b)$$

$$\hat{\mathbf{h}}_{w,k}^b = \mathbf{A}\mathbf{I}_w(\boldsymbol{\omega}_{w,k} + \mathbf{A}^T\hat{\boldsymbol{\omega}}_{ob,k}^b) \quad (5.65c)$$

$$\hat{\boldsymbol{\omega}}_{ob,k+1}^b = (\mathbf{I}^b)^{-1}\mathbf{R}_e(\eta_{s,k}, \boldsymbol{\epsilon}_{s,k})^T(\hat{\mathbf{h}}_k^b - \hat{\mathbf{h}}_{w,k}^b) \quad (5.65d)$$

$$\hat{\mathbf{q}}_{k+1} = \hat{\mathbf{q}}_k + \frac{1}{2} \begin{bmatrix} -\hat{\boldsymbol{\epsilon}}_k^T \\ \hat{\eta}_k\mathbf{I} + \mathbf{S}(\hat{\boldsymbol{\epsilon}}_k) \end{bmatrix} (\hat{\boldsymbol{\omega}}_{ob,k}^b + \frac{1}{2}k_v\mathbf{R}_e(\eta_{s,k}, \boldsymbol{\epsilon}_{s,k})(\mathbf{I}^b)^{-1}\mathbf{R}_e(\eta_{s,k}, \boldsymbol{\epsilon}_{s,k})^T\mathbf{e}_k\text{sgn}(\mathbf{e}_{0,k}))\Delta t \quad (5.65e)$$

$$\mathbf{e}_{0,k} = \eta_{s,k}\hat{\boldsymbol{\eta}}_k + \boldsymbol{\epsilon}_{s,k}^T\hat{\boldsymbol{\epsilon}}_k \quad (5.65f)$$

$$\mathbf{e}_k = \hat{\eta}_k\boldsymbol{\epsilon}_{s,k} - \eta_{s,k}\hat{\boldsymbol{\epsilon}}_k + \mathbf{S}(\boldsymbol{\epsilon}_{s,k})\hat{\boldsymbol{\epsilon}}_k \quad (5.65g)$$

When using measurements from more than one attitude sensor the problem of sensor fusion arise. The measurements from the two star sensor may be combined to produce one quaternion by calculating the mean attitude as

$$\mathbf{q}_{c,k} = \mathbf{q}_{s2,k} \otimes \left[ \sqrt{1 - \|\frac{1}{2}\Delta\epsilon_{s,k}\|^2} \right. \\ \left. \frac{1}{2}\Delta\epsilon_{s,k} \right] \quad (5.66)$$

where

$$\Delta\mathbf{q}_{s,k} = \begin{bmatrix} \Delta\eta_{s,k} \\ \Delta\epsilon_{s,k} \end{bmatrix} = \mathbf{q}_{s1,k} \otimes (\mathbf{q}_{s2,k})^{-1} \quad (5.67)$$

By using the combined measurement,  $\mathbf{q}_{c,k}$ , instead of the single star measurement,  $\mathbf{q}_{s,k}$ , in (5.65) the attitude from two star measurements may be determined.

### 5.3.4 Nonlinear observer using Star- and Sun-sensors

In between the star measurements, only sun measurements are available. The attitude determination is in this time period underdetermined, and deriving the attitude from the sun measurement is thus not possible. By using the following observer dynamics, the attitude may be estimated by the sun vector measurement.

$$\hat{\mathbf{h}}_{k+1}^b = \hat{\mathbf{h}}_k^b + \mathbf{R}_e(\hat{\eta}, \hat{\epsilon})[\hat{\mathbf{g}}_k^b + l_1\mathbf{I}\mathbf{H}_k^\dagger\boldsymbol{\nu}_{sun,k}]/\Delta t \quad (5.68a)$$

$$\hat{\mathbf{h}}_{w,k}^b = \mathbf{A}\mathbf{I}_w(\boldsymbol{\omega}_{w,k} + \mathbf{A}^\top\hat{\boldsymbol{\omega}}_{ob,k}^b) \quad (5.68b)$$

$$\hat{\boldsymbol{\omega}}_{ob,k+1}^b = (\mathbf{I}^b)^{-1}\mathbf{R}_e(\hat{\eta}, \hat{\epsilon})^\top(\hat{\mathbf{h}}_k^b - \hat{\mathbf{h}}_{w,k}^b) \quad (5.68c)$$

$$\hat{\mathbf{q}}_{k+1} = \hat{\mathbf{q}}_k + \frac{1}{2} \begin{bmatrix} -\hat{\boldsymbol{\epsilon}}_k^\top \\ \hat{\eta}_k\mathbf{I} + \mathbf{S}(\hat{\boldsymbol{\epsilon}}_k) \end{bmatrix} (\hat{\boldsymbol{\omega}}_{ob,k}^b + l_2\mathbf{I}\mathbf{H}_k^\dagger\boldsymbol{\nu}_{sun,k})\Delta t \quad (5.68d)$$

$$(5.68e)$$

where  $l_1$  and  $l_2$  are scalar observer gains, and  $\mathbf{H}_k$  is based on the epsilon part of the sun measurements matrix ,(5.36), now defined as

$$\mathbf{H}_k = 2\mathbf{S}(\hat{\mathbf{s}}_k^b) \quad (5.69)$$

where the estimated sun vector,  $\hat{\mathbf{s}}_k^b$ , is

$$\hat{\mathbf{s}}_k^b = \mathbf{R}_e(\hat{\eta}, \hat{\epsilon})^\top \mathbf{s}_{ref,k}^o \quad (5.70)$$

The estimation error , $\boldsymbol{\nu}_{sun,k}$ , is defined in a similar fashion as in the EKF, by

$$\boldsymbol{\nu}_{sun,k} = \mathbf{s}_k^b - \hat{\mathbf{s}}_k^b \quad (5.71)$$

Since the sun measurement can't produce full attitude information, stability or convergence proofs of just the presented sun observer does not exist. The combined filter must rely on the sun measurements dynamic observability properties, and its star measurement corrections.

### 5.3.5 Nonlinear observer using Star-, Sun- and Earth sensors

The same problem as in the previous section arise here. The nonlinear observer requires the measurements in quaternion form, while the sun and earth sensor produces vector measurements and non complete Euler angles, respectively. By them selves, they do not contain 3-axis attitude information, but combined they contain redundant attitude information. This suggests using the Gauss-Newton method yet again to produce complete attitude information from the two measurements.

The sensor fusion is performed as in section 5.2.7, and the resulting quaternion is utilized by the nonlinear observer in the same manner as the star sensor measurement, leading to two similar observers in the form of (5.65), running at different intervals. Since the Gauss-Newton quaternion is produced from the earth and sun measurements, it is less accurate then the star sensor quaternion and the respective observer gains must be designed thereafter.

# Chapter 6

## Performance Analysis

The demands on satellite performance are challenging in terms of attitude determination. The desired determination accuracy of  $0.001^\circ$  about all axes must be met with the use of either a EKF or a nonlinear observer with the presented sensor configurations. The determination schemes must determine the attitude from initially unknown state, and maintain the accuracies during the operation span.

### 6.1 Simulation environment

The attitude of the satellite is investigated by simulating the satellite as a gravity-gradient stabilized satellite with active control torque. A block diagram of the simulated system is shown in 6.1.

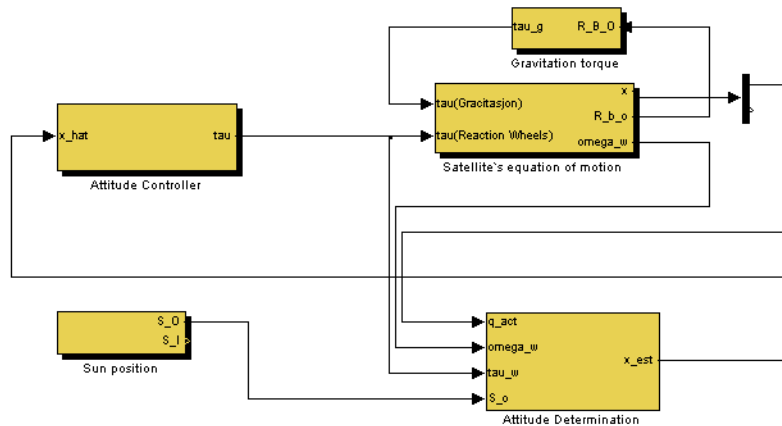


Figure 6.1: Simulink model overview

The lower left part of the diagram shows the sun reference vector propagation using (3.17). The upper right part consists of the satellite's attitude propagation being driven by the gravitational force,  $\mathbf{g}^b$ , and the control torque (upper left part),  $\boldsymbol{\tau}_w$ . The attitude propagation is done accord-

ing to the nonlinear model (4.13), and is used as reference when determining the accuracy of the determination schemes. The bottom right part is according to chosen sensor configuration, one of the presented attitude determination schemes in chapter 5.

**Table 6.1:** Satellite parameters

Parameter	Value
Inertia matrix	$\text{diag}\{4, 4, 3\} [kgm^2]$
Orbit altitude	600 km
Orbit angular velocity - $\omega_o$	$1.083 \times 10^{-3} [\text{rad/s}]$
Reaction wheels inertia $\mathbf{I}_w$	$\text{diag}\{1, 1, 1, 1\} \times 10^{-3} [kgm^2]$
R.W. configuration $\mathbf{A}$ :	$\mathbf{t}_1 = [\sqrt{\frac{1}{3}}, \sqrt{\frac{2}{3}}, 0]^T$ $\mathbf{t}_2 = [\sqrt{\frac{1}{3}}, -\sqrt{\frac{2}{3}}, 0]^T$ $\mathbf{t}_3 = [-\sqrt{\frac{1}{3}}, 0, -\sqrt{\frac{2}{3}}]^T$ $\mathbf{t}_4 = [-\sqrt{\frac{1}{3}}, 0, \sqrt{\frac{2}{3}}]^T$
Attitude control:	$\mathbf{K}_p = \text{diag}\{0.3, 0.3, 0.3\}$ $\mathbf{K}_d = \text{diag}\{1, 1, 1\}$
Disturbance torque	$\sigma = 1 \times 10^{-8} [Nm]$

The satellite is simulated in continuous-time, while the attitude determinations are, as they would in real life, run in discrete-time. The distinction is performed in order to make the simulations as close to real life as possible, and thus obtain a more actual performance analysis. Since the satellite is propagated by the ode45 solver, i.e. Runge-Kutta integration (Egeland et.al. 2002), the stability issues indicated by Kyrkjebø (2000) may be disregarded. According to chosen sensor configuration, the attitude determination runs at either 8 Hz or 40 Hz, and the discrete sensor models are implemented according to chapter 3. The main simulation parameters are given in table 6.1

To represent the disturbances of aerodynamic drag and solar pressure affecting the satellite, a disturbance torque of covariance  $\sigma^2$  is introduced to the process model. Simulations has shown that the stabilizing noise representing the quaternion part of the parameter noise may be discarded, making  $\mathbf{Q}_q = \mathbf{0}$ . No perturbations of the moments of inertia has been exploited in the simulations, as these are assumed eliminated by in-flight calibration using star sensor measurements.

The initial attitude acquisition of each shembe is investigated by propagating the satellite from a fixed initial attitude, while the filters and observers believes the attitude to be somewhat different. This initial difference is kept small, since attitude acquisition is normally performed shortly after a computer reset of fault. The initial attitude acquisition, i.e. after satellite de-tumbling has been performed, is believed to place the satellite in a stable state (Soglo 1994), and by using either gps-receivers or star sensor measurements as the initial attitude guess, it will correspond to acquiring the satellite attitude for relatively small deviances. By increasing the assumed process noise covariance in the filters or increasing the observer gains at start-up, a larger initial deviations

may be accounted for. The initial values are presented in table 6.2, and an initial drop angle,  $\beta_0$ , of  $90^\circ$  corresponds to an initial ECI position right above the north pole.

**Table 6.2:** Initial values

Parameter	Satellite	Determination
attitude $\Theta$ [Deg]	$[10, 10, 10]^T$	$[5, 5, 5]^T$
angular velocity $\omega_{ob}^b$ [rad/s]	$[5, 5, 5]^T \times 10^{-4}$	$[2, 2, 2]^T \times 10^{-3}$
Wheel spin $\omega_w$ [rad/s]	$[0, 0, 0, 0]^T$	
Position $\beta_0$ [Deg]	90	

The satellite is initially simulated without attitude control for a period of time, thereafter subjected to control using estimated state feedback the remanding time. This is done to investigate transient and steady-state performances of the attitude determinations, and display its implications on control performance. The simulation span is 5000 seconds, which roughly corresponds to one orbit.

Matlab(v7.0) and Matlab/Simulink(v6.0) are chosen as the simulation tool, and all simulation files are present on the accompanying cd (appendix D). Because of the large number of implemented determination schemes, their performances are concise presented in form of plots and tables.

## 6.2 Extended kalman filter

### 6.2.1 EKF using Star sensors

The star filters determines the attitude at a rate of 8 Hz, and the resulting performances are presented in the table 6.2(a) and figure 6.2.

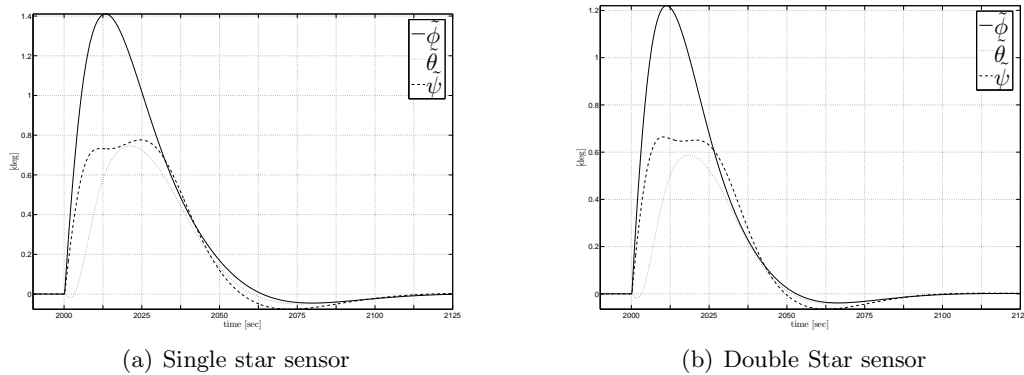


**Figure 6.2:** Star filters transient errors

The figure presents an graphical representation of the estimation error,  $\tilde{\Theta} = \Theta - \hat{\Theta}$ , in the period after attitude control is applied, and illustrates the transient performances of the filters. The table

presents the numerical Euler angle and angular velocity estimation errors in the period before and after the transient period, and illustrates the filters steady-state performances. Table 6.2(b) displays the attitude control performances when using estimated state feedback. The performance of the remaining determination schemes will be displayed in the same manner as presented here.

(a) Euler angle estimation errors			(b) controller errors		
	Single	Double		Single	Double
Conv.:	1.5 sec	1.1 sec	Conv.:	87 sec	74 sec
$\tilde{\Theta}$ RMS:	$\begin{bmatrix} 2.316 \\ 2.480 \\ 2.442 \end{bmatrix} \cdot 10^{-5}$	$\begin{bmatrix} 1.974 \\ 2.035 \\ 1.760 \end{bmatrix} \cdot 10^{-5}$	$\Theta$ RMS	$\begin{bmatrix} 4.167 \\ 0.356 \\ 3.656 \end{bmatrix} \cdot 10^{-4}$	$\begin{bmatrix} 4.139 \\ 0.334 \\ 3.658 \end{bmatrix} \cdot 10^{-4}$
$\tilde{\omega}_{ob}^b$ RMS:	$\begin{bmatrix} 4.040 \\ 4.308 \\ 4.210 \end{bmatrix} \cdot 10^{-8}$	$\begin{bmatrix} 3.820 \\ 3.874 \\ 3.733 \end{bmatrix} \cdot 10^{-8}$			

**Table 6.3:** Star filters steady-state errors

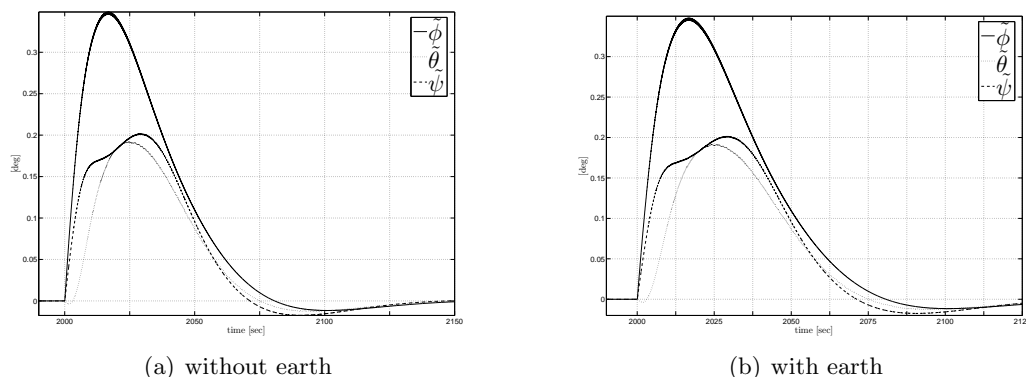
The time after initializing, to the estimation error is contained between  $\pm 0.001^\circ$ , are for the single star filter and the double star filter respectively 1.5 and 1.1 second. The the root-mean-square (RMS) estimation error at steady state indicates that the star filters determines the attitude well within the requirements, with the latter filter showing slightly improved precision.

The transient error of the determination may also be referred to as its tracking error, and is interpreted as the ability at following changing satellite states. The changes are caused by the satellite's introduction to active control torque, driving the attitude from  $[51^\circ \ 12^\circ \ 24^\circ]$  to within  $0.1^\circ$  in a time span of 87 and 74 seconds. The faster control convergence in the double star filter case, is achieved by the transient errors being smaller thus enabling faster converging of the estimates back to the true attitude. While there exists differences in the control convergence for the two systems, there are none when considering the steady-state control errors. Even if the latter filter produces more precise estimates at steady-state, it is not utilized by the presented controller.

### 6.2.2 EKF using Star-, Sun-, and Earth-sensors

The combined filters determines the attitude at a rate of 40 Hz, where they are corrected by two star measurements at every fifth iteration. Their performances are presented in table 6.4 and figure 6.3. The combined filter without earth is defined as the star and sun filter presented in section 5.2.4, while the combined filter with earth is the filter presented in section 5.2.5.

Initial attitude acquisition for the combined filters are 1.1 and 1.3 seconds, making them almost equal to the star filters. The stable-state errors for the combined filters are almost identical, and both indicate a deterioration of performance from the accuracy observed using only double star sensor. The reduced performance is caused by the two filters including of either sun sensor or sun and earth sensors, whom's less accurate measurements reduces the filters measurement sensitivity. The sensitivity reduction is traced back to the combined filters increased measurement covariances.

**Figure 6.3:** Combined filters' transient errors

	(a) Euler angle estimation errors		(b) controller errors	
	Without Earth	With Earth	Without Earth	With Earth
Conv.:	1.1 sec	1.3 sec	62 sec	62 sec
$\tilde{\Theta}$ RMS:	$\begin{bmatrix} 3.098 \\ 2.871 \\ 2.796 \end{bmatrix} \cdot 10^{-5}$	$\begin{bmatrix} 2.987 \\ 2.728 \\ 2.679 \end{bmatrix} \cdot 10^{-5}$	$\begin{bmatrix} 4.279 \\ 0.449 \\ 3.844 \end{bmatrix} \cdot 10^{-4}$	$\begin{bmatrix} 4.285 \\ 0.436 \\ 3.833 \end{bmatrix} \cdot 10^{-4}$
$\tilde{\omega}_{ob}^b$ RMS:	$\begin{bmatrix} 4.818 \\ 4.576 \\ 4.263 \end{bmatrix} \cdot 10^{-8}$	$\begin{bmatrix} 4.815 \\ 4.471 \\ 4.260 \end{bmatrix} \cdot 10^{-8}$		

**Table 6.4:** Combined filters steady-state errors

Even if the combined filters produces less accurate estimates at each timestep compared to the double star filter, they generate the estimates at 5 times the rate. The gain of increasing the filters determination rate is illustrated in figure 6.4. Here the discrete roll estimates,  $\hat{\phi}$ , produced by the star and sun filter, (dotted), and the double star filter, (dashed), are plotted against their actual continuous counterpart,  $\phi$  (solid). By considering the continuous estimation error as the area between the estimated trajectory and the actual trajectory, the estimation improvement becomes obvious.

The combined filters transient errors are even smaller than in the case of star filters. Again, this implies faster error convergence and further on to a faster control convergence, indicated by the shortened settle time of 62 seconds. By illustrating the control error as in the form of fig 6.4, it is seen that the combined filters estimates produces the most accurate attitude control.

### 6.2.3 Modified EKF

The observability properties of the satellite are investigated by calculating the observability Gramian for each of the measurements at two points in time. First shortly after initialization to inspect the static observability property, and secondly at the end of the first orbit to examine dynamic observ-

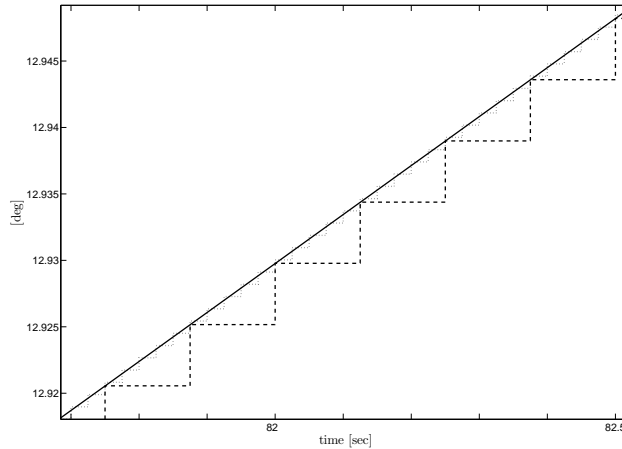


**Figure 6.4:** Double star vs. Star and sun filter

ability. Dividing the observability Gramian into four  $3 \times 3$  submatrices, the upper left part indicates the attitude observability. Due to the minor relations between the satellite's attitude and its angular velocity, the total Gramian matrices are close to singular after just 5 seconds after initialization. If only the attitude part is considered, the star measurements Gramian submatrix has condition number equal to 1, indicating a well defined, nonsingular matrix and thus static observability. The Sun and Earth measurements produced Gramian submatrices displaying condition numbers in the magnitude of  $10^4$ , indicating ill conditioned matrices. This confirms the previous statement of the system being in practical close to non observable in the static sense.

By evaluating observability at the end of the first orbit, only sun and earth Gramians are of interest. They now produce attitude submatrices with condition numbers 1.8, 31.4 and the combined 2.9, indicating that the attitude is almost fully observable by the sun measurements within one orbit, but not so observable by the earth sensor. A notable fact is that the combined sun and earth Gramian observes the attitude worse than just the sun sensor does.

Since the star sensor may become inaccessible due to image smearing, issues concerning the EKF for systems exploiting dynamic observability must be examined. The problem is illustrated by simulating a loss of star measurements over a time period of 500 seconds. The loss is examined on the star, sun, and earth filter, resulting in an determination system exploiting dynamic observability. The resulting attitude estimation errors is presented in 6.5(a). Here it is seen that the determination quickly becomes inaccurate and leaves the requirements, with  $\hat{\psi}$  continuing to diverge until the star sensor is available again.

The main problem of the EKF is that its covariance matrix fails to accurately describe the uncertainty in the estimates. This uncertainty is included in the calculation of the Kalman gains, which results in inaccurate state updates. The uncertainties in the covariance matrix is caused by the application of linear filter equations to the linearized system equations. The sensor fusion problem suffers from two effects, which combined generate poor EKF performance. First,  $\mathbf{H}_{se}$  has strong dependence on the uncertain states, which promotes the inaccuracy of the covariance matrix.

Secondly, the accuracy of the covariance matrix is important because it contains information about previous measurements.

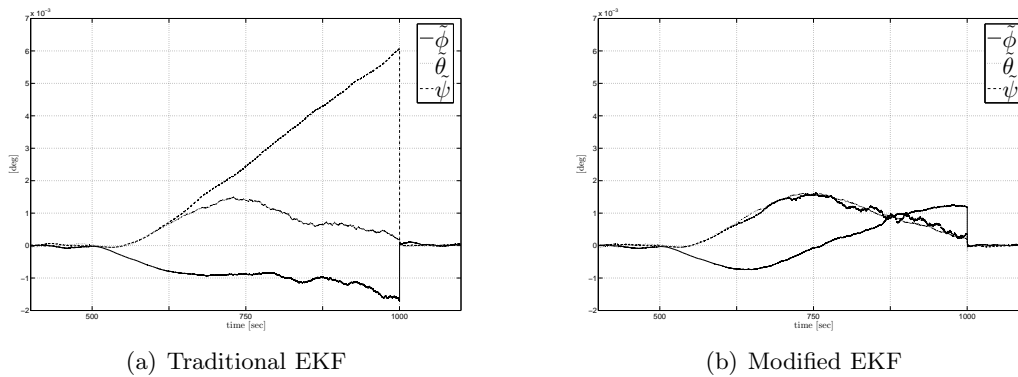


**Figure 6.5:** Simulated loss of star measurement

By modifying the star, sun and earth filter according to section 5.2.7, the above presented EKF issues may be solved. From its performance, figure 6.5(b), it is seen that compared with its traditional counterpart, the estimation error is more contained in the case of star measurement loss. It still does not meet the requirements, but more so than the alternative. The improved performance of the modified filter comes from the determination now exploiting static observable with just the sun and earth sensor, and the modified EKF having linear measurement matrix, reducing the inaccuracies in the covariance matrix.

## 6.3 Nonlinear observer

### 6.3.1 Nonlinear observer using Star sensors

As with the star filters, the nonlinear star observers determine the attitude at a rate of 8 Hz, and their performances are given in table 6.5 and figure 6.6.

The star observer shows similar points of distinction as the star filters, where the double star version displays best performances. Compared to the filters, the observers have slower initial attitude acquisition and greater steady-state and errors. While the errors are greater, the steady-state control performances are maintained, and the settling times of 59 and 50 seconds indicate faster determination dynamics.

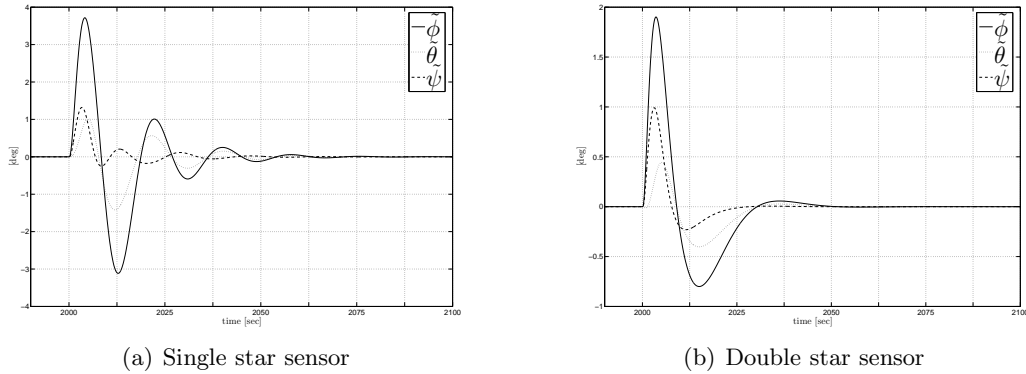


Figure 6.6: Star observers transient errors

	Single	Double		Single	Double
(a) Euler angle estimation errors			(b) controller errors		
Conv.:	12.2 sec	12.1 sec	Conv.:	59 sec	50 sec
$\tilde{\Theta}$ RMS:	$\begin{bmatrix} 5.501 \\ 5.472 \\ 6.387 \end{bmatrix} \cdot 10^{-5}$	$\begin{bmatrix} 3.666 \\ 3.764 \\ 4.325 \end{bmatrix} \cdot 10^{-5}$	$\Theta$ RMS	$\begin{bmatrix} 4.224 \\ 0.429 \\ 3.707 \end{bmatrix} \cdot 10^{-4}$	$\begin{bmatrix} 4.183 \\ 0.043 \\ 3.685 \end{bmatrix} \cdot 10^{-4}$
$\tilde{\omega}_{ob}^b$ RMS:	$\begin{bmatrix} 4.181 \\ 4.058 \\ 6.148 \end{bmatrix} \cdot 10^{-8}$	$\begin{bmatrix} 2.166 \\ 2.224 \\ 3.414 \end{bmatrix} \cdot 10^{-7}$			

Table 6.5: Star observers steady-state errors

### 6.3.2 Nonlinear observer using Star-, Sun- and Earth-sensors

As with the combined filters, the combined observers determines the attitude at a rate of 40 Hz, where they are corrected by two star measurements at every fifth iteration. The combined observers does not display the same relative performance as the combined filters, and where the combined filters indicated similar performances, the combined observers performances greatly differ.

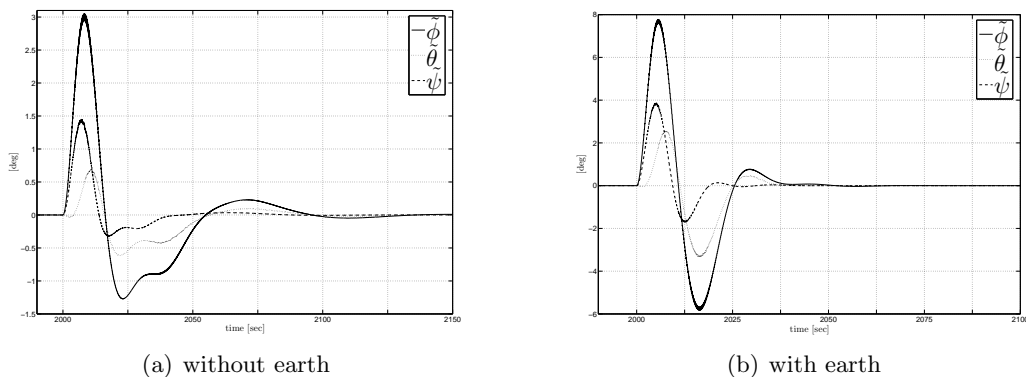


Figure 6.7: Combined observers transient errors

The combined observers initial attitude acquisitions are the slowest of all the presented determination schemes at 65 and 30 seconds. While the star, sun, and earth observers display improved determination compared to the double star observer, the star and sun observer deteriorates the determination. The improved and worsened performances of the combined observers are also apparent in the resulting control performance. Considering the increased performances of the star, sun, and earth observer and its increased determination rate, the resulting performance is superior to the other presented observers and slightly better than the star, sun, and earth filter.

(a) Euler angle estimation errors			(b) controller errors		
	Without Earth	With Earth		Without Earth	With Earth
Conv.:	65 sec	30 sec	Conv.:	139.6 sec	50.6 sec
$\tilde{\Theta}$ RMS:	$\begin{bmatrix} 0.277 \\ 1.399 \\ 1.842 \end{bmatrix} \cdot 10^{-4}$	$\begin{bmatrix} 2.252 \\ 2.401 \\ 2.789 \end{bmatrix} \cdot 10^{-5}$	$\Theta$ RMS	$\begin{bmatrix} 0.0052 \\ 0.0003 \\ 0.0046 \end{bmatrix}$	$\begin{bmatrix} 4.198 \\ 0.041 \\ 3.703 \end{bmatrix} \cdot 10^{-4}$
$\tilde{\omega}_{ob}^b$ RMS:	$\begin{bmatrix} 1.205 \\ 7.435 \\ 8.217 \end{bmatrix} \cdot 10^{-6}$	$\begin{bmatrix} 0.900 \\ 0.940 \\ 1.476 \end{bmatrix} \cdot 10^{-7}$			

**Table 6.6:** Combined observers steady-state errors

The poor performance of the star and sun observer is caused by the observer requiring full attitude information while the sun sensor only yields underdetermined attitude information. The observer does not utilize the star measurements dynamic observability property as the EKF does through its calculation of a covariance matrix.

## 6.4 Effect of attitude determination

By comparing the performance of the attitude control using the star filters estimates as state-feedback with the attitude control using sensor measurements directly as state-feedback, the determination effect may be illustrated. Since the controller is dependent on the satellite's angular velocities,  $\omega_{ob}^b$ , it must be computed directly from the star sensor measurements. By using the kinematic equations, (4.10), the angular velocities may be calculated as

$$\omega_{ob,k}^b = 2\mathbf{J}^T(\mathbf{q}_{star,k})\dot{\mathbf{q}}_k \quad (6.1)$$

where

$$\mathbf{J}(\mathbf{q}_k) = \begin{bmatrix} \epsilon_k^T \\ \eta_k \mathbf{I}_{3 \times 3} + \mathbf{S}(\epsilon_k) \end{bmatrix} \quad (6.2)$$

and the quaternion derivate,  $\dot{\mathbf{q}}_k$ , is computed from knowledge of current and last measurement as

$$\dot{\mathbf{q}}_k = \mathbf{q}_{star,k} - \mathbf{q}_{star,k-1} \quad (6.3)$$

The differences of using the single star filters estimates versus the measurements directly as state feedback is presented in figure 6.8.

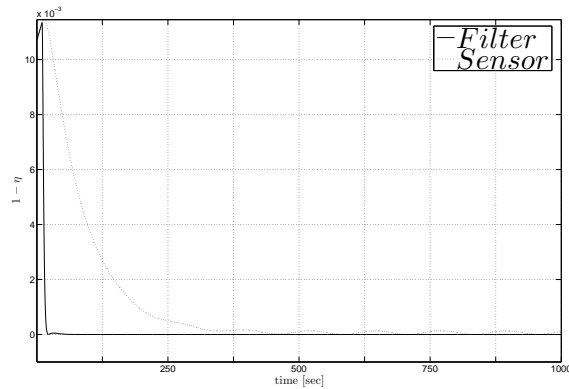


**Figure 6.8:** Satellite propagation simulink overview

Here the controller is turned on within 10 seconds of filter initialization. The control using only star measurement directly is slow in converging, and at steady-state oscillate with magnitude  $2^\circ$  about  $0^\circ$ . The performance using estimated feedback is discussed in section 6.2.1, and compared with using the star measurements directly, a far better approach. By using the above calculations to produce the attitude and angular velocity, it introduces some major errors. The angular velocities are colored by not compensating for noisy measurements, and thus include the differensiated noise component. The noise are usually fast changing, and a large error component in the calculation of the angular velocity is therefor introduced.

## Chapter 7

# Concluding Remarks and Recommendations

This thesis develops attitude determination schemes for an active stabilized and gravity-gradient stable small satellite. Its small size excludes the use of inertial measurements units, and attitude determination is based on observations of the relative positions of the Sun, the Earth, and the surrounding stars.

### 7.1 Conclusion

The attitude determination has desired accuracy demands of  $0.001^\circ$  about each axis, and these are sought met by employing either an extended Kalman filter or a nonlinear observer. While the Kalman filter relies on mathematical models of the satellite and sensors, combined with noise assumptions, the nonlinear observer relies just on the satellite model to estimate the satellite's attitude and angular velocity. Each of the two determination schemes derive the attitude based on four different sensor configurations.

The accuracy demands of the attitude determination system are easily met by all the presented determination schemes. Best determination is attained using the sun and earth measurements, at an output rate of 40 Hz, as main sensors, and performing corrections with two star sensors at every fifth iteration. Compared to just using the accurate star sensors the resulting determination displays similar root-mean-square (RMS) errors while generating them at 5 times the rate. Best determination is achieved with the EKF and by using all available sensors to determine the attitude with a RMS error of  $0.00003^\circ$  from their true values. Including active attitude control does not affect attitude determination as its performance is identical before and after control is introduced.

When the attitude determination system is exactly determined or overdetermined, as is the case using only star sensors or star sensors in combination with sun and earth sensors, the nonlinear observer gives improved performance compared to the EKF. While producing similar RMS errors as its counterpart, the advantage is indicated by a shorter settling time of the attitude control.

In the event of an underdetermined determination system, achieved by using star and sun sensors, the EKF shows its strengths and outperforms the nonlinear observer. By storing information

of previous measurements through the calculation of a covariance matrix, the filter exploits the dynamic observability property of the sun measurements. The resulting determination produces attitude estimates with RMS errors of  $0.00003^\circ$ .

## 7.2 Recommendations

The attitude determination in this thesis does not address implementation issues. Computation demands of the presented determination schemes should be investigated. If the computations are proven to be too demanding, lowering the output rates of the sensors and examine the resulting attitude determination could be explored. A more sophisticated attitude controller, like the LQR, may be introduced to exactly investigate attainable attitude control based on the presented determination schemes.

By the implications of this thesis, further development of the nonlinear observer should be performed. Because of their ad hoc design method and simplicity, issues concerning robustness and optimality should be clarified.

# References

- Appel, P., "Attitude estimation from magnetometer and earth-albedo-corrected coarse sun sensor measurement", (In press) *Acta Astronautica*, IAA, 2004.
- Bak, T., *Spacecraft Attitude Determination - a Magnetometer Approach*, PhD thesis, Aalborg University, Denmark, 2000.
- Bar-Itzhack, I.Y., Markley, F.L., and Deutchmann, J., "Quaternion normalization in additive EKF for spacecraft attitude determination", *Flight Mechanics/Estimation Symposium*, 1991.
- Boldrini, F., Monnini, E., *The officine galileo digital sun sensor*, Officine Galileo B.U. Spazio-Firenze Plant, Italy, 2001.
- Chen, C. T., *Linear System Theory and Design*, Third Edition, Oxford University Press, New York, 1999.
- Chou, J.C.K., "Quaternion Kinematic and Dynamic Differential Equation", *IEEE Transaction on Robotics and Automation*, **RA-8**(1), pp.53-64, 1992.
- Egeland, O. and Gravdahl, J. T., *Modeling and Simulation for Automatic Control*, Department of Engineering Cybernetics, NTNU, 2002.
- Farrell, J.A., Barth, M., *Global Positioning System & Inertial Navigation*, McGraw-Hill, USA, 1998.
- Farrell, J.L., *Integrated Aircraft Navigation*, Academic, New York, 1976.
- Fauske, K. M., *nCube attitude control*, Project report, Department of Engineering Cybernetics, NTNU, 2002.
- Fossen, Thor I., *Marine Control System*, Marine Cybernetics AS, Norway, 2002.
- Gelb, A., editor. *Applied Optimal Estimation*. The M.I.T. Press, Cambridge, Massachusetts, 1974.
- Goeree, B., Chatel, G., *UASat Attitude Dynamics*, Technial Note(Draft), University of Arizona, USA, 1999.
- Huster, A., "Relative position sensing by fusing monocular vision and inertial rate sensors", submitted dissertation, Dep. of Electrical Engineering, Stanford University, USA, 2003.
- Jazwinski, A. H., *Stochastic Processes and Filtering Theory, Mathematics in Science and Engineering*, Vol. 64, Academic Press, New York, 1970

- Jørgensen, J. L., Denver, T., Betto, M., Jørgensen, P.S., *Microasc a miniature star tracker*, Technical University of Denmark, Dept. of Measurement and Instrumentation, Denmark, 2001.
- Kailath, T., Sayed, A. H., Hassibi, B., *Linear Astimation*, Prentis Hall, 2000.
- Kalman, R.E., "A New Approach to Linear Filtering and Prediction Problems", *Transactions of ASME, Series D, Journal of Basic Engineering*, Vol.82, March 1960, pp.35-45.
- Krogstad, T, *Attitude control of satellites in clusters*, Master thesis, Department of Engineering Cybernetics, NTNU, 2004.
- Kyrkjebø, E., *Three-axis attitude determination using magnetometers and a star tracker*, Master thesis, Department of Engineering Cybernetics, NTNU, 2000.
- Lefferts, E.J., Markley, F.L. and Shuster, M.D., "Kalman Filtering for Spacecraft Attitude Estimation" *Journal of Guidance, Control and Dynamics*, Vol.5, No.5, 1982, pp.417-429.
- Marins, J.L., *An Extended Kalman filter for Quaternion-based Attitude Estimation*, Engineer Deree's Thesis, Naval Postgraduate School, Monterey, California, 2000.
- Marins, J.L., Yun, X., Bachmann, E.R., McGhee, R.B., and Zyda, M.J., "An Extended Kalman Filter for Quaternion-Based Orientation Estimation Using MARG Sensors", *International Conference on Intelligent Robots and Systems*, Maui, Hawaii, USA, 29 Oct. - 03 Nov., 2001.
- Maybeck, P. S., *Stochastic Models, Estimation, and Control*, Vol. 2, Academic Press, New York, 1982.
- Nocedal, J. and Wright, S.J., *Numerical Optimization*, Springer-Verlag, New York, 1999.
- Ose, S., *Attitude determination for the Norwegian student satelite nCube*, Master thesis, Department of Engineering Cybernetics, NTNU, 2004.
- Psiaki, M. L., Martel, F., Pal, P. K., "Three-Axis Attitude Determination via Kalman Filtering of Magnetometer Data", *Journal of Guidance, Control and Dynamics*, Vol. 13, No. 3, pp 506-514, 1990.
- Rao, N.S.V., "Multisensor Fusion Under Unknown Distributions: Finite Sample Performance Guarantees", *Multisensor Fusion*, 2002.
- Salcudea, S., "A globally converfant angular velocity observer for digid body motion", *IEEE Transaction on Automatic Control*, Vol. 36, No. 12, 1991.
- Schmidt, S.F., "Computational Techniques in Kalman Filtering", AGARDograph 139, NATO Advisory Group for Aerospace Reasearch and Development, London, 1970.
- Shuster, M. D., "Three-axis attitude determination from vector observations", *Journal of Guidance and Control*, Vol. 4, No. 1, 1981.
- Soglo, P. K., 3-aksestyring av gravitasjonsstabilisert satellitt ved bruk av magnetpoler. Siv. Ing. Thesis, Department of Engineering Cybernetics, NTNU, 1994, (In Norwegian)
- Stengel, R. F., *Optimal Control and Estimation*, Dover Publications, Inc.,New York, 1994.

- Svartveit, K., *Attitude determination of the NCUBE satellite*, Master thesis, Department of Engineering Cybernetics, NTNU, 2003.
- Vallado, David A., *Fundamentals of Astrodynamics and Applications*, Second Edition, Microcosm Press & Kluwer Academic Publishers, USA, 2001.
- Wiger, Ø., *Modellering og simulering for orienteringsregulering av minisatellitt*, Project report, Department of Engineering Cybernetics, NTNU, 2003.



# Appendix A

## Reference frames

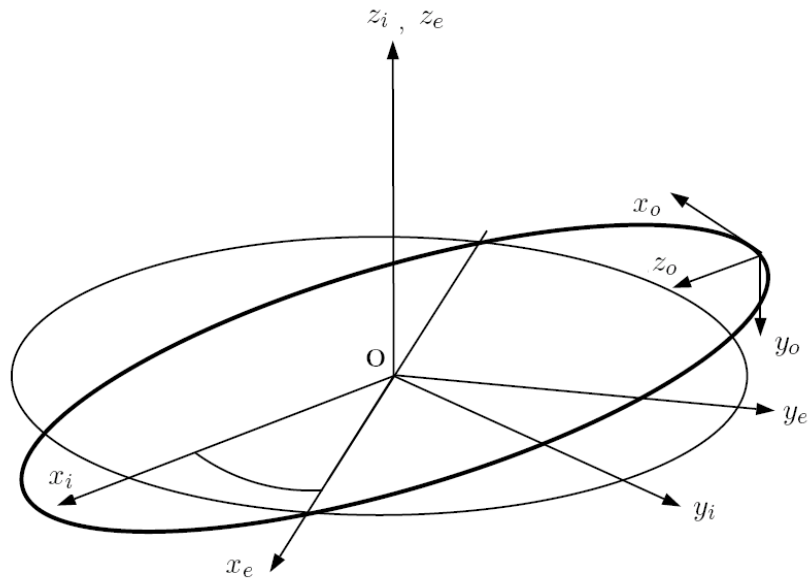
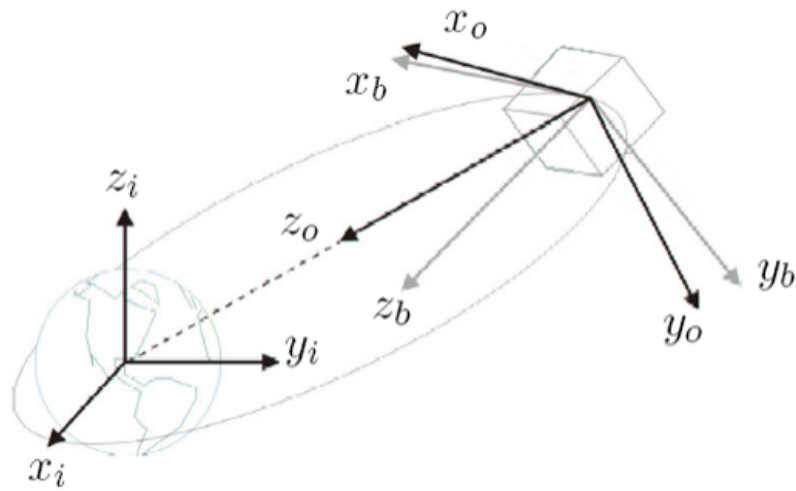


Figure A.1: ECI, ECEF, and Orbit frame



**Figure A.2:** Body, Orbit, and ECI frame

## Appendix B

# Attitude determination summary

### B.1 Extended Kalman Filter

#### B.1.1 EKF using a single Star sensor

$$\mathbf{K}_{star,k} = \bar{\mathbf{P}}_{r,k} \mathbf{H}_{star}^T [\mathbf{H}_{star} \bar{\mathbf{P}}_{r,k} \mathbf{H}_{star}^T + \mathbf{R}_{star,k}]^{-1} \quad (\text{B.1a})$$

$$\Delta \mathbf{q}_k = \mathbf{q}_{star,k} \otimes \bar{\mathbf{q}}_k^{-1} \quad (\text{B.1b})$$

$$\hat{\mathbf{q}}_k = \bar{\mathbf{q}}_k \otimes \left[ \frac{\sqrt{1 - \|\mathbf{K}_{star,\epsilon,k} \Delta \epsilon_k\|^2}}{\mathbf{K}_{star,\epsilon,k} \Delta \epsilon_k} \right] \quad (\text{B.1c})$$

$$\bar{\Delta} \epsilon_k = \epsilon_{star,k} - \bar{\epsilon}_k \quad (\text{B.1d})$$

$$\hat{\omega}_{ob,k}^b = \bar{\omega}_{ob,k}^b + \mathbf{K}_{star,\omega,k} \bar{\Delta} \epsilon_k \quad (\text{B.1e})$$

$$\hat{\mathbf{P}}_{r,k} = [\mathbf{I} - \mathbf{K}_{star,k} \mathbf{H}_{star}] \bar{\mathbf{P}}_{r,k} [\mathbf{I} - \mathbf{K}_{star,k} \mathbf{H}_{star}]^T + \mathbf{K}_{star,k} \mathbf{R}_{star,k} \mathbf{K}_{star,k}^T \quad (\text{B.1f})$$

$$\bar{\mathbf{x}}_{k+1} = \hat{\Phi}_k \hat{\mathbf{x}}_k + \mathbf{\Gamma}_k \tau_{w,k} \quad (\text{B.1g})$$

$$\bar{\mathbf{q}}_{k+1} = \frac{\bar{\mathbf{q}}_{k+1}}{\|\bar{\mathbf{q}}_{k+1}\|} \quad (\text{B.1h})$$

$$\bar{\mathbf{P}}_{r,k+1} = \hat{\Phi}_{r,k} \hat{\mathbf{P}}_{r,k} \hat{\Phi}_{r,k}^T + \mathbf{Q}_r \quad (\text{B.1i})$$

#### B.1.2 EKF using two Star sensors

$$\mathbf{K}_{stars,k} = \bar{\mathbf{P}}_{r,k} \mathbf{H}_{stars}^T [\mathbf{H}_{stars} \bar{\mathbf{P}}_{r,k} \mathbf{H}_{stars}^T + \mathbf{R}_{stars,k}]^{-1} \quad (\text{B.2a})$$

$$\Delta \mathbf{q}_{1,k} = \mathbf{q}_{star1,k} \otimes \bar{\mathbf{q}}_k^{-1} \quad (\text{B.2b})$$

$$\Delta \mathbf{q}_{2,k} = \mathbf{q}_{star2,k} \otimes \bar{\mathbf{q}}_k^{-1} \quad (\text{B.2c})$$

$$\hat{\mathbf{q}}_k = \bar{\mathbf{q}}_k \otimes \left[ \frac{\sqrt{1 - \|\mathbf{K}_{star1,\epsilon,k} \Delta \epsilon_{1,k} + \mathbf{K}_{star2,\epsilon,k} \Delta \epsilon_{2,k}\|^2}}{\mathbf{K}_{star1,\epsilon,k} \Delta \epsilon_{1,k} + \mathbf{K}_{star1,\epsilon,k} \Delta \epsilon_{1,k}} \right] \quad (\text{B.2d})$$

$$\bar{\Delta}\epsilon_{1,k} = \epsilon_{star1,k} - \bar{\epsilon}_k \quad (\text{B.2e})$$

$$\bar{\Delta}\epsilon_{2,k} = \epsilon_{star2,k} - \bar{\epsilon}_k \quad (\text{B.2f})$$

$$\hat{\omega}_{ob,k}^b = \bar{\omega}_{ob,k}^b + \mathbf{K}_{star1,\omega,k} \bar{\Delta}\epsilon_{1,k} + \mathbf{K}_{star2,\omega,k} \bar{\Delta}\epsilon_{2,k} \quad (\text{B.2g})$$

$$\hat{\mathbf{P}}_{r,k} = [\mathbf{I} - \mathbf{K}_{stars,k} \mathbf{H}_{stars}] \bar{\mathbf{P}}_{r,k} [\mathbf{I} - \mathbf{K}_{stars,k} \mathbf{H}_{stars}]^T + \mathbf{K}_{stars,k} \mathbf{R}_{stars,k} \mathbf{K}_{stars,k}^T \quad (\text{B.2h})$$

$$\bar{\mathbf{x}}_{k+1} = \hat{\Phi}_k \hat{\mathbf{x}}_k + \mathbf{\Gamma}_k \boldsymbol{\tau}_{w,k} \quad (\text{B.2i})$$

$$\bar{\mathbf{q}}_{k+1} = \frac{\bar{\mathbf{q}}_{k+1}}{\|\bar{\mathbf{q}}_{k+1}\|} \quad (\text{B.2j})$$

$$\bar{\mathbf{P}}_{r,k+1} = \hat{\Phi}_{r,k} \hat{\mathbf{P}}_{r,k} \hat{\Phi}_{r,k}^T + \mathbf{E}_{r,k} \mathbf{Q}_r \mathbf{E}_{r,k}^T \quad (\text{B.2k})$$

### B.1.3 EKF using Star- and Sun-sensors

$$\mathbf{H}_{sun,k} = [2\mathbf{S}(\bar{\mathbf{s}}_k^b) \quad 0_{3 \times 3}] \quad (\text{B.3a})$$

$$\mathbf{K}_{sun,k} = \bar{\mathbf{P}}_{r,k} \mathbf{H}_{sun,k}^T [\mathbf{H}_{sun,k} \bar{\mathbf{P}}_{r,k} \mathbf{H}_{sun,k}^T + \mathbf{R}_{sun,k}]^{-1} \quad (\text{B.3b})$$

$$\boldsymbol{\nu}_{s,k} = \mathbf{s}_k^b - \bar{\mathbf{s}}_k^b \quad (\text{B.3c})$$

$$\hat{\mathbf{q}}_k = \bar{\mathbf{q}}_k \otimes \begin{bmatrix} \sqrt{1 - \|\mathbf{K}_{sun,\epsilon,k} \boldsymbol{\nu}_{s,k}\|^2} \\ \mathbf{K}_{sun,\epsilon,k} \boldsymbol{\nu}_{s,k} \end{bmatrix} \quad (\text{B.3d})$$

$$\hat{\omega}_{ob,k}^b = \bar{\omega}_{ob,k}^b + \mathbf{K}_{sun,\omega,k} \boldsymbol{\nu}_{s,k} \quad (\text{B.3e})$$

$$\hat{\mathbf{P}}_{r,k} = [\mathbf{I} - \mathbf{K}_{sun,k} \mathbf{H}_{sun,k}] \bar{\mathbf{P}}_{r,k} [\mathbf{I} - \mathbf{K}_{sun,k} \mathbf{H}_{sun,k}]^T + \mathbf{K}_{sun,k} \mathbf{R}_{sun,k} \mathbf{K}_{sun,k}^T \quad (\text{B.3f})$$

(if star measurement available)

$$\mathbf{K}_{stars,k} = \bar{\mathbf{P}}_{r,k} \mathbf{H}_{stars}^T [\mathbf{H}_{stars} \bar{\mathbf{P}}_{r,k} \mathbf{H}_{stars}^T + \mathbf{R}_{stars,k}]^{-1} \quad (\text{B.3g})$$

$$\Delta \mathbf{q}_{1,k} = \mathbf{q}_{star1,k} \otimes \bar{\mathbf{q}}_k^{-1} \quad (\text{B.3h})$$

$$\Delta \mathbf{q}_{2,k} = \mathbf{q}_{star2,k} \otimes \bar{\mathbf{q}}_k^{-1} \quad (\text{B.3i})$$

$$\hat{\mathbf{q}}_k = \bar{\mathbf{q}}_k \otimes \begin{bmatrix} \sqrt{1 - \|\mathbf{K}_{star1,\epsilon,k} \Delta \epsilon_{1,k} + \mathbf{K}_{star2,\epsilon,k} \Delta \epsilon_{2,k}\|^2} \\ \mathbf{K}_{star1,\epsilon,k} \Delta \epsilon_{1,k} + \mathbf{K}_{star2,\epsilon,k} \Delta \epsilon_{2,k} \end{bmatrix} \quad (\text{B.3j})$$

$$\bar{\Delta}\epsilon_{1,k} = \epsilon_{star1,k} - \bar{\epsilon}_k \quad (\text{B.3k})$$

$$\bar{\Delta}\epsilon_{2,k} = \epsilon_{star2,k} - \bar{\epsilon}_k \quad (\text{B.3l})$$

$$\hat{\omega}_{ob,k}^b = \bar{\omega}_{ob,k}^b + \mathbf{K}_{star1,\omega,k} \bar{\Delta}\epsilon_{1,k} + \mathbf{K}_{star2,\omega,k} \bar{\Delta}\epsilon_{2,k} \quad (\text{B.3m})$$

$$\hat{\mathbf{P}}_{r,k} = [\mathbf{I} - \mathbf{K}_{stars,k} \mathbf{H}_{stars}] \bar{\mathbf{P}}_{r,k} [\mathbf{I} - \mathbf{K}_{stars,k} \mathbf{H}_{stars}]^T + \mathbf{K}_{stars,k} \mathbf{R}_{stars,k} \mathbf{K}_{stars,k}^T \quad (\text{B.3n})$$

end if

$$\bar{\mathbf{x}}_{k+1} = \hat{\Phi}_k \hat{\mathbf{x}}_k + \mathbf{\Gamma}_k \boldsymbol{\tau}_{w,k} \quad (\text{B.3o})$$

$$\bar{\mathbf{q}}_{k+1} = \frac{\bar{\mathbf{q}}_{k+1}}{\|\bar{\mathbf{q}}_{k+1}\|} \quad (\text{B.3p})$$

$$\bar{\mathbf{P}}_{r,k+1} = \hat{\Phi}_{r,k} \hat{\mathbf{P}}_{r,k} \hat{\Phi}_{r,k}^T + \mathbf{E}_{r,k} \mathbf{Q}_r \mathbf{E}_{r,k}^T \quad (\text{B.3q})$$

## B.1.4 EKF using Star-, Sun-, and Earth-sensors

$$\mathbf{H}_{sun,k} == [2\mathbf{S}(\bar{\mathbf{s}}_k^b) \quad 0_{3 \times 3}] \quad (\text{B.4a})$$

$$\mathbf{H}_{earth,k} = \left. \frac{\partial}{\partial \mathbf{x}_r} (\mathbf{y}_e^b) \right|_{\mathbf{x}_r = \bar{\mathbf{x}}_r} \quad (\text{B.4b})$$

$$\mathbf{H}_{se,k} = \begin{bmatrix} \mathbf{H}_{sun,k} \\ \mathbf{H}_{earth,k} \end{bmatrix} \quad (\text{B.4c})$$

$$\mathbf{K}_{se,k} = \bar{\mathbf{P}}_{r,k} \mathbf{H}_{se,k}^T [\mathbf{H}_{se,k} \bar{\mathbf{P}}_{r,k} \mathbf{H}_{se,k}^T + \mathbf{R}_{se,k}]^{-1} \quad (\text{B.4d})$$

$$\boldsymbol{\nu}_{se,k} = \begin{bmatrix} \boldsymbol{\nu}_{sun,k} \\ \boldsymbol{\nu}_{earth,k} \end{bmatrix} = \begin{bmatrix} \mathbf{s}_k^b - \bar{\mathbf{s}}_k^b \\ \mathbf{y}_e^b - \bar{\mathbf{y}}_e^b \end{bmatrix} \quad (\text{B.4e})$$

$$\hat{\mathbf{q}}_k = \bar{\mathbf{q}}_k \otimes \begin{bmatrix} \sqrt{1 - \|\mathbf{K}_{se,\epsilon,k} \boldsymbol{\nu}_{se,k}\|^2} \\ \mathbf{K}_{se,\epsilon,k} \boldsymbol{\nu}_{se,k} \end{bmatrix} \quad (\text{B.4f})$$

$$\hat{\boldsymbol{\omega}}_{ob,k}^b = \bar{\boldsymbol{\omega}}_{ob,k}^b + \mathbf{K}_{se,\omega,k} \boldsymbol{\nu}_{se,k} \quad (\text{B.4g})$$

$$\hat{\mathbf{P}}_{r,k} = [\mathbf{I} - \mathbf{K}_{se,k} \mathbf{H}_{se,k}] \bar{\mathbf{P}}_{r,k} [\mathbf{I} - \mathbf{K}_{se,k} \mathbf{H}_{se,k}]^T + \mathbf{K}_{se,k} \mathbf{R}_{se,k} \mathbf{K}_{se,k}^T \quad (\text{B.4h})$$

(if star measurement available)

$$\mathbf{K}_{stars,k} = \bar{\mathbf{P}}_{r,k} \mathbf{H}_{stars}^T [\mathbf{H}_{stars} \bar{\mathbf{P}}_{r,k} \mathbf{H}_{stars}^T + \mathbf{R}_{stars,k}]^{-1} \quad (\text{B.4i})$$

$$\Delta \mathbf{q}_{1,k} = \mathbf{q}_{star1,k} \otimes \bar{\mathbf{q}}_k^{-1} \quad (\text{B.4j})$$

$$\Delta \mathbf{q}_{2,k} = \mathbf{q}_{star2,k} \otimes \bar{\mathbf{q}}_k^{-1} \quad (\text{B.4k})$$

$$\hat{\mathbf{q}}_k = \bar{\mathbf{q}}_k \otimes \begin{bmatrix} \sqrt{1 - \|\mathbf{K}_{star1,\epsilon,k} \Delta \boldsymbol{\epsilon}_{1,k} + \mathbf{K}_{star2,\epsilon,k} \Delta \boldsymbol{\epsilon}_{2,k}\|^2} \\ \mathbf{K}_{star1,\epsilon,k} \Delta \boldsymbol{\epsilon}_{1,k} + \mathbf{K}_{star2,\epsilon,k} \Delta \boldsymbol{\epsilon}_{2,k} \end{bmatrix} \quad (\text{B.4l})$$

$$\bar{\Delta} \boldsymbol{\epsilon}_{1,k} = \boldsymbol{\epsilon}_{star1,k} - \bar{\boldsymbol{\epsilon}}_k \quad (\text{B.4m})$$

$$\bar{\Delta} \boldsymbol{\epsilon}_{2,k} = \boldsymbol{\epsilon}_{star2,k} - \bar{\boldsymbol{\epsilon}}_k \quad (\text{B.4n})$$

$$\hat{\boldsymbol{\omega}}_{ob,k}^b = \bar{\boldsymbol{\omega}}_{ob,k}^b + \mathbf{K}_{star1,\omega,k} \bar{\Delta} \boldsymbol{\epsilon}_{1,k} + \mathbf{K}_{star2,\omega,k} \bar{\Delta} \boldsymbol{\epsilon}_{2,k} \quad (\text{B.4o})$$

$$\hat{\mathbf{P}}_{r,k} = [\mathbf{I} - \mathbf{K}_{stars,k} \mathbf{H}_{stars}] \bar{\mathbf{P}}_{r,k} [\mathbf{I} - \mathbf{K}_{stars,k} \mathbf{H}_{stars}]^T + \mathbf{K}_{stars,k} \mathbf{R}_{stars,k} \mathbf{K}_{stars,k}^T \quad (\text{B.4p})$$

end if

$$\bar{\mathbf{x}}_{k+1} = \hat{\boldsymbol{\Phi}}_k \hat{\mathbf{x}}_k + \boldsymbol{\Gamma}_k \boldsymbol{\tau}_w \quad (\text{B.4q})$$

$$\bar{\mathbf{q}}_{k+1} = \frac{\bar{\mathbf{q}}_{k+1}}{\|\bar{\mathbf{q}}_{k+1}\|} \quad (\text{B.4r})$$

$$\bar{\mathbf{P}}_{r,k+1} = \hat{\boldsymbol{\Phi}}_{r,k} \hat{\mathbf{P}}_{r,k} \hat{\boldsymbol{\Phi}}_{r,k}^T + \mathbf{E}_{r,k} \mathbf{Q}_r \mathbf{E}_{r,k}^T \quad (\text{B.4s})$$

## B.1.5 Modified EKF

$$J = - \left[ \left( \frac{\partial \mathbf{M}}{\partial \eta_{g,k}} \mathbf{y}_m^b \right) \left( \frac{\partial \mathbf{M}}{\partial \epsilon_{g,1,k}} \mathbf{y}_m^b \right) \left( \frac{\partial \mathbf{M}}{\partial \epsilon_{g,2,k}} \mathbf{y}_m^b \right) \left( \frac{\partial \mathbf{M}}{\partial \epsilon_{g,3,k}} \mathbf{y}_m^b \right) \right] \quad (\text{B.5a})$$

$$\hat{\mathbf{q}}_{g,k+1} = \hat{\mathbf{q}}_{g,k} - [J^T(\hat{\mathbf{q}}_{g,k})J(\hat{\mathbf{q}}_{g,k})]^{-1} J^T(\hat{\mathbf{q}}_{g,k}) \boldsymbol{\varepsilon}^o(\hat{\mathbf{q}}_{g,k}) \quad (\text{B.5b})$$

$$\mathbf{K}_{gauss,k} = \bar{\mathbf{P}}_{r,k} \mathbf{H}_{gauss}^T [\mathbf{H}_{gauss} \bar{\mathbf{P}}_{r,k} \mathbf{H}_{gauss}^T + \mathbf{R}_{gauss}]^{-1} \quad (\text{B.5c})$$

$$\Delta \mathbf{q}_k = \hat{\mathbf{q}}_{g,k} \otimes \hat{\mathbf{q}}_k^{-1} \quad (\text{B.5d})$$

$$\hat{\mathbf{q}}_k = \bar{\mathbf{q}}_k \otimes \left[ \frac{\sqrt{1 - \|\mathbf{K}_{gauss,\epsilon,k} \Delta \boldsymbol{\epsilon}_k\|^2}}{\mathbf{K}_{gauss,\epsilon,k} \Delta \boldsymbol{\epsilon}_k} \right] \quad (\text{B.5e})$$

$$\bar{\Delta} \boldsymbol{\epsilon}_k = \boldsymbol{\epsilon}_{g,k} - \hat{\boldsymbol{\epsilon}}_k \quad (\text{B.5f})$$

$$\hat{\boldsymbol{\omega}}_{ob,k}^b = \bar{\boldsymbol{\omega}}_{ob,k}^b + \mathbf{K}_{gauss,\omega,k} \bar{\Delta} \boldsymbol{\epsilon}_k \quad (\text{B.5g})$$

$$\hat{\mathbf{P}}_{r,k} = [\mathbf{I} - \mathbf{K}_{gauss,k} \mathbf{H}_{gauss}] \bar{\mathbf{P}}_{r,k} [\mathbf{I} - \mathbf{K}_{gauss,k} \mathbf{H}_{gauss}]^T + \mathbf{K}_{gauss,k} \mathbf{R}_{gauss} \mathbf{K}_{gauss,k}^T \quad (\text{B.5h})$$

(if star measurement available)

$$\mathbf{K}_{stars,k} = \bar{\mathbf{P}}_{r,k} \mathbf{H}_{stars}^T [\mathbf{H}_{stars} \bar{\mathbf{P}}_{r,k} \mathbf{H}_{stars}^T + \mathbf{R}_{stars,k}]^{-1} \quad (\text{B.5i})$$

$$\Delta \mathbf{q}_{1,k} = \mathbf{q}_{star1,k} \otimes \bar{\mathbf{q}}_k^{-1} \quad (\text{B.5j})$$

$$\Delta \mathbf{q}_{2,k} = \mathbf{q}_{star2,k} \otimes \bar{\mathbf{q}}_k^{-1} \quad (\text{B.5k})$$

$$\hat{\mathbf{q}}_k = \bar{\mathbf{q}}_k \otimes \left[ \frac{\sqrt{1 - \|\mathbf{K}_{star1,\epsilon,k} \Delta \boldsymbol{\epsilon}_{1,k} + \mathbf{K}_{star2,\epsilon,k} \Delta \boldsymbol{\epsilon}_{2,k}\|^2}}{\mathbf{K}_{star1,\epsilon,k} \Delta \boldsymbol{\epsilon}_{1,k} + \mathbf{K}_{star2,\epsilon,k} \Delta \boldsymbol{\epsilon}_{2,k}} \right] \quad (\text{B.5l})$$

$$\bar{\Delta} \boldsymbol{\epsilon}_{1,k} = \boldsymbol{\epsilon}_{star1,k} - \bar{\boldsymbol{\epsilon}}_k \quad (\text{B.5m})$$

$$\bar{\Delta} \boldsymbol{\epsilon}_{2,k} = \boldsymbol{\epsilon}_{star2,k} - \bar{\boldsymbol{\epsilon}}_k \quad (\text{B.5n})$$

$$\hat{\boldsymbol{\omega}}_{ob,k}^b = \bar{\boldsymbol{\omega}}_{ob,k}^b + \mathbf{K}_{star1,\omega,k} \bar{\Delta} \boldsymbol{\epsilon}_{1,k} + \mathbf{K}_{star2,\omega,k} \bar{\Delta} \boldsymbol{\epsilon}_{2,k} \quad (\text{B.5o})$$

$$\hat{\mathbf{P}}_{r,k} = [\mathbf{I} - \mathbf{K}_{stars,k} \mathbf{H}_{stars}] \bar{\mathbf{P}}_{r,k} [\mathbf{I} - \mathbf{K}_{stars,k} \mathbf{H}_{stars}]^T + \mathbf{K}_{stars,k} \mathbf{R}_{stars,k} \mathbf{K}_{stars,k}^T \quad (\text{B.5p})$$

end if

$$\bar{\mathbf{x}}_{k+1} = \hat{\boldsymbol{\Phi}}_k \hat{\mathbf{x}}_k + \boldsymbol{\Gamma}_k \boldsymbol{\tau}_{w,k} \quad (\text{B.5q})$$

$$\bar{\mathbf{q}}_{k+1} = \frac{\bar{\mathbf{q}}_{k+1}}{\|\bar{\mathbf{q}}_{k+1}\|} \quad (\text{B.5r})$$

$$\bar{\mathbf{P}}_{r,k+1} = \hat{\boldsymbol{\Phi}}_{r,k} \bar{\mathbf{P}}_{r,k} \hat{\boldsymbol{\Phi}}_{r,k}^T + \mathbf{E}_{r,k} \mathbf{Q}_r \mathbf{E}_{r,k}^T \quad (\text{B.5s})$$

## B.2 Nonlinear Observer

### B.2.1 Nonlinear observer using a single star sensor

$$\hat{\mathbf{g}}_k^b = 3\omega_o^2 \hat{\mathbf{c}}_{3,k} \times \mathbf{I}^b \hat{\mathbf{c}}_{3,k} \quad (\text{B.6a})$$

$$\hat{\mathbf{h}}_{k+1}^b = \hat{\mathbf{h}}_k^b + \mathbf{R}_e(\eta_{s,k}, \epsilon_{s,k}) [\hat{\mathbf{g}}_k^b + \frac{1}{2} k_p (\mathbf{I}^b)^{-1} \mathbf{e}_k \text{sgn}(e_{0,k})] \Delta t \quad (\text{B.6b})$$

$$\hat{\mathbf{h}}_{w,k}^b = \mathbf{A} \mathbf{I}_w (\boldsymbol{\omega}_{w,k} + \mathbf{A}^T \hat{\boldsymbol{\omega}}_{ob,k}^b) \quad (\text{B.6c})$$

$$\hat{\boldsymbol{\omega}}_{ob,k+1}^b = (\mathbf{I}^b)^{-1} \mathbf{R}_e(\eta_{s,k}, \epsilon_{s,k})^T (\hat{\mathbf{h}}_k^b - \hat{\mathbf{h}}_{w,k}^b) \quad (\text{B.6d})$$

$$\hat{\mathbf{q}}_{k+1} = \hat{\mathbf{q}}_k + \frac{1}{2} \begin{bmatrix} -\hat{\boldsymbol{\epsilon}}_k^T \\ \hat{\eta}_k \mathbf{I} + \mathbf{S}(\hat{\boldsymbol{\epsilon}}_k) \end{bmatrix} \left( \hat{\boldsymbol{\omega}}_{ob,k}^b + \frac{1}{2} k_v \mathbf{R}_e(\eta_{s,k}, \epsilon_{s,k}) (\mathbf{I}^b)^{-1} \mathbf{R}_e(\eta_{s,k}, \epsilon_{s,k})^T \mathbf{e}_k \text{sgn}(e_{0,k}) \right) \Delta t \quad (\text{B.6e})$$

$$e_{0,k} = \eta_{s,k} \hat{\eta}_k + \boldsymbol{\epsilon}_{s,k}^T \hat{\boldsymbol{\epsilon}}_k \quad (\text{B.6f})$$

$$\mathbf{e}_k = \hat{\eta}_k \boldsymbol{\epsilon}_{s,k} - \eta_{s,k} \hat{\boldsymbol{\epsilon}}_k + \mathbf{S}(\boldsymbol{\epsilon}_{s,k}) \hat{\boldsymbol{\epsilon}}_k \quad (\text{B.6g})$$

### B.2.2 Nonlinear observer using two star sensors

$$\Delta \mathbf{q}_k = \begin{bmatrix} \Delta \eta_k \\ \Delta \boldsymbol{\epsilon}_k \end{bmatrix} = \mathbf{q}_{s1,k} \otimes (\mathbf{q}_{s2,k})^{-1} \quad (\text{B.7a})$$

$$\mathbf{q}_{c,k} = \mathbf{q}_{s2,k} \otimes \begin{bmatrix} \sqrt{1 - \|\frac{1}{2} \Delta \boldsymbol{\epsilon}_k\|^2} \\ \frac{1}{2} \Delta \boldsymbol{\epsilon}_k \end{bmatrix} \quad (\text{B.7b})$$

$$e_{0,k} = \eta_{c,k} \hat{\eta}_k + \boldsymbol{\epsilon}_{c,k}^T \hat{\boldsymbol{\epsilon}}_k \quad (\text{B.7c})$$

$$\mathbf{e}_k = \hat{\eta}_k \boldsymbol{\epsilon}_{c,k} - \eta_{c,k} \hat{\boldsymbol{\epsilon}}_k + \mathbf{S}(\boldsymbol{\epsilon}_{c,k}) \hat{\boldsymbol{\epsilon}}_k \quad (\text{B.7d})$$

$$\hat{\mathbf{g}}_k^b = 3\omega_o^2 \hat{\mathbf{c}}_{3,k} \times \mathbf{I}^b \hat{\mathbf{c}}_{3,k} \quad (\text{B.7e})$$

$$\hat{\mathbf{h}}_{k+1}^b = \hat{\mathbf{h}}_k^b + \mathbf{R}_e(\eta_{c,k}, \epsilon_{c,k}) [\hat{\mathbf{g}}_k^b + \frac{1}{2} k_p (\mathbf{I}^b)^{-1} \mathbf{e}_k \text{sgn}(e_{0,k})] \Delta t \quad (\text{B.7f})$$

$$\hat{\mathbf{h}}_{w,k}^b = \mathbf{A} \mathbf{I}_w (\boldsymbol{\omega}_{w,k} + \mathbf{A}^T \hat{\boldsymbol{\omega}}_{ob,k}^b) \quad (\text{B.7g})$$

$$\hat{\boldsymbol{\omega}}_{ob,k+1}^b = (\mathbf{I}^b)^{-1} \mathbf{R}_e(\eta_{c,k}, \epsilon_{c,k})^T (\hat{\mathbf{h}}_k^b - \hat{\mathbf{h}}_{w,k}^b) \quad (\text{B.7h})$$

$$\hat{\mathbf{q}}_{k+1} = \hat{\mathbf{q}}_k + \frac{1}{2} \begin{bmatrix} -\hat{\boldsymbol{\epsilon}}_k^T \\ \hat{\eta}_k \mathbf{I} + \mathbf{S}(\hat{\boldsymbol{\epsilon}}_k) \end{bmatrix} \left( \hat{\boldsymbol{\omega}}_{ob,k}^b + \frac{1}{2} k_v \mathbf{R}_e(\eta_{c,k}, \epsilon_{c,k}) (\mathbf{I}^b)^{-1} \mathbf{R}_e(\eta_{c,k}, \epsilon_{c,k})^T \mathbf{e}_k \text{sgn}(e_{0,k}) \right) \Delta t \quad (\text{B.7i})$$

### B.2.3 Nonlinear observer using stars and sun sensors

$$\hat{\mathbf{S}}_k^b = \mathbf{R}_e(\hat{\boldsymbol{\eta}}_k, \hat{\boldsymbol{\epsilon}}_k)^T \mathbf{s}_{ref,k}^o \quad (\text{B.8a})$$

$$\boldsymbol{\nu}_{sun,k} = \mathbf{s}_k^b - \hat{\mathbf{S}}_k^b \quad (\text{B.8b})$$

$$\mathbf{H}_k = 2\mathbf{S}(\hat{\mathbf{S}}_k^b) \quad (\text{B.8c})$$

$$\hat{\mathbf{g}}_k^b = 3\omega_o^2 \hat{\mathbf{c}}_{3,k} \times \mathbf{I}^b \hat{\mathbf{c}}_{3,k} \quad (\text{B.8d})$$

$$\hat{\mathbf{h}}_{k+1}^b = \hat{\mathbf{h}}_k^b + \mathbf{R}_e(\hat{\boldsymbol{\eta}}, \hat{\boldsymbol{\epsilon}})[\hat{\mathbf{g}}_k^b + l_1 \mathbf{I} \mathbf{H}_k^\dagger \boldsymbol{\nu}_{sun,k}] \Delta t \quad (\text{B.8e})$$

$$\hat{\mathbf{h}}_{w,k}^b = \mathbf{A} \mathbf{I}_w (\boldsymbol{\omega}_{w,k} + \mathbf{A}^T \hat{\boldsymbol{\omega}}_{ob,k}^b) \quad (\text{B.8f})$$

$$\hat{\boldsymbol{\omega}}_{ob,k+1}^b = (\mathbf{I}^b)^{-1} \mathbf{R}_e(\hat{\boldsymbol{\eta}}, \hat{\boldsymbol{\epsilon}})^T (\hat{\mathbf{h}}_k^b - \hat{\mathbf{h}}_{w,k}^b) \quad (\text{B.8g})$$

$$\hat{\mathbf{q}}_{k+1} = \hat{\mathbf{q}}_k + \frac{1}{2} \begin{bmatrix} -\hat{\boldsymbol{\epsilon}}_k^T \\ \hat{\boldsymbol{\eta}}_k \mathbf{I} + \mathbf{S}(\hat{\boldsymbol{\epsilon}}_k) \end{bmatrix} (\hat{\boldsymbol{\omega}}_{ob,k}^b + l_2 \mathbf{I} \mathbf{H}_k^\dagger \boldsymbol{\nu}_{sun,k}) \Delta t \quad (\text{B.8h})$$

if (star measurement available)

$$\Delta \mathbf{q}_k = \begin{bmatrix} \Delta \eta_k \\ \Delta \boldsymbol{\epsilon}_k \end{bmatrix} = \mathbf{q}_{s1,k} \otimes (\mathbf{q}_{s2,k})^{-1} \quad (\text{B.8i})$$

$$\mathbf{q}_{c,k} = \mathbf{q}_{s2,k} \otimes \begin{bmatrix} \sqrt{1 - \|\frac{1}{2} \Delta \boldsymbol{\epsilon}_k\|^2} \\ \frac{1}{2} \Delta \boldsymbol{\epsilon}_k \end{bmatrix} \quad (\text{B.8j})$$

$$e_{0,k} = \eta_{c,k} \hat{\boldsymbol{\eta}}_k + \boldsymbol{\epsilon}_{c,k}^T \hat{\boldsymbol{\epsilon}}_k \quad (\text{B.8k})$$

$$\mathbf{e}_k = \hat{\boldsymbol{\eta}}_k \boldsymbol{\epsilon}_{c,k} - \eta_{c,k} \hat{\boldsymbol{\epsilon}}_k + \mathbf{S}(\boldsymbol{\epsilon}_{c,k}) \hat{\boldsymbol{\epsilon}}_k \quad (\text{B.8l})$$

$$\hat{\mathbf{g}}_k^b = 3\omega_o^2 \hat{\mathbf{c}}_{3,k} \times \mathbf{I}^b \hat{\mathbf{c}}_{3,k} \quad (\text{B.8m})$$

$$\hat{\mathbf{h}}_{k+1}^b = \hat{\mathbf{h}}_k^b + \mathbf{R}_e(\eta_{c,k}, \boldsymbol{\epsilon}_{c,k}) [\hat{\mathbf{g}}_k^b + \frac{1}{2} k_p (\mathbf{I}^b)^{-1} \mathbf{e}_k \text{sgn}(e_{0,k})] \Delta t \quad (\text{B.8n})$$

$$\hat{\mathbf{h}}_{w,k}^b = \mathbf{A} \mathbf{I}_w (\boldsymbol{\omega}_{w,k} + \mathbf{A}^T \hat{\boldsymbol{\omega}}_{ob,k}^b) \quad (\text{B.8o})$$

$$\hat{\boldsymbol{\omega}}_{ob,k+1}^b = (\mathbf{I}^b)^{-1} \mathbf{R}_e(\eta_{c,k}, \boldsymbol{\epsilon}_{c,k})^T (\hat{\mathbf{h}}_k^b - \hat{\mathbf{h}}_{w,k}^b) \quad (\text{B.8p})$$

$$\hat{\mathbf{q}}_{k+1} = \hat{\mathbf{q}}_k + \frac{1}{2} \begin{bmatrix} -\hat{\boldsymbol{\epsilon}}_k^T \\ \hat{\boldsymbol{\eta}}_k \mathbf{I} + \mathbf{S}(\hat{\boldsymbol{\epsilon}}_k) \end{bmatrix} (\hat{\boldsymbol{\omega}}_{ob,k}^b + \frac{1}{2} k_v \mathbf{R}_e(\eta_{c,k}, \boldsymbol{\epsilon}_{c,k}) (\mathbf{I}^b)^{-1} \mathbf{R}_e(\eta_{c,k}, \boldsymbol{\epsilon}_{c,k})^T \mathbf{e}_k \text{sgn}(e_{0,k})) \Delta t \quad (\text{B.8q})$$

end if

## B.2.4 Nonlinear observer using stars, sun, and earth sensors

$$J = - \left[ \left( \frac{\partial \mathbf{M}}{\partial \eta_{g,k}} \mathbf{y}_m^b \right) \left( \frac{\partial \mathbf{M}}{\partial \epsilon_{g,1,k}} \mathbf{y}_m^b \right) \left( \frac{\partial \mathbf{M}}{\partial \epsilon_{g,2,k}} \mathbf{y}_m^b \right) \left( \frac{\partial \mathbf{M}}{\partial \epsilon_{g,3,k}} \mathbf{y}_m^b \right) \right] \quad (\text{B.9a})$$

$$\hat{\mathbf{q}}_{g,k+1} = \hat{\mathbf{q}}_{g,k} - [J^T(\hat{\mathbf{q}}_{g,k})J(\hat{\mathbf{q}}_{g,k})]^{-1} J^T(\hat{\mathbf{q}}_{g,k}) \boldsymbol{\varepsilon}^o(\hat{\mathbf{q}}_{g,k}) \quad (\text{B.9b})$$

$$e_{0,k} = \hat{\eta}_{g,k} \hat{\eta}_k + \hat{\boldsymbol{\epsilon}}_{g,k}^T \hat{\boldsymbol{\epsilon}}_k \quad (\text{B.9c})$$

$$\mathbf{e}_k = \hat{\eta}_k \hat{\boldsymbol{\epsilon}}_{g,k} - \hat{\eta}_{g,k} \hat{\boldsymbol{\epsilon}}_k + \mathbf{S}(\hat{\boldsymbol{\epsilon}}_{g,k}) \hat{\boldsymbol{\epsilon}}_k \quad (\text{B.9d})$$

$$\hat{\mathbf{g}}_k^b = 3\omega_o^2 \hat{\mathbf{c}}_{3,k} \times \mathbf{I}^b \hat{\mathbf{c}}_{3,k} \quad (\text{B.9e})$$

$$\hat{\mathbf{h}}_{k+1}^b = \hat{\mathbf{h}}_k^b + \mathbf{R}_e(\hat{\eta}_{g,k}, \hat{\boldsymbol{\epsilon}}_{g,k}) [\hat{\mathbf{g}}_k^b + \frac{1}{2} k_p (\mathbf{I}^b)^{-1} \mathbf{e}_k \text{sgn}(e_{0,k})] \Delta t \quad (\text{B.9f})$$

$$\hat{\mathbf{h}}_{w,k}^b = \mathbf{A} \mathbf{I}_w (\boldsymbol{\omega}_{w,k} + \mathbf{A}^T \hat{\boldsymbol{\omega}}_{ob,k}^b) \quad (\text{B.9g})$$

$$\hat{\boldsymbol{\omega}}_{ob,k+1}^b = (\mathbf{I}^b)^{-1} \mathbf{R}_e(\hat{\eta}_{g,k}, \hat{\boldsymbol{\epsilon}}_{g,k})^T (\hat{\mathbf{h}}_k^b - \hat{\mathbf{h}}_{w,k}^b) \quad (\text{B.9h})$$

$$\hat{\mathbf{q}}_{k+1} = \hat{\mathbf{q}}_k + \frac{1}{2} \begin{bmatrix} -\hat{\boldsymbol{\epsilon}}_k^T \\ \hat{\eta}_k \mathbf{I} + \mathbf{S}(\hat{\boldsymbol{\epsilon}}_k) \end{bmatrix} \left( \hat{\boldsymbol{\omega}}_{ob,k}^b + \frac{1}{2} k_v \mathbf{R}_e(\hat{\eta}_{g,k}, \hat{\boldsymbol{\epsilon}}_{g,k}) (\mathbf{I}^b)^{-1} \mathbf{R}_e(\hat{\eta}_{g,k}, \hat{\boldsymbol{\epsilon}}_{g,k})^T \mathbf{e}_k \text{sgn}(e_{0,k}) \right) \Delta t \quad (\text{B.9i})$$

(if star measurement available)

$$\Delta \mathbf{q}_k = \begin{bmatrix} \Delta \eta_k \\ \Delta \boldsymbol{\epsilon}_k \end{bmatrix} = \mathbf{q}_{s1,k} \otimes (\mathbf{q}_{s2,k})^{-1} \quad (\text{B.9j})$$

$$\mathbf{q}_{c,k} = \mathbf{q}_{s2,k} \otimes \begin{bmatrix} \sqrt{1 - \|\frac{1}{2} \Delta \boldsymbol{\epsilon}_k\|^2} \\ \frac{1}{2} \Delta \boldsymbol{\epsilon}_k \end{bmatrix} \quad (\text{B.9k})$$

$$e_{0,k} = \eta_{c,k} \hat{\eta}_k + \boldsymbol{\epsilon}_{c,k}^T \hat{\boldsymbol{\epsilon}}_k \quad (\text{B.9l})$$

$$\mathbf{e}_k = \hat{\eta}_k \boldsymbol{\epsilon}_{c,k} - \eta_{c,k} \hat{\boldsymbol{\epsilon}}_k + \mathbf{S}(\boldsymbol{\epsilon}_{c,k}) \hat{\boldsymbol{\epsilon}}_k \quad (\text{B.9m})$$

$$\hat{\mathbf{g}}_k^b = 3\omega_o^2 \hat{\mathbf{c}}_{3,k} \times \mathbf{I}^b \hat{\mathbf{c}}_{3,k} \quad (\text{B.9n})$$

$$\hat{\mathbf{h}}_{k+1}^b = \hat{\mathbf{h}}_k^b + \mathbf{R}_e(\eta_{c,k}, \boldsymbol{\epsilon}_{c,k}) [\hat{\mathbf{g}}_k^b + \frac{1}{2} k_p (\mathbf{I}^b)^{-1} \mathbf{e}_k \text{sgn}(e_{0,k})] \Delta t \quad (\text{B.9o})$$

$$\hat{\mathbf{h}}_{w,k}^b = \mathbf{A} \mathbf{I}_w (\boldsymbol{\omega}_{w,k} + \mathbf{A}^T \hat{\boldsymbol{\omega}}_{ob,k}^b) \quad (\text{B.9p})$$

$$\hat{\boldsymbol{\omega}}_{ob,k+1}^b = (\mathbf{I}^b)^{-1} \mathbf{R}_e(\eta_{c,k}, \boldsymbol{\epsilon}_{c,k})^T (\hat{\mathbf{h}}_k^b - \hat{\mathbf{h}}_{w,k}^b) \quad (\text{B.9q})$$

$$\hat{\mathbf{q}}_{k+1} = \hat{\mathbf{q}}_k + \frac{1}{2} \begin{bmatrix} -\hat{\boldsymbol{\epsilon}}_k^T \\ \hat{\eta}_k \mathbf{I} + \mathbf{S}(\hat{\boldsymbol{\epsilon}}_k) \end{bmatrix} \left( \hat{\boldsymbol{\omega}}_{ob,k}^b + \frac{1}{2} k_v \mathbf{R}_e(\eta_{c,k}, \boldsymbol{\epsilon}_{c,k}) (\mathbf{I}^b)^{-1} \mathbf{R}_e(\eta_{c,k}, \boldsymbol{\epsilon}_{c,k})^T \mathbf{e}_k \text{sgn}(e_{0,k}) \right) \Delta t \quad (\text{B.9r})$$

end if



# Appendix C

## Linearization

### C.1 Added inertia model

$$\begin{aligned}
 \frac{\partial \mathbf{f}_{inertadd,1}}{\partial \mathbf{x}} &= \frac{\partial}{\partial \mathbf{x}} \left( \frac{1}{I_x} (-e_2(\omega_{ob,3}^b - c_{32}\omega_o) + e_3(\omega_{ob,2}^b - c_{22}\omega_o)) \right) \\
 &= \frac{1}{I_x} \left[ -\frac{\partial}{\partial \mathbf{x}}(e_2)\omega_{ob,3}^b - e_2 \frac{\partial}{\partial \mathbf{x}}(\omega_{ob,3}^b) + \frac{\partial}{\partial \mathbf{x}}(e_2)c_{32}\omega_o + e_2 \frac{\partial}{\partial \mathbf{x}}(c_{32})\omega_o \right. \\
 &\quad \left. + \frac{\partial}{\partial \mathbf{x}}(e_3)\omega_{ob,2}^b + e_3 \frac{\partial}{\partial \mathbf{x}}(\omega_{ob,2}^b) - \frac{\partial}{\partial \mathbf{x}}(e_3)c_{22}\omega_o - e_3 \frac{\partial}{\partial \mathbf{x}}(c_{22})\omega_o \right]
 \end{aligned} \tag{C.1}$$

$$\begin{aligned}
 \frac{\partial \mathbf{f}_{inertadd,2}}{\partial \mathbf{x}} &= \frac{\partial}{\partial \mathbf{x}} \left( \frac{1}{I_y} (e_1(\omega_{ob,3}^b - c_{32}\omega_o) - e_3(\omega_{ob,1}^b - c_{12}\omega_o)) \right) \\
 &= \frac{1}{I_y} \left[ \frac{\partial}{\partial \mathbf{x}}(e_1)\omega_{ob,3}^b + e_1 \frac{\partial}{\partial \mathbf{x}}(\omega_{ob,3}^b) - \frac{\partial}{\partial \mathbf{x}}(e_1)c_{32}\omega_o - e_1 \frac{\partial}{\partial \mathbf{x}}(c_{32})\omega_o \right. \\
 &\quad \left. - \frac{\partial}{\partial \mathbf{x}}(e_3)\omega_{ob,1}^b - e_3 \frac{\partial}{\partial \mathbf{x}}(\omega_{ob,1}^b) + \frac{\partial}{\partial \mathbf{x}}(e_3)c_{12}\omega_o + e_3 \frac{\partial}{\partial \mathbf{x}}(c_{12})\omega_o \right]
 \end{aligned} \tag{C.2}$$

$$\begin{aligned}
 \frac{\partial \mathbf{f}_{inertadd,3}}{\partial \mathbf{x}} &= \frac{\partial}{\partial \mathbf{x}} \left( \frac{1}{I_z} (-e_1(\omega_{ob,2}^b - c_{22}\omega_o) + e_2(\omega_{ob,1}^b - c_{12}\omega_o)) \right) \\
 &= \frac{1}{I_z} \left[ -\frac{\partial}{\partial \mathbf{x}}(e_1)\omega_{ob,2}^b - e_1 \frac{\partial}{\partial \mathbf{x}}(\omega_{ob,2}^b) + \frac{\partial}{\partial \mathbf{x}}(e_1)c_{22}\omega_o + e_1 \frac{\partial}{\partial \mathbf{x}}(c_{22})\omega_o \right. \\
 &\quad \left. + \frac{\partial}{\partial \mathbf{x}}(e_2)\omega_{ob,1}^b + e_2 \frac{\partial}{\partial \mathbf{x}}(\omega_{ob,1}^b) - \frac{\partial}{\partial \mathbf{x}}(e_2)c_{12}\omega_o - e_2 \frac{\partial}{\partial \mathbf{x}}(c_{12})\omega_o \right]
 \end{aligned} \tag{C.3}$$

By evaluating (C.1), (C.2), and (C.3) with respect to the kalman states one gets:

$$\frac{\partial \mathbf{f}_{inertadd,1}}{\partial \eta} = \frac{1}{I_x} \left[ \frac{\partial}{\partial \eta}(e_2)(c_{32}\omega_o - \omega_{ob,3}^b) - 2e_2\epsilon_1\omega_o + \frac{\partial}{\partial \eta}(e_3)(\omega_{ob,2}^b - c_{22}\omega_o) - 2e_3\eta\omega_o \right] \tag{C.4}$$

$$\frac{\partial \mathbf{f}_{inertadd,2}}{\partial \eta} = \frac{1}{I_y} \left[ \frac{\partial}{\partial \eta}(e_1)(\omega_{ob,3}^b - c_{32}\omega_o) + 2e_1\epsilon_1\omega_o + \frac{\partial}{\partial \eta}(e_3)(c_{12}\omega_o - \omega_{ob,1}^b) - 2e_3\epsilon_3\omega_o \right] \tag{C.5}$$

$$\frac{\partial \mathbf{f}_{inertadd,3}}{\partial \eta} = \frac{1}{I_z} \left[ \frac{\partial}{\partial \eta}(e_1)(c_{22}\omega_o - \omega_{ob,2}^b) + 2e_1\eta\omega_o + \frac{\partial}{\partial \eta}(e_2)(\omega_{ob,1}^b - c_{12}\omega_o) - 2e_2\epsilon_3\omega_o \right] \tag{C.6}$$

where

$$\begin{aligned}
\frac{\partial}{\partial \eta}(e_j) &= \frac{\partial}{\partial \eta} \left[ i_w \sum_{i=1}^4 a_{ji}(\omega_{w,i} + \sum_{k=1}^3 (a_{ki}(\omega_{ob,k}^b - c_{k2}\omega_o))) \right], \text{ for } j = 1, \dots, 3 \\
&= i_w \sum_{i=1}^4 a_{ji}(\omega_{w,i} + \sum_{k=1}^3 \frac{\partial}{\partial \eta} (a_{ki}(\omega_{ob,k}^b - c_{k2}\omega_o))), \text{ for } j = 1, \dots, 3 \\
&= i_w \sum_{i=1}^4 a_{ji}(\omega_{w,i} + \sum_{k=1}^3 (-a_{ki} \frac{\partial}{\partial \eta} (c_{k2}\omega_o))), \text{ for } j = 1, \dots, 3 \\
&= i_w \sum_{i=1}^4 a_{ji}(\omega_{w,i} - a_{1i}2\epsilon_3\omega_o - a_{2i}2\eta\omega_o + a_{3i}2\epsilon_1\omega_o), \text{ for } j = 1, \dots, 3 \tag{C.7}
\end{aligned}$$

$$\frac{\partial \mathbf{f}_{inertadd,1}}{\partial \epsilon_1} = \frac{1}{I_x} \left[ \frac{\partial}{\partial \epsilon_1} (e_2)(c_{32}\omega_o - \omega_{ob,3}^b) - 2e_2\eta\omega_o + \frac{\partial}{\partial \epsilon_1} (e_3)(\omega_{ob,2}^b - c_{22}\omega_o) + 2e_3\epsilon_1\omega_o \right] \tag{C.8}$$

$$\frac{\partial \mathbf{f}_{inertadd,2}}{\partial \epsilon_1} = \frac{1}{I_y} \left[ \frac{\partial}{\partial \epsilon_1} (e_1)(\omega_{ob,3}^b - c_{32}\omega_o) + 2e_1\eta\omega_o + \frac{\partial}{\partial \epsilon_1} (e_3)(c_{12}\omega_o - \omega_{ob,1}^b) - 2e_3\epsilon_2\omega_o \right] \tag{C.9}$$

$$\frac{\partial \mathbf{f}_{inertadd,3}}{\partial \epsilon_1} = \frac{1}{I_z} \left[ \frac{\partial}{\partial \epsilon_1} (e_1)(c_{22}\omega_o - \omega_{ob,2}^b) - 2e_1\epsilon_1\omega_o + \frac{\partial}{\partial \epsilon_1} (e_2)(\omega_{ob,1}^b - c_{12}\omega_o) - 2e_2\epsilon_2\omega_o \right] \tag{C.10}$$

where

$$\begin{aligned}
\frac{\partial}{\partial \epsilon_1}(e_j) &= \frac{\partial}{\partial \epsilon_1} \left[ i_w \sum_{i=1}^4 a_{ji}(\omega_{w,i} + \sum_{k=1}^3 (a_{ki}(\omega_{ob,k}^b - c_{k2}\omega_o))) \right], \text{ for } j = 1, \dots, 3 \\
&= i_w \sum_{i=1}^4 a_{ji}(\omega_{w,i} + \sum_{k=1}^3 (-a_{ki} \frac{\partial}{\partial \epsilon_1} (c_{k2}\omega_o))), \text{ for } j = 1, \dots, 3 \\
&= i_w \sum_{i=1}^4 a_{ji}(\omega_{w,i} - a_{1i}2\epsilon_2\omega_o + a_{2i}2\epsilon_1\omega_o + a_{3i}2\eta\omega_o), \text{ for } j = 1, \dots, 3 \tag{C.11}
\end{aligned}$$

$$\frac{\partial \mathbf{f}_{inertadd,1}}{\partial \epsilon_2} = \frac{1}{I_x} \left[ \frac{\partial}{\partial \epsilon_2} (e_2)(c_{32}\omega_o - \omega_{ob,3}^b) + 2e_2\epsilon_3\omega_o + \frac{\partial}{\partial \epsilon_2} (e_3)(\omega_{ob,2}^b - c_{22}\omega_o) - 2e_3\epsilon_2\omega_o \right] \tag{C.12}$$

$$\frac{\partial \mathbf{f}_{inertadd,2}}{\partial \epsilon_2} = \frac{1}{I_y} \left[ \frac{\partial}{\partial \epsilon_2} (e_1)(\omega_{ob,3}^b - c_{32}\omega_o) - 2e_1\epsilon_3\omega_o + \frac{\partial}{\partial \epsilon_2} (e_3)(c_{12}\omega_o - \omega_{ob,1}^b) + 2e_3\epsilon_1\omega_o \right] \tag{C.13}$$

$$\frac{\partial \mathbf{f}_{inertadd,3}}{\partial \epsilon_2} = \frac{1}{I_z} \left[ \frac{\partial}{\partial \epsilon_2} (e_1)(c_{22}\omega_o - \omega_{ob,2}^b) + 2e_1\epsilon_2\omega_o + \frac{\partial}{\partial \epsilon_2} (e_2)(\omega_{ob,1}^b - c_{12}\omega_o) - 2e_2\epsilon_1\omega_o \right] \tag{C.14}$$

where

$$\begin{aligned}
\frac{\partial}{\partial \epsilon_2}(e_j) &= \frac{\partial}{\partial \epsilon_2} \left[ i_w \sum_{i=1}^4 a_{ji}(\omega_{w,i} + \sum_{k=1}^3 (a_{ki}(\omega_{ob,k}^b - c_{k2}\omega_o))) \right], \text{ } j = 1, \dots, 3 \\
&= i_w \sum_{i=1}^4 a_{ji}(\omega_{w,i} + \sum_{k=1}^3 (-a_{ki} \frac{\partial}{\partial \epsilon_2} (c_{k2}\omega_o))), \text{ } j = 1, \dots, 3 \\
&= i_w \sum_{i=1}^4 a_{ji}(\omega_{w,i} - a_{1i}2\epsilon_1\omega_o - a_{2i}2\epsilon_2\omega_o + a_{3i}2\epsilon_3\omega_o), \text{ } j = 1, \dots, 3 \tag{C.15}
\end{aligned}$$

$$\frac{\partial \mathbf{f}_{inertadd,1}}{\partial \epsilon_3} = \frac{1}{I_x} \left[ \frac{\partial}{\partial \epsilon_3} (e_2)(c_{32}\omega_o - \omega_{ob,3}^b) + 2e_2\epsilon_2\omega_o + \frac{\partial}{\partial \epsilon_3} (e_3)(\omega_{ob,2}^b - c_{22}\omega_o) + 2e_3\epsilon_3\omega_o \right] \quad (C.16)$$

$$\frac{\partial \mathbf{f}_{inertadd,2}}{\partial \epsilon_3} = \frac{1}{I_y} \left[ \frac{\partial}{\partial \epsilon_3} (e_1)(\omega_{ob,3}^b - c_{32}\omega_o) - 2e_1\epsilon_2\omega_o + \frac{\partial}{\partial \epsilon_3} (e_3)(c_{12}\omega_o - \omega_{ob,1}^b) - 2e_3\eta\omega_o \right] \quad (C.17)$$

$$\frac{\partial \mathbf{f}_{inertadd,3}}{\partial \epsilon_3} = \frac{1}{I_z} \left[ \frac{\partial}{\partial \epsilon_3} (e_1)(c_{22}\omega_o - \omega_{ob,2}^b) - 2e_1\epsilon_3\omega_o + \frac{\partial}{\partial \epsilon_3} (e_2)(\omega_{ob,1}^b - c_{12}\omega_o) - 2e_2\eta\omega_o \right] \quad (C.18)$$

where

$$\begin{aligned} \frac{\partial}{\partial \epsilon_3} (e_j) &= \frac{\partial}{\partial \epsilon_3} \left[ i_w \sum_{i=1}^4 a_{ji}(\omega_{w,i} + \sum_{k=1}^3 (a_{ki}(\omega_{ob,k}^b - c_{k2}\omega_o))) \right], \quad \text{for } j = 1, \dots, 3 \\ &= i_w \sum_{i=1}^4 a_{ji}(\omega_{w,i} + \sum_{k=1}^3 (-a_{ki} \frac{\partial}{\partial \epsilon_3} (c_{k2}\omega_o))), \quad \text{for } j = 1, \dots, 3 \\ &= i_w \sum_{i=1}^4 a_{ji}(\omega_{w,i} - a_{1i}2\eta\omega_o + a_{2i}2\epsilon_3\omega_o + a_{3i}2\epsilon_2\omega_o), \quad \text{for } j = 1, \dots, 3 \end{aligned} \quad (C.19)$$

$$\frac{\partial \mathbf{f}_{inertadd,1}}{\partial \omega_{ob,1}^b} = \frac{1}{I_x} \left[ \frac{\partial}{\partial \omega_{ob,1}^b} (e_2)(c_{32}\omega_o - \omega_{ob,3}^b) + \frac{\partial}{\partial \omega_{ob,1}^b} (e_3)(\omega_{ob,2}^b - c_{22}\omega_o) \right] \quad (C.20)$$

$$\frac{\partial \mathbf{f}_{inertadd,2}}{\partial \omega_{ob,1}^b} = \frac{1}{I_y} \left[ \frac{\partial}{\partial \omega_{ob,1}^b} (e_1)(\omega_{ob,3}^b - c_{32}\omega_o) + \frac{\partial}{\partial \omega_{ob,1}^b} (e_3)(c_{12}\omega_o - \omega_{ob,1}^b) - e_3 \right] \quad (C.21)$$

$$\frac{\partial \mathbf{f}_{inertadd,1}}{\partial \omega_{ob,1}^b} = \frac{1}{I_z} \left[ \frac{\partial}{\partial \omega_{ob,1}^b} (e_1)(c_{22}\omega_o - \omega_{ob,2}^b) + \frac{\partial}{\partial \omega_{ob,1}^b} (e_2)(\omega_{ob,1}^b - c_{12}\omega_o) + e_2 \right] \quad (C.22)$$

where

$$\begin{aligned} \frac{\partial}{\partial \omega_{ob,1}^b} (e_j) &= \frac{\partial}{\partial \omega_{ob,1}^b} \left[ i_w \sum_{i=1}^4 a_{ji}(\omega_{w,i} + \sum_{k=1}^3 (a_{ki}(\omega_{ob,k}^b - c_{k2}\omega_o))) \right], \quad \text{for } j = 1, \dots, 3 \\ &= i_w \sum_{i=1}^4 a_{ji}(\omega_{w,i} + \sum_{k=1}^3 \frac{\partial}{\partial \omega_{ob,1}^b} (a_{ki}(\omega_{ob,k}^b - c_{k2}\omega_o))), \quad \text{for } j = 1, \dots, 3 \\ &= i_w \sum_{i=1}^4 a_{ji}(\omega_{w,i} + \sum_{k=1}^3 (a_{ki} \frac{\partial}{\partial \omega_{ob,1}^b} (\omega_{ob,k}^b))), \quad \text{for } j = 1, \dots, 3 \\ &= i_w \sum_{i=1}^4 a_{ji}(\omega_{w,i} + a_{1i}), \quad \text{for } j = 1, \dots, 3 \end{aligned} \quad (C.23)$$

$$\frac{\partial \mathbf{f}_{inertadd,1}}{\partial \omega_{ob,2}^b} = \frac{1}{I_x} \left[ \frac{\partial}{\partial \omega_{ob,2}^b} (e_2)(c_{32}\omega_o - \omega_{ob,3}^b) + \frac{\partial}{\partial \omega_{ob,2}^b} (e_3)(\omega_{ob,2}^b - c_{22}\omega_o) + e_3 \right] \quad (C.24)$$

$$\frac{\partial \mathbf{f}_{inertadd,2}}{\partial \omega_{ob,2}^b} = \frac{1}{I_y} \left[ \frac{\partial}{\partial \omega_{ob,2}^b} (e_1)(\omega_{ob,3}^b - c_{32}\omega_o) + \frac{\partial}{\partial \omega_{ob,2}^b} (e_3)(c_{12}\omega_o - \omega_{ob,1}^b) \right] \quad (C.25)$$

$$\frac{\partial \mathbf{f}_{inertadd,1}}{\partial \omega_{ob,2}^b} = \frac{1}{I_z} \left[ \frac{\partial}{\partial \omega_{ob,2}^b} (e_1)(c_{22}\omega_o - \omega_{ob,2}^b) - e_1 + \frac{\partial}{\partial \omega_{ob,2}^b} (e_2)(\omega_{ob,1}^b - c_{12}\omega_o) \right] \quad (C.26)$$

where

$$\begin{aligned}
\frac{\partial}{\partial \omega_{ob,2}^b}(e_j) &= \frac{\partial}{\partial \omega_{ob,2}^b} \left[ i_w \sum_{i=1}^4 a_{ji}(\omega_{w,i} + \sum_{k=1}^3 (a_{ki}(\omega_{ob,k}^b - c_{k2}\omega_o))) \right], \text{ for } j = 1, \dots, 3 \\
&= i_w \sum_{i=1}^4 a_{ji}(\omega_{w,i} + \sum_{k=1}^3 (a_{ki} \frac{\partial}{\partial \omega_{ob,2}^b}(\omega_{ob,k}^b))), \text{ for } j = 1, \dots, 3 \\
&= i_w \sum_{i=1}^4 a_{ji}(\omega_{w,i} + a_{2i}), \text{ for } j = 1, \dots, 3
\end{aligned} \tag{C.27}$$

$$\frac{\partial \mathbf{f}_{inertadd,1}}{\partial \omega_{ob,3}^b} = \frac{1}{I_x} \left[ \frac{\partial}{\partial \omega_{ob,3}^b}(e_2)(c_{32}\omega_o - \omega_{ob,3}^b) - e_2 + \frac{\partial}{\partial \omega_{ob,3}^b}(e_3)(\omega_{ob,2}^b - c_{22}\omega_o) \right] \tag{C.28}$$

$$\frac{\partial \mathbf{f}_{inertadd,2}}{\partial \omega_{ob,3}^b} = \frac{1}{I_y} \left[ \frac{\partial}{\partial \omega_{ob,3}^b}(e_1)(\omega_{ob,3}^b - c_{32}\omega_o) + e_1 + \frac{\partial}{\partial \omega_{ob,3}^b}(e_3)(c_{12}\omega_o - \omega_{ob,1}^b) \right] \tag{C.29}$$

$$\frac{\partial \mathbf{f}_{inertadd,1}}{\partial \omega_{ob,3}^b} = \frac{1}{I_z} \left[ \frac{\partial}{\partial \omega_{ob,3}^b}(e_1)(c_{22}\omega_o - \omega_{ob,2}^b) + \frac{\partial}{\partial \omega_{ob,3}^b}(e_2)(\omega_{ob,1}^b - c_{12}\omega_o) \right] \tag{C.30}$$

where

$$\begin{aligned}
\frac{\partial}{\partial \omega_{ob,3}^b}(e_j) &= \frac{\partial}{\partial \omega_{ob,3}^b} \left[ i_w \sum_{i=1}^4 a_{ji}(\omega_{w,i} + \sum_{k=1}^3 (a_{ki}(\omega_{ob,k}^b - c_{k2}\omega_o))) \right], \text{ for } j = 1, \dots, 3 \\
&= i_w \sum_{i=1}^4 a_{ji}(\omega_{w,i} + \sum_{k=1}^3 (a_{ki} \frac{\partial}{\partial \omega_{ob,3}^b}(\omega_{ob,k}^b))), \text{ for } j = 1, \dots, 3 \\
&= i_w \sum_{i=1}^4 a_{ji}(\omega_{w,i} + a_{3i}), \text{ for } j = 1, \dots, 3
\end{aligned} \tag{C.31}$$

## C.2 Angular velocity model

By combining the results of the above section with the results from Kyrkjebø (2000), the linearized angular model can now be expressed as

$$\mathbf{F}_{\text{vel}} = \begin{bmatrix} b_{51} & b_{52} & b_{53} & b_{54} & b_{55} & b_{56} & b_{57} \\ b_{61} & b_{62} & b_{63} & b_{64} & b_{65} & b_{66} & b_{67} \\ b_{71} & b_{72} & b_{73} & b_{74} & b_{75} & b_{76} & b_{77} \end{bmatrix} \tag{C.32}$$

where the components  $b_{ij}$  are defined as

$$\begin{aligned}
b_{51} = & 2k_x\omega_o(\epsilon_1(\omega_{ob,2}^b - c_{22}\omega_o) - \eta(\omega_{ob,3}^b - c_{32}\omega_o)) - 6k_x\omega_o^2(\epsilon_1c_{33} + \eta c_{23}) + 2(\eta\omega_{ob,3}^b + \epsilon_1\omega_{ob,2}^b)\omega_o \\
& + \frac{1}{I_x}[2i_w\omega_o(a_{21} + a_{22} + a_{23} + a_{24})(-\epsilon_3(a_{11} + a_{12} + a_{13} + a_{14}) - \eta(a_{21} + a_{22} + a_{23} + a_{24})) \\
& + \epsilon_1(a_{31} + a_{32} + a_{33} + a_{34}) + a_{21}\omega_{w,1} + \frac{1}{2\omega_o}(\omega_{w,2} + \omega_{w,3} + \omega_{w,4})))(c_{32}\omega_o - \omega_{ob,3}^b) \\
& - 2\epsilon_1\omega_o e_2 + 2i_w\omega_o(a_{31} + a_{32} + a_{33} + a_{34})(\epsilon_3(-a_{11} - a_{12} - a_{13} - a_{14}) + \eta(-a_{21} - a_{22} - a_{23} - a_{24})) \\
& + \epsilon_1(-a_{31} + a_{32} + a_{33} + a_{34}) + \frac{1}{2\omega_o}(\omega_{w,1} + a_{32}\omega_{w,2} + \omega_{w,3} + \omega_{w,4})))(\omega_{ob,2}^b - c_{22}\omega_o) \\
& - 2\eta\omega_o e_3] \tag{C.33}
\end{aligned}$$

$$\begin{aligned}
b_{52} = & 2k_x\omega_o(\eta(\omega_{ob,2}^b - c_{22}\omega_o) - \epsilon_1(\omega_{ob,3}^b - c_{32}\omega_o)) + 6k_x\omega_o^2(\epsilon_1c_{23} - \eta c_{33}) + 2(\eta\omega_{ob,2}^b - \epsilon_1\omega_{ob,3}^b)\omega_o \\
& + \frac{1}{I_x}[2i_w\omega_o(a_{21} + a_{22} + a_{23} + a_{24})(-\epsilon_2(a_{11} + a_{12} + a_{13} + a_{14}) + \epsilon_1(a_{21} + a_{22} + a_{23} + a_{24})) \\
& + \eta(a_{31} + a_{32} + a_{33} + a_{34}) + a_{21}\omega_{w,1} + \frac{1}{2\omega_o}(\omega_{w,2} + \omega_{w,3} + \omega_{w,4})))(\omega_{ob,3}^b - c_{32}\omega_o) \\
& - 2\eta\omega_o e_2 + 2i_w\omega_o(a_{31} + a_{32} + a_{33} + a_{34})(-\epsilon_2(a_{11} + a_{12} + a_{13} + a_{14}) + \epsilon_1(a_{21} + a_{22} + a_{23} + a_{24})) \\
& + \eta(a_{31} + a_{32} + a_{33} + a_{34}) + \frac{1}{2\omega_o}(\omega_{w,1} + \omega_{w,2} + \omega_{w,3} + \omega_{w,4})))(\omega_{ob,1}^b - c_{22}\omega_o) \\
& + 2\epsilon_1\omega_o e_3] \tag{C.34}
\end{aligned}$$

$$\begin{aligned}
b_{53} = & -2k_x\omega_o(\epsilon_3(\omega_{ob,2}^b - c_{22}\omega_o) - \epsilon_2(\omega_{ob,3}^b - c_{32}\omega_o)) + 6k_x\omega_o^2(\epsilon_2c_{23} - \epsilon_3c_{33}) + 2(\epsilon_3\omega_{ob,3}^b - \epsilon_3\omega_{ob,2}^b)\omega_o \\
& + \frac{1}{I_x}[2i_w\omega_o(a_{21} + a_{22} + a_{23} + a_{24})(-\epsilon_1(a_{11} + a_{12} + a_{13} + a_{14}) + \epsilon_2(a_{21} + a_{22} + a_{23} + a_{24})) \\
& + \epsilon_3(a_{31} + a_{32} + a_{33} + a_{34}) + a_{21}\omega_{w,1} + \frac{1}{2\omega_o}(\omega_{w,2} + \omega_{w,3} + \omega_{w,4})))(\omega_{ob,3}^b - c_{32}\omega_o) \\
& + 2\epsilon_3\omega_o e_2 + 2i_w\omega_o(a_{31} + a_{32} + a_{33} + a_{34})(-\epsilon_1(a_{11} + a_{12} + a_{13} + a_{14}) + \epsilon_2(a_{21} + a_{22} + a_{23} + a_{24})) \\
& + \epsilon_3(a_{31} + a_{32} + a_{33} + a_{34}) + \frac{1}{2\omega_o}(\omega_{w,1} + \omega_{w,2} + \omega_{w,3} + \omega_{w,4})))(\omega_{ob,1}^b - c_{22}\omega_o) \\
& - 2\epsilon_2\omega_o e_3] \tag{C.35}
\end{aligned}$$

$$\begin{aligned}
b_{54} = & 2k_x\omega_o(\epsilon_3(\omega_{ob,3}^b - c_{32}\omega_o) - \eta(\omega_{ob,2}^b - c_{22}\omega_o)) - 6k_x\omega_o^2(\epsilon_2c_{33} + \epsilon_3c_{23}) - 2(\epsilon_3\omega_{ob,3}^b + \epsilon_2\omega_{ob,2}^b)\omega_o \\
& + \frac{1}{I_x}[2i_w\omega_o(a_{21} + a_{22} + a_{23} + a_{24})(-\eta(a_{11} + a_{12} + a_{13} + a_{14}) + \epsilon_3(a_{21} + a_{22} + a_{23} + a_{24})) \\
& + \epsilon_2(a_{31} + a_{32} + a_{33} + a_{34}) + a_{21}\omega_{w,1} + \frac{1}{2\omega_o}(\omega_{w,2} + \omega_{w,3} + \omega_{w,4})))(\omega_{ob,3}^b - c_{32}\omega_o) \\
& + 2\epsilon_2\omega_o e_2 + 2i_w\omega_o(a_{31} + a_{32} + a_{33} + a_{34})(-\eta(a_{11} + a_{12} + a_{13} + a_{14}) + \epsilon_3(a_{21} + a_{22} + a_{23} + a_{24})) \\
& + \epsilon_2(a_{31} + a_{32} + a_{33} + a_{34}) + \frac{1}{2\omega_o}(\omega_{w,1} + \omega_{w,2} + \omega_{w,3} + \omega_{w,4})))(\omega_{ob,1}^b - c_{22}\omega_o) \\
& + 2\epsilon_3\omega_o e_3] \tag{C.36}
\end{aligned}$$

$$\begin{aligned}
b_{55} = & \frac{1}{I_x} [(i_w(a_{21}(\omega_{w,1} + a_{11}) + a_{22}(\omega_{w,2} + a_{12}) + a_{23}(\omega_{w,3} + a_{13}) + a_{24}(\omega_{w,4} + a_{14}))) (c_{32}\omega_o - \omega_{ob,3}^b) \\
& + (i_w(a_{31}(\omega_{w,1} + a_{11}) + a_{32}(\omega_{w,2} + a_{12}) + a_{33}(\omega_{w,3} + a_{13}) + a_{34}(\omega_{w,4} + a_{14}))) (\omega_{ob,2}^b - c_{22}\omega_o)] \\
& \tag{C.37}
\end{aligned}$$

$$\begin{aligned}
b_{56} = & k_x(\omega_{ob,3}^b - c_{32}\omega_o) - c_{32}\omega_o + \frac{1}{I_x} [(i_w(a_{21}(\omega_{w,1} + a_{21}) + a_{22}(\omega_{w,2} + a_{22}) + a_{23}(\omega_{w,3} + a_{23}) \\
& + a_{24}(\omega_{w,4} + a_{24}))) (c_{32}\omega_o - \omega_{ob,3}^b) + (i_w(a_{31}(\omega_{w,1} + a_{21}) + a_{32}(\omega_{w,2} + a_{22}) + a_{33}(\omega_{w,3} + a_{23}) \\
& + a_{34}(\omega_{w,4} + a_{24}))) (\omega_{ob,2}^b - c_{22}\omega_o) + e_3] \\
& \tag{C.38}
\end{aligned}$$

$$\begin{aligned}
b_{57} = & k_x(\omega_{ob,2}^b - c_{22}\omega_o) + c_{22}\omega_o + \frac{1}{I_x} [(i_w(a_{21}(\omega_{w,1} + a_{31}) + a_{22}(\omega_{w,2} + a_{32}) + a_{23}(\omega_{w,3} + a_{33}) \\
& + a_{24}(\omega_{w,4} + a_{34}))) (c_{32}\omega_o - \omega_{ob,3}^b) + (i_w(a_{31}(\omega_{w,1} + a_{31}) + a_{32}(\omega_{w,2} + a_{32}) + a_{33}(\omega_{w,3} + a_{33}) \\
& + a_{34}(\omega_{w,4} + a_{34}))) (\omega_{ob,2}^b - c_{22}\omega_o) - e_2] \\
& \tag{C.39}
\end{aligned}$$

$$\tag{C.40}$$

$$\begin{aligned}
b_{61} = & 2k_y\omega_o(\epsilon_3(\omega_{ob,z}^b - c_{32}\omega_o) - \epsilon_1(\omega_{ob,x}^b - c_{12}\omega_o)) + 6k_y\omega_o^2(\eta c_{13} + \epsilon_2 c_{33}) - 2(\epsilon_1\omega_{ob,x}^b + \epsilon_3\omega_{ob,z}^b)\omega_o \\
& + \frac{1}{I_y} [2i_w\omega_o(a_{11} + a_{12} + a_{13} + a_{14})(-\epsilon_3(a_{11} + a_{12} + a_{13} + a_{14}) - \eta(a_{21} + a_{22} + a_{23} + a_{24})) \\
& + \epsilon_1(a_{31} + a_{32} + a_{33} + a_{34}) + \frac{1}{2\omega_o}(\omega_{w,1} + \omega_{w,2} + \omega_{w,3} + \omega_{w,4}))(\omega_{ob,3}^b - c_{32}\omega_o) \\
& + 2\epsilon_1\omega_o e_1 + 2i_w\omega_o(a_{31} + a_{32} + a_{33} + a_{34})(-\epsilon_3(a_{11} + a_{12} + a_{13} + a_{14}) - \eta(a_{21} + a_{22} + a_{23} + a_{24})) \\
& + \epsilon_1(a_{31} + a_{32} + a_{33} + a_{34}) + \frac{1}{2\omega_o}(\omega_{w,1} + \omega_{w,2} + \omega_{w,3} + \omega_{w,4}))(\omega_{ob,2}^b - c_{22}\omega_o) \\
& - 2\epsilon_3\omega_o e_3] \\
& \tag{C.41}
\end{aligned}$$

$$\begin{aligned}
b_{62} = & 2k_y\omega_o(\epsilon_2(\omega_{ob,z}^b - c_{32}\omega_o) - \eta(\omega_{ob,x}^b - c_{12}\omega_o)) + 6k_y\omega_o^2(\epsilon_3 c_{33} - \epsilon_1 c_{13}) - 2(\eta\omega_{ob,x}^b + \epsilon_2\omega_{ob,z}^b)\omega_o \\
& + \frac{1}{I_y} [2i_w\omega_o(a_{11} + a_{12} + a_{13} + a_{14})(-\epsilon_2(a_{11} + a_{12} + a_{13} + a_{14}) + \epsilon_1(a_{21} + a_{22} + a_{23} + a_{24})) \\
& + \eta(a_{31} + a_{32} + a_{33} + a_{34}) + \frac{1}{2\omega_o}(\omega_{w,1} + \omega_{w,2} + \omega_{w,3} + \omega_{w,4}))(\omega_{ob,3}^b - c_{32}\omega_o) \\
& + 2\eta\omega_o e_1 + 2i_w\omega_o(a_{31} + a_{32} + a_{33} + a_{34})(-\epsilon_2(a_{11} + a_{12} + a_{13} + a_{14}) + \epsilon_1(a_{21} + a_{22} + a_{23} + a_{24})) \\
& + \eta(a_{31} + a_{32} + a_{33} + a_{34}) + \frac{1}{2\omega_o}(\omega_{w,1} + \omega_{w,2} + \omega_{w,3} + \omega_{w,4}))(\omega_{ob,2}^b - c_{22}\omega_o) \\
& - 2\epsilon_2\omega_o e_3] \\
& \tag{C.42}
\end{aligned}$$

$$\begin{aligned}
b_{63} = & 2k_y\omega_o(\epsilon_1(\omega_{ob,z}^b - c_{32}\omega_o) - \epsilon_3(\omega_{ob,x}^b - c_{12}\omega_o)) - 6k_y\omega_o^2(\eta c_{33} - \epsilon_2 c_{13}) + 2(\epsilon_3\omega_{ob,x}^b - \eta\omega_{ob,z}^b)\omega_o \\
& + \frac{1}{I_y}[2i_w\omega_o(a_{11} + a_{12} + a_{13} + a_{14})(-\epsilon_1(a_{11} + a_{12} + a_{13} + a_{14}) - \epsilon_2(a_{21} + a_{22} + a_{23} + a_{24})) \\
& + \epsilon_3(a_{31} + a_{32} + a_{33} + a_{34}) + \frac{1}{2\omega_o}(\omega_{w,1} + \omega_{w,2} + \omega_{w,3} + \omega_{w,4}))(\omega_{ob,3}^b - c_{32}\omega_o) \\
& - 2\epsilon_3\omega_o e_1 + 2i_w\omega_o(a_{31} + a_{32} + a_{33} + a_{34})(-\epsilon_1(a_{11} + a_{12} + a_{13} + a_{14}) - \epsilon_2(a_{21} + a_{22} + a_{23} + a_{24})) \\
& + \epsilon_3(a_{31} + a_{32} + a_{33} + a_{34}) + \frac{1}{2\omega_o}(\omega_{w,1} + \omega_{w,2} + \omega_{w,3} + \omega_{w,4}))(\omega_{ob,2}^b - c_{22}\omega_o) \\
& + 2\epsilon_1\omega_o e_3] \tag{C.43}
\end{aligned}$$

$$\begin{aligned}
b_{64} = & 2k_y\omega_o(\eta(\omega_{ob,z}^b - c_{32}\omega_o) - \epsilon_2(\omega_{ob,x}^b - c_{12}\omega_o)) + 6k_y\omega_o^2(\epsilon_1 c_{33} + \epsilon_3 c_{13}) + 2(\epsilon_3\omega_{ob,z}^b - \eta\omega_{ob,x}^b)\omega_o \\
& + \frac{1}{I_y}[2i_w\omega_o(a_{11} + a_{12} + a_{13} + a_{14})(-\eta(a_{11} + a_{12} + a_{13} + a_{14}) + \epsilon_3(a_{21} + a_{22} + a_{23} + a_{24})) \\
& + \epsilon_2(a_{31} + a_{32} + a_{33} + a_{34}) + \frac{1}{2\omega_o}(\omega_{w,1} + \omega_{w,2} + \omega_{w,3} + \omega_{w,4}))(\omega_{ob,3}^b - c_{32}\omega_o) \\
& - 2\epsilon_2\omega_o e_1 + 2i_w\omega_o(a_{31} + a_{32} + a_{33} + a_{34})(-\eta(a_{11} + a_{12} + a_{13} + a_{14}) + \epsilon_3(a_{21} + a_{22} + a_{23} + a_{24})) \\
& + \epsilon_2(a_{31} + a_{32} + a_{33} + a_{34}) + \frac{1}{2\omega_o}(\omega_{w,1} + \omega_{w,2} + \omega_{w,3} + \omega_{w,4}))(\omega_{ob,2}^b - c_{22}\omega_o) \\
& - 2\eta\omega_o e_3] \tag{C.44}
\end{aligned}$$

$$\begin{aligned}
b_{65} = & -k_y(\omega_{ob,z}^b - c_{32}\omega_o) + c_{32}\omega_o + \frac{1}{I_y}[i_w(a_{11}(\omega_{w,1} + a_{11}) + a_{12}(\omega_{w,2} + a_{12}) + a_{13}(\omega_{w,3} + a_{13}) \\
& + a_{14}(\omega_{w,4} + a_{14}))(\omega_{ob,3}^b - c_{32}\omega_o) + (i_w(a_{31}(\omega_{w,1} + a_{11}) + a_{32}(\omega_{w,2} + a_{12}) + a_{33}(\omega_{w,3} + a_{13}) \\
& + a_{34}(\omega_{w,4} + a_{14}))) (c_{12}\omega_o - \omega_{ob,1}^b) - e_3] \tag{C.45}
\end{aligned}$$

$$\begin{aligned}
b_{66} = & \frac{1}{I_y}[i_w(a_{11}(\omega_{w,1} + a_{21}) + a_{12}(\omega_{w,2} + a_{22}) + a_{13}(\omega_{w,3} + a_{23}) + a_{14}(\omega_{w,4} + a_{24}))(\omega_{ob,3}^b - c_{32}\omega_o) \\
& + (i_w(a_{31}(\omega_{w,1} + a_{21}) + a_{32}(\omega_{w,2} + a_{22}) + a_{33}(\omega_{w,3} + a_{23}) + a_{34}(\omega_{w,4} + a_{24}))) (c_{12}\omega_o - \omega_{ob,1}^b)] \tag{C.46}
\end{aligned}$$

$$\begin{aligned}
b_{67} = & -k_y(\omega_{ob,x}^b - c_{12}\omega_o) - c_{12}\omega_o + \frac{1}{I_y}[i_w(a_{11}(\omega_{w,1} + a_{31}) + a_{12}(\omega_{w,2} + a_{32}) + a_{13}(\omega_{w,3} + a_{33}) \\
& + a_{14}(\omega_{w,4} + a_{34}))(\omega_{ob,3}^b - c_{32}\omega_o) + e_1 + (i_w(a_{31}(\omega_{w,1} + a_{31}) + a_{32}(\omega_{w,2} + a_{32}) + a_{33}(\omega_{w,3} + a_{33}) \\
& + a_{34}(\omega_{w,4} + a_{34}))) (c_{12}\omega_o - \omega_{ob,1}^b)] \tag{C.47}
\end{aligned}$$

$$\begin{aligned}
b_{71} = & 2k_z\omega_o(\epsilon_3(\omega_{ob,y}^b - c_{22}\omega_o) + \eta(\omega_{ob,x}^b - c_{12}\omega_o)) + 6k_z\omega_o^2(\epsilon_1c_{13} - \epsilon_2c_{23}) + 2(\epsilon_3\omega_{ob,x}^b - \eta\omega_{ob,x}^b)\omega_o \\
& + \frac{1}{I_z}[2i_w\omega_o(a_{11} + a_{12} + a_{13} + a_{14})(-\epsilon_3(a_{11} + a_{12} + a_{13} + a_{14}) - \eta(a_{21} + a_{22} + a_{23} + a_{24})) \\
& + \epsilon_1(a_{31} + a_{32} + a_{33} + a_{34}) + \frac{1}{2\omega_o}(\omega_{w,1} + \omega_{w,2} + \omega_{w,3} + \omega_{w,4}))(c_{22}\omega_o - \omega_{ob,2}^b) \\
& + 2\eta\omega_o e_1 + 2i_w\omega_o(a_{11} + a_{12} + a_{13} + a_{14})(-\epsilon_3(a_{11} + a_{12} + a_{13} + a_{14}) - \eta(a_{21} + a_{22} + a_{23} + a_{24})) \\
& + \epsilon_1(a_{31} + a_{32} + a_{33} + a_{34}) + \frac{1}{2\omega_o}(\omega_{w,1} + \omega_{w,2} + \omega_{w,3} + \omega_{w,4}))(c_{12}\omega_o - \omega_{ob,1}^b) \\
& - 2\epsilon_3\omega_o e_2] \tag{C.48}
\end{aligned}$$

$$\begin{aligned}
b_{72} = & 2k_z\omega_o(\epsilon_2(\omega_{ob,y}^b - c_{22}\omega_o) - \epsilon_1(\omega_{ob,x}^b - c_{12}\omega_o)) + 6k_z\omega_o^2(\epsilon_3c_{23} + \eta c_{13}) + 2(\epsilon_1\omega_{ob,x}^b + \epsilon_2\omega_{ob,y}^b)\omega_o \\
& + \frac{1}{I_z}[2i_w\omega_o(a_{11} + a_{12} + a_{13} + a_{14})(-\epsilon_2(a_{11} + a_{12} + a_{13} + a_{14}) + \epsilon_1(a_{21} + a_{22} + a_{23} + a_{24})) \\
& + \eta(a_{31} + a_{32} + a_{33} + a_{34}) + \frac{1}{2\omega_o}(\omega_{w,1} + \omega_{w,2} + \omega_{w,3} + \omega_{w,4}))(c_{22}\omega_o - \omega_{ob,2}^b) \\
& - 2\epsilon_1\omega_o e_1 + 2i_w\omega_o(a_{11} + a_{12} + a_{13} + a_{14})(-\epsilon_2(a_{11} + a_{12} + a_{13} + a_{14}) + \epsilon_1(a_{21} + a_{22} + a_{23} + a_{24})) \\
& + \eta(a_{31} + a_{32} + a_{33} + a_{34}) + \frac{1}{2\omega_o}(\omega_{w,1} + \omega_{w,2} + \omega_{w,3} + \omega_{w,4}))(c_{12}\omega_o - \omega_{ob,1}^b) \\
& - 2\epsilon_2\omega_o e_2] \tag{C.49}
\end{aligned}$$

$$\begin{aligned}
b_{73} = & 2k_z\omega_o(\epsilon_1(\omega_{ob,y}^b - c_{22}\omega_o) + \epsilon_2(\omega_{ob,x}^b - c_{12}\omega_o)) + 6k_z\omega_o^2(\epsilon_3c_{13} - \eta c_{23}) + 2(\epsilon_1\omega_{ob,y}^b - \epsilon_2\omega_{ob,x}^b)\omega_o \\
& + \frac{1}{I_z}[2i_w\omega_o(a_{11} + a_{12} + a_{13} + a_{14})(-\epsilon_1(a_{11} + a_{12} + a_{13} + a_{14}) - \epsilon_2(a_{21} + a_{22} + a_{23} + a_{24})) \\
& + \epsilon_3(a_{31} + a_{32} + a_{33} + a_{34}) + \frac{1}{2\omega_o}(\omega_{w,1} + \omega_{w,2} + \omega_{w,3} + \omega_{w,4}))(c_{22}\omega_o - \omega_{ob,2}^b) \\
& + 2\epsilon_2\omega_o e_1 + 2i_w\omega_o(a_{11} + a_{12} + a_{13} + a_{14})(-\epsilon_1(a_{11} + a_{12} + a_{13} + a_{14}) - \epsilon_2(a_{21} + a_{22} + a_{23} + a_{24})) \\
& + \epsilon_3(a_{31} + a_{32} + a_{33} + a_{34}) + \frac{1}{2\omega_o}(\omega_{w,1} + \omega_{w,2} + \omega_{w,3} + \omega_{w,4}))(c_{12}\omega_o - \omega_{ob,1}^b) \\
& - 2\epsilon_1\omega_o e_2] \tag{C.50}
\end{aligned}$$

$$\begin{aligned}
b_{74} = & 2k_z\omega_o(\eta(\omega_{ob,y}^b - c_{22}\omega_o) - \epsilon_3(\omega_{ob,x}^b - c_{12}\omega_o)) + 6k_z\omega_o^2(\epsilon_1c_{23} + \epsilon_2c_{13}) + 2(\epsilon_3\omega_{ob,x}^b + \eta\omega_{ob,y}^b)\omega_o \\
& + \frac{1}{I_z}[2i_w\omega_o(a_{11} + a_{12} + a_{13} + a_{14})(-\eta(a_{11} + a_{12} + a_{13} + a_{14}) + \epsilon_3(a_{21} + a_{22} + a_{23} + a_{24})) \\
& + \epsilon_2(a_{31} + a_{32} + a_{33} + a_{34}) + \frac{1}{2\omega_o}(\omega_{w,1} + \omega_{w,2} + \omega_{w,3} + \omega_{w,4}))(c_{22}\omega_o - \omega_{ob,2}^b) \\
& - 2\epsilon_3\omega_o e_1 + 2i_w\omega_o(a_{11} + a_{12} + a_{13} + a_{14})(-\eta(a_{11} + a_{12} + a_{13} + a_{14}) + \epsilon_3(a_{21} + a_{22} + a_{23} + a_{24})) \\
& + \epsilon_2(a_{31} + a_{32} + a_{33} + a_{34}) + \frac{1}{2\omega_o}(\omega_{w,1} + \omega_{w,2} + \omega_{w,3} + \omega_{w,4}))(c_{12}\omega_o - \omega_{ob,1}^b) \\
& - 2\eta\omega_o e_2] \tag{C.51}
\end{aligned}$$

$$\begin{aligned}
b_{75} = & -k_z(\omega_{ob,y}^b - c_{22}\omega_o) - c_{22}\omega_o + \frac{1}{I_z}[i_w(a_{11}(\omega_{w,1} + a_{11}) + a_{12}(\omega_{w,2} + a_{12}) + a_{13}(\omega_{w,3} + a_{13}) \\
& + a_{14}(\omega_{w,4} + a_{14}))(c_{22}\omega_o - \omega_{ob,2}^b) + (i_w(a_{21}(\omega_{w,1} + a_{11}) + a_{22}(\omega_{w,2} + a_{12}) + a_{23}(\omega_{w,3} + a_{13}) \\
& + a_{24}(\omega_{w,4} + a_{14}))) (\omega_{ob,1}^b - c_{12}\omega_o) + e_2] \tag{C.52}
\end{aligned}$$

$$\begin{aligned}
b_{76} = & -k_z(\omega_{ob,x}^b - c_{12}\omega_o) + c_{12}\omega_o + \frac{1}{I_z}[i_w(a_{11}(\omega_{w,1} + a_{21}) + a_{12}(\omega_{w,2} + a_{22}) + a_{13}(\omega_{w,3} + a_{23}) \\
& + a_{14}(\omega_{w,4} + a_{24}))(c_{22}\omega_o - \omega_{ob,2}^b) - e_1 + (i_w(a_{21}(\omega_{w,1} + a_{21}) + a_{22}(\omega_{w,2} + a_{22}) + a_{23}(\omega_{w,3} + a_{23}) \\
& + a_{24}(\omega_{w,4} + a_{24}))) (\omega_{ob,1}^b - c_{12}\omega_o)] \tag{C.53}
\end{aligned}$$

$$\begin{aligned}
b_{77} = & \frac{1}{I_z}[i_w(a_{11}(\omega_{w,1} + a_{31}) + a_{12}(\omega_{w,2} + a_{32}) + a_{13}(\omega_{w,3} + a_{33}) + a_{14}(\omega_{w,4} + a_{34}))(c_{22}\omega_o - \omega_{ob,2}^b) \\
& + (i_w(a_{21}(\omega_{w,1} + a_{31}) + a_{22}(\omega_{w,2} + a_{32}) + a_{23}(\omega_{w,3} + a_{33}) + a_{24}(\omega_{w,4} + a_{34}))) (\omega_{ob,1}^b - c_{12}\omega_o)] \tag{C.54}
\end{aligned}$$

where  $e_1$ ,  $e_2$ , and  $e_3$  are defined by (4.25).

### C.3 Earth sensor measurement matrix

$$\mathbf{H}_{earth,k} = \frac{\partial}{\partial \mathbf{x}_r}(\mathbf{y}_e^b)|_{\mathbf{x}_r=\bar{\mathbf{x}}_r} = \begin{bmatrix} \frac{\partial \phi}{\partial \epsilon_1} & \cdots & \frac{\partial \phi}{\partial \omega_{ob,3}^b} \\ \frac{\partial \theta}{\partial \epsilon_1} & \cdots & \frac{\partial \theta}{\partial \omega_{ob,3}^b} \end{bmatrix}_{\mathbf{x}_r=\bar{\mathbf{x}}_r} \tag{C.55}$$

The roll part is linearized as

$$\frac{\partial \phi}{\partial \mathbf{x}_r} = \frac{\partial}{\partial \mathbf{x}_r}(\tan^{-1}(u)) = \frac{1}{1+u^2} \frac{\partial}{\partial \mathbf{x}_r}(u) \tag{C.56}$$

where

$$u = \frac{2(\bar{\epsilon}_2\bar{\epsilon}_3 + \bar{\eta}\bar{\epsilon}_1)}{\bar{\eta}^2 - \bar{\epsilon}_1^2 - \bar{\epsilon}_2^2 + \bar{\epsilon}_3^2} \tag{C.57}$$

$$\frac{\partial}{\partial \epsilon_1}(u) = \frac{2\eta(\eta^2 - \epsilon_1^2 - \epsilon_2^2 + \epsilon_3^2) + 2\epsilon_1(2(\epsilon_2\epsilon_3 + \eta\epsilon_1))}{(\eta^2 - \epsilon_1^2 - \epsilon_2^2 + \epsilon_3^2)^2} \tag{C.58a}$$

$$\frac{\partial}{\partial \epsilon_2}(u) = \frac{2\epsilon_3(\eta^2 - \epsilon_1^2 - \epsilon_2^2 + \epsilon_3^2) + 2\epsilon_2(2(\epsilon_2\epsilon_3 + \eta\epsilon_1))}{(\eta^2 - \epsilon_1^2 - \epsilon_2^2 + \epsilon_3^2)^2} \tag{C.58b}$$

$$\frac{\partial}{\partial \epsilon_3}(u) = \frac{2\epsilon_2(\eta^2 - \epsilon_1^2 - \epsilon_2^2 + \epsilon_3^2) - 2\epsilon_3(2(\epsilon_2\epsilon_3 + \eta\epsilon_1))}{(\eta^2 - \epsilon_1^2 - \epsilon_2^2 + \epsilon_3^2)^2} \tag{C.58c}$$

$$\frac{\partial}{\partial \omega_{ob,1}^b}(u) = \frac{\partial}{\partial \omega_{ob,2}^b}(u) = \frac{\partial}{\partial \omega_{ob,3}^b}(u) = 0 \tag{C.58d}$$

and the pitch part as

$$\frac{\partial \theta}{\partial \mathbf{x}_r} = \frac{\partial}{\partial \mathbf{x}_r} \left( \tan^{-1} \left( \frac{v}{\sqrt{1-v^2}} \right) \right) = \frac{1}{1 + \left( \frac{v}{\sqrt{1-v^2}} \right)^2} \frac{\partial}{\partial \mathbf{x}_r} \left( \frac{v}{\sqrt{1-v^2}} \right) \quad (\text{C.59})$$

where

$$v = 2(\epsilon_1 \epsilon_3 - \eta \epsilon_2) \quad (\text{C.60})$$

and

$$\frac{\partial}{\partial \epsilon_1} \left( \frac{v}{\sqrt{1-v^2}} \right) = \frac{2\epsilon_3 \sqrt{1-v^2} - 4\epsilon_1 \epsilon_3^2 \frac{v}{\sqrt{1-v^2}}}{1-v^2} \quad (\text{C.61a})$$

$$\frac{\partial}{\partial \epsilon_2} \left( \frac{v}{\sqrt{1-v^2}} \right) = \frac{-2\eta \sqrt{1-v^2} - 4\eta^2 \epsilon_2^2 \frac{v}{\sqrt{1-v^2}}}{1-v^2} \quad (\text{C.61b})$$

$$\frac{\partial}{\partial \epsilon_3} \left( \frac{v}{\sqrt{1-v^2}} \right) = \frac{2\epsilon_1 \sqrt{1-v^2} - 4\epsilon_1^2 \epsilon_3 \frac{v}{\sqrt{1-v^2}}}{1-v^2} \quad (\text{C.61c})$$

$$\frac{\partial}{\partial \omega_{ob,1}^b} \left( \frac{v}{\sqrt{1-v^2}} \right) = \frac{\partial}{\partial \omega_{ob,2}^b} \left( \frac{v}{\sqrt{1-v^2}} \right) = \frac{\partial}{\partial \omega_{ob,3}^b} \left( \frac{v}{\sqrt{1-v^2}} \right) = 0 \quad (\text{C.61d})$$

**Appendix D**

**CD Contents**

Folder	File	Description
common:	initSat.m	Initializes the satellite
	euler2q.m	Compute Euler param. from Euler angles
	q2euler.m	Compute Euler angles from Euler param.
	Rquat.m	Computes the rotaion matrix from Euler param.
	qProd.m	Compute the product of two Euler param.
	qProdiv.m	Compute the inv. product of two Euler param.
	nonlinearPropRW.m	Computes the nonlin. propagation
	linearsystemRRW	Computes F
	genJacobieD	Computes the Jacobiematrix
KF/Star	DEKFStar	Model of system
KF/Star	initFilterStar.m	Initializes determination scheme
KF/Star	kalmanStar.m	Discrete EKF
KF/DoubleStar	DEKFDoubleStar	Model of system
KF/DoubleStar	initFilterDoubleStar.m	Init determination scheme
KF/DoubleStar	kalmanStar.m	Discrete EKF
KF/StarSun	DEKFStar	Model of system
KF/StarSun	initFilterStarSun.m	Init determination scheme
KF/StarSun	kalmanStar.m	Discrete EKF
KF/SunEarthStar	EKFSunEarthStar	Model of system
KF/SunEarthStar	initFilterStar.m	Init determination scheme
KF/SunEarthStar	kalmanStarSun.m	Discrete EKF
KF/SunEarthStar	kalmanSunEarthStarMod.m	Modified EKF
KF/SunEarthStar	EarthLinH.m	Lin. earth matrix
Observer/Star	ObserverStar	Model of system
Observer/Star	initObserverStar.m	Init determination scheme
Observer/Star	ObserverStar.m	Discrete observer
Observer/StarDouble	ObserverStarDouble	Model of system
Observer/StarDouble	initObserverStarDouble.m	Init determination scheme
Observer/StarDouble	ObserverStarDouble.m	Discrete observer
Observer/StarSun	ObserverStarSun	Model of system
Observer/StarSun	initObserverStarSun.m	Init determination scheme
Observer/StarDouble	ObserverStarSun.m	Discrete observer
Observer/SunEarthStar	ObserverSunEarthStar	Model of system
Observer/SunEarthStar	initObserverSunEarthStar.m	Init determination scheme
Observer/SunEarthStar	observerSunEarthStar.m	Discrete observer